AD_____

GRANT NO: DAMD17-94-J-4272

TITLE: Immunogenic Structural Features of a Breast Tumor-Specific Epitope for Cancer Immunotherapy

PRINCIPAL INVESTIGATOR(S): Kenneth E. Dombrowski, Ph.D.
Co-PI: Stephen E. Wright, MD
CONTRACTING ORGANIZATION: Harrington Regional Medical Center
Amarillo, Texas 79106

REPORT DATE: September 1995

TYPE OF REPORT: Annual

PREPARED FOR: U.S. Army Medical Research and Materiel Command
Fort Detrick, Maryland 21702-5012

REPORT DOCUMENTATION PAGE

Form Approved
OMB No. 0704-0188

1. AGENCY USE ONLY (Leave blank)	2. REPORT DATE	3. REPORT TYPE AND DATES COVERED
	September 1995	Annual (1 Sep 94 - 31 Aug 95)

4. TITLE AND SUBTITLE
Immunogenic Structural Features of a Breast Tumor-Specific Epitope for Cancer Immunotherapy

5. FUNDING NUMBERS
DAMD17-94-J-4272

6. AUTHOR(S)
Kenneth E. Dombrowski, Ph.D.
Stephen E. Wright, M.D.

7. PERFORMING ORGANIZATION NAME(S) AND ADDRESS(ES)
Harrington Regional Medical Center
Amarillo, Texas 79106

8. PERFORMING ORGANIZATION REPORT NUMBER

9. SPONSORING/MONITORING AGENCY NAME(S) AND ADDRESS(ES)
U.S. Army Medical Research and Materiel Command
Fort Detrick, Maryland 21702-5012

10. SPONSORING/MONITORING AGENCY REPORT NUMBER

11. SUPPLEMENTARY NOTES

12a. DISTRIBUTION/AVAILABILITY STATEMENT
Approved for publicrelease; distribution unlimited

12b. DISTRIBUTION CODE

13. ABSTRACT *(Maximum 200 words)*

The objectives of the research program are to understand the structure-immunogenicity relationships of tumor-specific mucin common to human breast adenocarcinomas, and the regulation of tumor-specific lymphoid cells that respond to the tumor-specific immunogen. Using the synthetic native MUC1 peptide PDTRPAPGSTAPPAHGVTSA and the mutated $T^3 \rightarrow N^3$ MUC1 (containing the mutation in the TSE) these relationships are being studied. The peptides were equal in immunogenicity with respect to cell proliferation and tumor-specific cytotoxicity. Both peptides also induced expansion of a narrow T cell population, each with a unique Vβ repertoire. The conformation of each peptide is being evaluated ^{1}H-NMR. Amino acids and carbohydrates found in the MUC1 molecule have been characterized by x-ray photoelectron spectroscopy. This method is also able to detect the point mutation within the TSE. Thus, we can design, construct and characterize the biophysical properties of immunogenic mucin peptides which can elicit tumor-specific responses. This progress in understanding of the structure-immunogenicity relationships of tumor-specific immunogens, and the regulation of the lymphoid cells responding to the immunogen, should maximize the use of synthetic peptide immunogens for the adoptive immunotherapy of adenocarcinomas and as a potential vaccine.

14. SUBJECT TERMS
Breast cancer, mucin, immunotherapy, structure, immunogenicity, tumor-specific epitopes, regulation

15. NUMBER OF PAGES
71

16. PRICE CODE

17. SECURITY CLASSIFICATION OF REPORT	18. SECURITY CLASSIFICATION OF THIS PAGE	19. SECURITY CLASSIFICATION OF ABSTRACT	20. LIMITATION OF ABSTRACT
Unclassified	Unclassified	Unclassified	Unlimited

FOREWORD

Opinions, interpretations, conclusions and recommendations are those of the author and are not necessarily endorsed by the US Army.

____ Where copyrighted material is quoted, permission has been obtained to use such material.

____ Where material from documents designated for limited distribution is quoted, permission has been obtained to use the material.

KE Citations of commercial organizations and trade names in this report do not constitute an official Department of Army endorsement or approval of the products or services of these organizations.

KE In conducting research using animals, the investigator(s) adhered to the "Guide for the Care and Use of Laboratory Animals," prepared by the Committee on Care and Use of Laboratory Animals of the Institute of Laboratory Resources, National Research Council (NIH Publication No. 86-23, Revised 1985).

KE For the protection of human subjects, the investigator(s) adhered to policies of applicable Federal Law 45 CFR 46.

KE In conducting research utilizing recombinant DNA technology, the investigator(s) adhered to current guidelines promulgated by the National Institutes of Health.

KE In the conduct of research utilizing recombinant DNA, the investigator(s) adhered to the NIH Guidelines for Research Involving Recombinant DNA Molecules.

KE In the conduct of research involving hazardous organisms, the investigator(s) adhered to the CDC-NIH Guide for Biosafety in Microbiological and Biomedical Laboratories.

9/27/95

PI - Signature Date

9/27/95

Table of Contents

Introduction. One of the current approaches in cancer therapy is the development of biological therapies, such as immunotherapy. Considerable advances have been made in identifying and understanding the regulation of immune cells which can distinguish between abnormal cells and normal cells. Several cell types have been identified which recognize and kill tumor cells in a specific manner [e.g. tumor-infiltrating lymphocytes (TIL); 1-5], as well as in a non-specific manner [e.g. lymphokine activated killer (LAK) cells and natural killer (NK) cells]. Pertinent to this research program, T-cells (6, 7) and B-cells (8) specific for breast, ovarian and pancreatic adenocarcinomas have been described. These observations demonstrate that the body does mount an immune response against several adenocarcinomas.

An epitope common to breast and several other adenocarcinomas recognized by cytotoxic T lymphocytes (CTL) is the tumor-specific epitope (TSE) of mucin. Mucin is the major glycoprotein of mucous secretions and is normally confined to the luminal surface of the glandular epithelial cells (9, 10). The core protein is heavily glycosylated with carbohydrate accounting for up to 80% of the glycoprotein mass (9, 10). It is the glycosylation which is responsible for the viscoelastic properties of mucus. The physicochemical properties and extracellular localization of mucin therefore suggest that this glycoprotein has a role in surface protection and lubrication of associated tissues.

Tumor-specific mucin is a normal protein that is aberrantly expressed on the tumor cells. The tumor-specific antigenicity and immunogenicity of normal mucin is inhibited by the extensive branching of the carbohydrate side chains. In contrast, the aberrant glycosylation of cancer-associated mucins exposes unique antigenic epitopes on the core protein which are masked in the fully glycosylated native form (10). This is made evident by the development of a tumor-specific monoclonal antibody, SM3, which recognizes tumor-specific mucins and fully deglycosylated native mucin, but not the fully glycosylated native mucin (10, 11).

The entire mucin core protein has been cloned and sequenced (10 and references therein). To date, at least 7 different mucin proteins have been described. The hallmark of mucins are tandem repeating sequences. MUC1 is the mucin associated with breast, ovarian, pancreatic and several other adenocarcinomas. MUC1 has the 20 amino acid repeat of $P^{1}DTRPAPGST^{10}APPAHGVTSA^{20}$ (MUC1-mucin tandem repeat; i.e., MUC1-mtr_1). Mucins are structurally polymorphic and generally contain between 40-100 tandem repeat sequences.

The structure of the MUC1-mtr_n , where n=1-3, has been partially characterized based on NMR, hydropathicity and structure prediction calculations (11-13). Viscosity measurements suggested that the structure is rod-shaped, but the state of aggregation was not reported (12). Residues $P^{1}DTRP^{5}$ are suggested to be poly-proline β-turn helices (12). It is the poly-proline β-turn regions of the core protein which are suggested to be within the SM3-reactive TSE (12). This model is also intriguing in that all of the potential glycosylation sites are either within, or surround, the TSE. Thus, glycosylation of any, or all, of these residues may result in altered immunogenicity of the TSE.

The objective of this research program is to characterize the TSE of human mucin common to breast, and other adenocarcinomas. This is essential for the development of immunotherapeutic modalities for the treatment and prevention of cancer. Understanding the structure-glycosylation patterns of the mtr and their relationship to the immunogenicity of the TSE is necessary for progress to be made in developing immunotherapeutic modalities for prevention and treatment of breast and other adenocarcinomas. In this regard, we have pursued studying the basic structure of the adenocarcinoma-specific epitope of human mucin.

The approach we have taken involves the development of synthetic peptides and recombinant mucin proteins as tumor-specific immunogens. The structure-immunogenicity relationships of these immunogens is being studied by biophysical approaches, such as NMR and x-ray photoelectron spectroscopy and correlated with the ability of the novel immunogens to develop and stimulate tumor-specific CTL.

Body. Development of Tumor-Specific CTL Lines (14). We have developed four tumor-specific human cytotoxic T-lymphocyte cell lines (CTL) from patients with adenocarcinomas. We have demonstrated that both a MUC1-mtr_1 non-glycosylated peptide and a mutated ($T^3 \rightarrow N^3$)MUC1-mtr_1 non-glycosylated peptide (containing the mutation in the tumo-specific monoclonal antibody epitope) can elicit a mucin specific response in both peripheral blood lymphocytes (PBL) and TIL. Specifically, peripheral blood mononuclear cells (PBMC) from a breast cancer patient, and TIL from both breast and ovarian tumor samples were cultured in the presence of either anti-CD3, interleukin 2 (IL2), MUC1-mtr_1+IL2 or ($T^3 \rightarrow N^3$)MUC1-mtr_1+IL2 for 14 and 29 days, respectively. The cultures were restimulated once with the same antigens. We assessed the expansion, phenotype [including T-cell receptor (TCR) Vß repertoire], and cytotoxicity of these activated cells.

Two of two experiments performed with PBMC from a single patient with breast cancer yielded similar results, indicating that our approach is reproducible within a single patient. The expansion of CTL from this patient induced by the peptides were comparable to anti-CD3 activated cells (Fig. 1 in ref. 14). However, the phenotype of the peptide-stimulated cultures showed higher levels of $CD8^+/CD56^+$ double positive T cells as compared to the anti-CD3 activated cells (Fig. 2 in ref. 14). The proliferative response, as measured by ^{3}H-thymidine incorporation, induced by ($T^3 \rightarrow N^3$)MUC1-mtr_1 was much higher than that of both MUC1-mtr_1 and anti-CD3 activated T cells (Fig. 3 in ref. 14). The cytotoxic response, as measured by ^{51}Cr release assay against the mucin expressing breast cell line MCF7 showed clearly that both peptide-stimulated PBMC cultures had significantly higher mucin-specific target cell lysis as compared to anti-CD3-stimulated cultures (Fig.4 in ref. 14). TCR analysis of these cultures indicated that each immunogen induced expansion of a narrow T cell population, with each population expressing a unique Vß repertoire (Figs. 5 & 6 in ref. 14). Anti-CD3 activated cultures showed polyclonal expansion of T cells with moderate increases in Vß 1 and 13 expressing cells. However, MUC1-mtr_1 stimulated cells showed predominantly Vß 2, 13, and 14 positive populations. On the other hand, Vß 18 positive cells were predominantly expanded in ($T^3 \rightarrow N^3$)MUC1-mtr_1 stimulated cultures.

Mucin specific CTL were also generated from an ovarian TIL sample (Figs. 7 & 8 in ref. 14). Ovarian TIL were cultured either in the presence of IL2, MUC1-mtr_1, or ($T^3 \rightarrow N^3$)MUC1-mtr_1 for 29 days and analyzed for the phenotype changes, cytotoxic potential and TCR repertoire. Under all conditions, the three cultures had similar phenotype profiles showing a predominant $CD4^+$ population. However, there was a clear difference in the cytotoxicity of these cells when tested against MCF7 target cells. The cultures expanded with IL2, but without mucin peptides, did not show any cytotoxicity against MCF7 target cells, whereas cultures stimulated with either mucin peptide showed killing activity. Significantly higher levels of lysis were observed when ($T^3 \rightarrow N^3$)MUC1-mtr_1 stimulated cells were used as effectors. TCR analysis showed different repertoires in both the MUC1-mtr_1 and the ($T^3 \rightarrow N^3$)MUC1-mtr_1 stimulated cultures. TIL cultured with IL2 alone showed Vβ 13.2 and 22.1 predominant populations. MUC1-mtr_1 stimulated TIL had a dominant Vß 18.1

population, whereas ($T^3 \rightarrow N^3$)MUC1-mtr_1 stimulated cultures showed Vß 2.b and 5.2 cells as the predominant populations. Functional correlations of the TCR specificity and response against the autologous tumor are in progress.

In addition, we have performed other experiments examining the response of an additional breast TIL culture to stimulation by the synthetic MUC1-mtr peptides. This culture responded similarly to MUC1-mtr_1 stimulation as the previously discussed cultures.

Vaccine Construction. Fowlpox viruses are capable of initiating infection of mammalian cells, but the infection is not productive, i.e., the virus does not replicate. Thus, fowlpox viruses have the potential of providing safe vaccines by producing antigens intracellularly (facilitating antigen presentation) when the inserted gene is designed to be expressed prior to replication. A fowlpox shuttle vector (pNZ1729R) containing an expression cassette and flanking poxvirus sequences (for homologous recombination) has been provided by Dr. K. Nazerian, along with a fowlpox virus isolate for use in preparing recombinant fowlpox virus (15, 16). We have successfully cloned two glycosylated, membrane associated virus antigens into the shuttle vector, and are currently defining conditions to efficiently generate recombinant fowlpox virus. Experiments are proceeding to subcloning mucin immunogens into the fowlpox virus for expression in mammalian cells. The recombinant viruses will be tested for expression and membrane association of the antigens, and for antigenicity in our CTL systems.

Surface Analysis of Native and Deglycosylated Mucin (19). X-ray photoelectron spectroscopy (XPS) is a surface sensitive analytical technique which measures the binding energy of non-valence electrons in atoms and molecules. The binding energy can be related to the molecular bonding or oxidation state of an element in the outermost layer of a material (<100Å). Thus, XPS is able to identify chemical species present on the surface of a molecule. Quantitative XPS results of C, O and N for various mucin related materials have been determined (Table 1 in ref. 17). Briefly, amino acids and proteins are comprised of 40-60 atom percent of carbon, 15-20 atom percent nitrogen (except for arginine which is 36 atom percent nitrogen), and 20-40 atom percent oxygen. Since the hydrogen 1s electrons appear in valence electron bonds, it is nearly impossible to determine its energy and intensity except in very simple systems, such as metal hydrides. Therefore, quantitative results do not include hydrogen.

One of the goals of the proposed research is to correlate the amount of carbohydrate coating (e.g., thickness) with immunological response for human mucin. By examining the XPS O 1s spectra of glycosylated and deglycosylated mucin, it was found that this surface technique can distinguish the carbohydrate coating from the mucin core protein. A representative scan of carbohydrate oxygen taken from a powdered mixture of Glc_{10}-Gal_{10}-GalNAc (to mimic the coating of human milk fat globule mucin) showed two major oxygen peaks observed in each of the oxygen scans, one at a binding energy of 532.2 eV and the other at 531.4 eV (Table 2 & Fig. 5 in ref. 17). The first peak is characteristic of O atoms of the carbohydrate coating and the latter is characteristic of the O atoms of the protein amide bond.

XPS examination of fully glycosylated and partially deglycosylated porcine mucin showed an increase in the N 1s photoelectron peak on the deglycosylated mucin relative to the native molecule. Since the XPS technique is surface sensitive, this increase would be expected if the C- and O-rich carbohydrate coating of the core protein is decreased, thus exposing the N-rich core protein. Similar XPS N 1s and O 1s spectra were obtained with

bovine submaxillary gland mucin. An estimate of the coating thickness on each mucin can be made, if one assumes that the carbohydrate coating is uniformly covering the protein. Using a mean free path of 2 nm for a 950 eV photoelectron, coating thicknesses of 3 and 1.4 nm for the glycosylated and deglycosylated bovine mucin and 1.5 and 0.5 nm for the porcine mucin were calculated. Deglycosylation exposes more of the nitrogen in the core protein of the bovine and porcine mucins. The data also suggests that not all the coating has been removed, since one might expect the N atomic concentration of the core protein to be > 15 %, based on the analyses of single amino acids and amino acid compositions prepared to mimic the mtr. (This observation is confirmed in the paper by Gerken et al. [18]). Work is in progress to determine the thickness of native and deglycosylated human breast milk mucin.

Structural Characterization. Initial NMR experiments have begun to confirm the conformation of the native MUC1-mtr$_1$ peptide and the ($T^3 \rightarrow N^3$)MUC1-mtr$_1$ peptide immunogen described above. NMR and mass spectroscopy have also been used effectiviely to assay the purity and level of derivitization of the synthetic peptide samples used in the immunological studies.

Extracellular Regulation of Lymphoid Cell Activity. A greater understanding of the regulation of CTL may enhance our understanding of how to better develop and expand tumor-specific CTL. We have obtained novel evidence suggesting that lymphoid cells are regulated by extracellular ATP (19-21). The mechanism by which CTL and NK cells are regulated is presently unknown, but our reports suggest that antigen recognition by CTL is dependent on the hydrolysis of extracellular ATP by the ectoATPase expressed by these cells.

Conclusions. We have demonstrated in this first year of the grant that a conservative mutation of a potential glycosylation site in a tumor-specific epitope is effective in eliciting an immunogenic response. This was achieved using synthetic mucin peptides containing the entire 20 amino acid tandem repeat sequence. Also, the immunogen with a mutation in a potential glycosylation site within the tumor-specific monoclonal antibody epitope is equal to, or better than, the native molecule in stimulating tumor-specific CTL derived from PBMC from patients with breast adenocarcinomas. There is oligoclonal expansion of the CTL stimulated with the mucin immunogens, thus demonstrating a limited TCR repertoire that recognizes and responds to the mucin immunogens.

The stimulation of PBMC with synthetic peptides presents several advantages over current methodologies using tumor as the immunogen. First, the use of synthetic peptides ensures that an unlimited supply of the synthetic immunogen can be obtained, whereas use of autologous tumor is limited to only the amount of tumor obtained. Another advantage to this approach is that non-glycosylated immunogenic peptides can be prepared reproducibly. Yet a third advantage of using chemically synthesized mucin immunogens is that lengthy cloning procedures may not be necessary to produce an immunogen for the ex vivo expansion of tumor-specific CTL for the potential adoptive therapy of adenocarcinomas.

The work accomplished in the first year of this grant is on schedule with regard to the specific aims of this grant; namely, the design and construction of potential mucin immunogens. In the following years of this grant the design, construction and characterization of additional mucin immunogens will be pursued. The immunogens will consist of mucins of different lengths and mutations in other potential glycosylation sites. Since it is now apparent that a single MUC1-mtr can elicit a tumor-specific response, it does

not appear necessary to clone this sequence into a mammalian expression vector to study the effect of glycosylation on the structure and immunogenicity of these immunogens. The more direct approach to addressing this aim is the in vitro glycosylation of the synthetic mucin peptides by purified or partially purified glycosyl transferases. In vitro glycosylation will eliminate the variability associated with using mammalian cells transfected with mucin genes for the expression and glycosylation of these immunogens (22). This approach will further define structural features of mucins necessary for its tumor-specific immunogenicity, as well as the role of glycosylation in determining the structure-immunogenicity relationships. Definition of these relationships is for developing reproducible sources of tumor-specific immunogens for use in the adoptive immunotherapy of breast and other adenocarcinomas, and as potential vaccines against this disease.

In developing CTL cell lines, it is important to understand other factors which also may contribute to antigen recognition. Work which we had begun prior to this grant has demonstrated that ectoATPase is important in antigen recognition. It becomes necessary to examine the culture conditions for the presence of extracellular nucleotides. This may have far ranging effects on the immunotherapy of cancers and in maintaining CTL activity.

The second focus of this work is on the structural characterization of our novel immunogens. Although not scheduled for work accomplished until year 2 of this grant, structural characterization (i.e., NMR and surface analysis) has already begun. Thus, the technologies and techniques for efficient characterization of tumor-specific mucin immunogens are well in place.

In conclusion, the work in this grant is proceeding on, or ahead, of schedule. We look forward in the coming years of this work to learning more on the structure-immunogenicity relationships of tumor-specific mucin immunogens and also the action and regulation of tumor-specific CTL as a basis for design of immunotherapies and vaccines.

References.

1. Stevenson, FK (1991) FASEB J. 5, 2250-2257.
2. Rosenberg, SA (1991) Cancer Res. 51, 5074s-5079s.
3. Greenberg, PD & Riddell, SR (1992) J. Natl. Cancer Inst. 84, 1059-1060.
4. Fiddler, IJ (1989) Cytometry 10, 673-680.
5. Kagan, JM & Fahey, JL (1987) J. Am. Med. Assoc. 258, 2988-2992.
6. Barnd, DL, Lan, MS, Metzgar, RS, Finn, OJ (1989) Proc. Natl. Acad. Sci. USA 86, 7159-7163.
7. Ioannides, C, Fisk, B, Jerome, KR, Irimura, T, Wharton, JT, Finn, OJ (1993) J. Immunol. 151, 3693-3703.
8. Rughetti, A, Turchi, V, Ghetti, CA, Scambia, G, Panici, PB, Roncucci, G, Mancuso, S, Frati, L, Nuti, M (1993) Cancer Res. 53, 2457-2459.
9. Sheehan, JK, Thornton, DJ, Somerville, M, Carlstedt, I (1991) Amer. Rev. Resp. Dis. 144, S4-S9.
10. Gendler, SJ, Spicer, AP, Lalani, E-N, Duhig, T, Peat, N, Burchell, J, Pemberton, L, Boshell, M, Taylor-Papadimitriou, J (1991) Amer. Rev. Resp. Dis. 144, S42-S47.
11. Price, MR, Hudecz, R, O'Sullivan, C, Baldwin, RW, Edwards, PM, Tendler, SJB (1990) Molec. Immunol. 27, 795-802.
12. Fontenot, JD, Domenech, N, Bu, D, Tjandra, N, Ho, C, Finn, OJ (1993) J. Cell. Biochem. Suppl. 17D, Abstr. #NZ504, p.125.

13. Scanlon, MJ, Morley, SD, Jackson, DE, Price, MR, Tendler, SJB (1992) Biochem. J. 284, 137-144.
14. Wright, SE, Lowe, KE, Talib, S, Kilinski, L, Dombrowski, KE, Lebkowski, JS, Philip, R (1995) J. Cell Biochem. Suppl. 21A, p. 182, Abstr. #C2-590, appended.
15. Nazerian, K, Dhawale, S, Payne, WS (1989) Avian Diseases 33, 458-465.
16. Nazerian, K, Lee, LF, Yanagida, N, Ogawa, R (1992) J. Virol. 66, 1409-1413.
17. Dombrowksi, KE, Wright, SE, Birkbeck, JC, Moddeman, WE (1995) in Methods in Protein Structure Analysis (Atassi, M.Z. & Appella, E., eds) Plenum, NY, in press, appended.
18. Gerken, TA, Gupta, R, Jentoft, N (1992) Biochemistry 31, 639-648.
19. Dombrowski, KE, Trevillyan, JM, Cone, JC, Lu, Y, Phillips, CA (1993) Biochemistry 32, 6515-6522.
20. Dombrowski, KE, Trevillyan, JM, Cone, JC, Lu, Y, Phillips, CA (1993) J. Immunol. 150, 208A, appended.
21. Dombrowski, KE, Ke, Y, Thompson, LF, Kapp, JA (1995) J. Immunol. 154, 6227-6237, appended.
22. Jerome, K, Bu, D, Finn, OJ (1992) Cancer Res. 52, 5985-5990.

Appendix.

Immunogenic Structural Features of a Breast Tumor-specific Epitope for Cancer Immunotherapy

Grant No: DMAD17-94-J-4272

The following appended publications, presentations and patent application have resulted from funding from the Department of the Army:

Publications:

1. Dombrowski, K.E., Wright, S.E., Birkbeck, J.C. & Moddeman, W.E. (1994) *X-ray Photoelectron Spectroscopy of Amino Acids, Polypeptides and Simple Carbohydrates* in Methods in Protein Structure Analysis (Atassi, M.Z. & Appella, E., eds) Plenum, NY, in press.

2. Dombrowski, K.E., Cone, J.C, Bjorndahl, J.M. & Phillips, C.A. (1994) *Irreversible Inhibition of Human Natural Killer Cell Natural Cytotoxicity by Modification of the Extracellular Membrane by the Adenine Nucleotide Analogue 5'-p-(Fluorosulfonyl)benzoyl Adenosine.* Cell. Immunol., 160, 199-204.

3. Dombrowski, KE, Ke,Y, Thompson, LF, and Kapp, JA (1995) *Antigen Recognition by CTL is Dependent upon EctoATPase Activity,* J. Immunol. 154, 6227-6237.

Abstracts published:

1. Wright, S.E., Lowe, K.E., Talib, S., Kilinski, L., Dombrowski, K.E., Lebkowski, J.S. & Philip, R. (1995) *Antigen-specific Cytotoxic T-lymphocyte (CTL) Response Induced by Tumor-specific Mucin Peptide in Breast Cancer.* J. Cell. Biochem. Suppl. 21A, p. 182, Abstr. #C2-590. (Poster presentation)

2. Dombrowski, K.E., Wright, S.E., Birkbeck, J.C. & Moddeman, W.E. (1995) *Surface analysis of proteins and related molecules by x-ray photoelectron spectroscopy.* Prot. Sci. 4, Suppl. 2, 161, Abstr. #567-M. (Poster presentation)

Presentations:

1. Dombrowski, K.E., Moddeman, W.E., Wright, S.E. (1994) *X-ray Photoelectron Spectroscopy of Human Mucin Proteins and Tandem Repeat Peptides.* 10th International Conference on Methods in Protein Structure Analysis, Snowbird, Utah, Sept. 8-13.

Patent Applications:

1. Invention disclosure: *Non-destructive Analysis of Proteins Bound to a Solid Support by X-ray Photoelectron Spectroscopy.* KE Dombrowski & WE Moddeman, inventors. (not appended)

preprint: in Methods in Protein Structure Analysis (Atassi, M.Z and Appella, E., eds) Plenum Press, NY, in press.

X-ray Photoelectron Spectroscopy of Amino Acids, Polypeptides and Simple Carbohydrates

Kenneth E. Dombrowski, Stephen E. Wright

Department of Veterans Affairs Medical Center and Department of Internal Medicine, Texas Tech University Health Sciences Center

Amarillo, TX 79106

Jannine C. Birkbeck, William E. Moddeman

Mason & Hanger-Silas Mason Co., Inc., Pantex Plant Amarillo, TX 79177

ABSTRACT

X-ray photoelectron spectroscopy (XPS) is a surface sensitive analytical technique which measures the binding energy of electrons in atoms and molecules. The binding energy can be related to the molecular bonding or oxidation state of an element in the outermost layer of a material, that is < 100 Å. Thus, XPS is able to identify chemical species present on the surface of a molecule. In this paper XPS is briefly described. Spectra demonstrating its potential use for probing the surface properties of amino acids, polypeptides, proteins, carbohydrates and glycoproteins are discussed.

INTRODUCTION

XPS has also been referred to as electron spectroscopy for chemical analysis (ESCA). The basis for XPS is the photoelectric effect (1). Irradiation of a material with monochromatic x-rays results in the expulsion of photoelectrons from electron orbitals (e.g., s-orbitals) of the

sample. The energy of an incident x-ray is transformed into the kinetic energy of a photo-emitted electron (Figure 1). By measuring the kinetic energy (E_k) of the ejected photoelectron and known x-ray photon energy ($h\nu$), the binding energy (E_b) of that electron can be deduced using the following equation:

$$E_b = h\nu - E_k - w$$

where w is the experimentally determined work function of the spectrometer.

XPS generates its information from two modes of analyses: low resolution, or survey, spectra and high resolution spectra. Qualitative information is normally obtained and atomic composition can be obtained from a survey spectrum of the sample surface. Detailed chemical bonding information (e.g., oxidation state) is acquired from high resolution scans on each element.

The binding energy of electrons in an element is unique to the element as well as unique to its chemical environment. E_b can change several eV due to changes in oxidation state. When examining inner-shell electrons, the binding energies of these electrons in any element, X, can be directly related to the oxidation state of that element in a molecule in the following progression: $X^- < X^{\delta-} < X^0 < X^{\delta+} < X^+$; i.e., the larger the positive charge on the element, the greater the affinity of the nucleus for the remaining electrons, and hence, the larger the E_b.

XPS has routinely been used to examine the chemical structure of various organic and inorganic materials (2). In an article on the microencapsulation of an explosive, which contains the elements of carbon, nitrogen and oxygen (similar to the biological compounds to be discussed), equations were written that allowed for the determination of the thickness of the coating and the mechanism of polymer bonding to the explosive (3).

XPS has not been extensively used in the study of biological systems. A few XPS papers have been published which examined the role of metals in biological systems. Chiu et al. (4) studied the bonding of oxygen to selenium in a glutathione peroxidase model system, Meisenheimer et al. (5) determined monovalent cation compositions in erythrocyte membranes, and Pickart et al. (6) studied Ca^{2+} flux in hepatoma cells during DNA synthesis. In the latter study, an intramembrane Ca^{2+} gradient was established with the highest levels of Ca^{2+} being at the cytoplasmic side and not towards the extracellular space. A few studies have been published that have made use of XPS for the characterization of surfaces of bacterial cells (7), and for estimating the protein content in seeds (8).

Only a few XPS studies have been performed to study in detail the surface chemistries of biological macromolecules such as proteins (9-11). These papers showed the zwitterionic nitrogen to be in a less positive state following amide formation. In this paper, low and high resolution XPS spectra for several amino acids related to the core protein of a glycoprotein are reported. These results show the potential usefulness of this technique in characterizing carbohydrate coatings on polypeptides and proteins.

EXPERIMENTATION

Samples are applied to a 25 mm^2 Au metal surface as a monolayer in one of the following methods: 1) as a powder, 2) as a solution in water (doubly distilled), 3) as a slurry in methanol, or 4) as a slurry in a mixture of water and methanol. In the latter cases, the solvents were allowed to evaporate before being placed in the analysis chamber.
The instrument used in this study was a Kratos AXIS spectrometer which uses a hemispherical electrostatic analyzer to determine electron kinetic energies. Following sample

introduction, the chamber was evacuated to $< 10^{-7}$ torr. The x-ray source was an aluminum monochromator that emits an x-ray beam of 1486.67 eV. The x-ray power was 300 watts (20 mA and 15 kV). During the photoelectron process, the surface acquires a positive charge. In order to minimize sample decomposition and charging, the sample was bathed in low energy electrons of about 1 eV by a charge neutralizer. In this work, copious amounts of electrons were generated by the neutralizer which were sufficient to minimize differential sample charging. Samples were irradiated until sufficient data were collected. The amount of x-ray degradation previously determined on glycine was found to be $< 1\%$ over two hours of irradiation. No detectable x-ray damage was noted on the samples analyzed in this paper. Data collection required about 90 min per sample.

XPS spectra were deconvoluted to a best fit using peak shapes of 70 % Gaussian and 30 % Lawrencian character to account for tailing toward the high E_b side. Atomic % compositions of each elemental species present were calculated by dividing the area under each XPS elemental peak by an instrumental sensitivity factor. The sensitivity factors were theoretically calculated (12) from photoionization cross-sectional data. It is very difficult for the XPS technique to quantify hydrogen since the H 1s electron is part of the valence level. These valence electrons are often associated with, or shared between, two or more elements and thus can not be easily be used for elemental quantification. Therefore, hydrogen is not included in the atomic % determinations.

RESULTS AND DISCUSSION

As discussed earlier, XPS data are often accumulated in two ways: either low resolution or high resolution. In the first case, the electron binding energies of a protein or

peptide are measured to approximately ± 1 eV. From this determination, qualitative and semi-quantitative information about the protein surface is acquired. That is, the elemental constituents are determined and the atomic % composition is calculated. In the second case, E_b are determined to within ± 0.1 eV. In our work, E_b are determined to < 0.1 eV. From these measurements, the electron distributions about each atom (or the charge distributions) in the molecule are determined, and oxidation state and chemical bonding information are inferred.

Low Resolution Spectra

Figure 2 illustrates a survey scan for the simple amino acid glycine. The spectrum shows the three major constituents found in most amino acids: C at 285 eV, N at 401 eV and O at 531 eV. After correcting for differences in sensitivity factors, the area under each photoelectron peak is proportional to the atomic concentration. For this amino acid, the experimentally determined composition (in atomic %) from the survey scan is 42 % C, 20 % N and 38% O. These values are in good agreement with the theoretically calculated atomic compositions of 40% C, 20% N and 40% O.

The atomic concentrations obtained from the XPS spectra of the nine different amino acids found in the human mucin tandem repeat sequence MUC1 (12, 13) are given in Table 1. MUC1 is a 20 amino acid polypeptide with the sequence GSTAPPAHGVTSAPDTRPAP. An amino acid mixture with the composition of $G_2S_2T_3A_4P_5HVDR$ corresponding to the MUC1 peptide was prepared and analyzed by XPS. Again, good agreement between experiment and theoretical values was noted. These amino acids have a range of carbon from 43% for Gly to 64% for Val. The nitrogen composition is much lower: from 12% for Asp

to 32% for Arg. The usual range for % N in proteins is about 15 to 20%. The % atomic composition of oxygen varies much like that of nitrogen. Ranges for this element are from 16% in Arg to 41% in Ser.

The full range of sensitivity of this technique for identifying specific amino acid substitutions in simple polypeptides and proteins is not fully established. Using a human mucin MUC1 tandem repeat peptide, we have preliminary evidence suggesting that XPS is capable of easily identifying a point mutation in a mutant peptide containing the $T^{16} \rightarrow N^{16}$ mutation. This mutant peptide represents a 20% decrease in the number of hydroxyl groups present on this peptide.

A survey of carbohydrate structures found in human mucins (13, 14) is beginning to reveal some similarities and differences between protein and carbohydrate in an XPS spectrum (Table 2). Carbohydrates are not too dissimilar from amino acids in carbon content (~ 55 % C in carbohydrates as compared to ~ 50% in amino acids). The % O is slightly higher in carbohydrates (~ 45-49 % O) than in protein (~ 35 % O). However, the major difference between amino acids and carbohydrates is their nitrogen content. In human mucins, an average of about 3 atomic % nitrogen can be observed in samples representing normal mucin oligosaccharide side chains to 0.3 atomic % N in the oligosaccharide side chains of breast cancer-associated mucin (13, 14).

The atomic % of nitrogen in carbohydrates are clearly distinguishable from the nitrogen composition of protein. For example, fully glycosylated porcine mucin showed a composition of 77 % C, 4.9 % N and 18 % O (Table 2). The measured composition of periodate-oxidized porcine mucin (Table 2) showed a decrease in the atomic % of carbon and an increase in the atomic % of both nitrogen and oxygen. This indicates that the mucin core

protein is being exposed by the removal of carbohydrate during periodate oxidation. Since the core protein of a related porcine mucin has a theoretical composition of 51% C, 16 % N and 33 % O (16), it can be concluded that the periodate treatment did not fully deglycosylate this mucin and that it still bears a high degree of oligosaccharide side chains branched on the GalNAc-O-Thr which are not susceptible to periodate oxidation (15). Similar to the porcine mucin, bovine mucin showed an increase in atomic % N content from 3.2% to 9.7% after periodate treatment. Again, indicating that bovine mucin is not fully susceptible to periodate oxidation to remove oligosaccharide side chains.

High Resolution Spectra

Figures 3 through 5 illustrate the XPS high resolution C 1s, N 1s and O 1s spectra, respectively, of one amino acid (glycine), one polypeptide (polyglycine with average M_r ~ 4,500) and one carbohydrate (glucose). The analyses of these data are given in Table 3. As can be seen from the data (also see Fig. 3a), glycine has two types of carbon atoms: one methylene and one carboxylate. (A small third carbon peak is also found to be present. Almost all materials contain a carboneous contaminant that is sometimes referred to as ubiquitous, or residual, carbon. The source is often not readily identifiable. The C 1s electrons from this carbon source is often found at an E_b of ~ 285 eV and has not been assigned to any specific carbon species of the amino acid.) The higher binding energy peak at 288.38 $\pm$ 0.07 eV corresponds to the carbon atom of the carboxylate group with the methylene carbon appearing at a lower binding energy of 286. 19 $\pm$ 0.07 eV. This is consistent with the molecular bonding and the electron charge distribution where the carbon of the carboxylate is at a higher positive oxidation state than the methylene carbon. Also, the

intensities of the peaks are in about a 1:1 ratio, consistent with their abundance in this amino acid. Fig. 3B illustrates the C 1s data from polyglycine. Again, two peaks are seen which are due to the amide carbon at 288.42 ± 0.07 eV. The glucose C 1s spectrum (Fig. 3c) is completely different from either of the above two glycine compounds. This carbohydrate contains two carbon atoms in different chemical environments: one at 286.60 eV characteristic of an alcohol and the other at 287.94 eV, characteristic of the anomeric carbon. Thus, the E_b's are distinguishable between the different oxidation states of each carbon species (i.e., a carboxylate of a zwitterion is identifiable from an anomeric carbon, or an alcohol or from aliphatic carbons). The binding energy data reported above is referenced to the C 1s level of the two methyl groups on Leu which was set at 285.00 eV.

Fig. 4 exhibits the high resolution N 1s spectra of glycine, polyglycine and glucose. A single N 1s peak is observed in both the glycine (Fig. 4a) and polyglycine (Fig. 4b) spectra, but no nitrogen is observed in the glucose spectrum (Fig. 4c). The N 1s peaks appear at different positions in the first two spectra: the nitrogen atoms in the zwitterionic form of glycine are observed at E_b = 401.45 ± 0.05 eV which is characteristic of nitrogen in a +1 oxidation state and the amide nitrogen at E_b = 400.19 ± 0.05 eV where nitrogen has a lone pair of electrons. These nitrogen results are similar to those reported previously (8-10).

Glycine has two oxygen atoms. However, these electrons are equivalent due to the resonance structures of the carboxylate anion of the acid. Fig. 5a depicts a single O 1s peak with a binding energy of 531.15 ± 0.06 eV. Upon polymerization to form the peptide, again, only one O 1s peak is observed (Fig. 5b), but the binding energy is increased to 531.78 ± 0.06 eV. The carbohydrate O 1s spectrum show a broad peak that has been deconvoluted into two structures: the primary one at 532.88 ± 0.04 eV and a smaller one

with approximately one-fifth the area at 533.62 ± 0.07 eV. These two peaks are characteristic of oxygen atoms of the alcohol and pyranose ring environments, respectively.

SUMMARY

XPS is a surface sensitive technique capable of distinguishing between core protein and carbohydrate coatings on glycoproteins. Deglycosylation of periodate-oxidized porcine and bovine mucin were not complete. There is a difference in the composition between coatings of normal and breast cancer-associated oligosaccharide side chains. Further examination of XPS in terms of its sensitivities for sample amount and limits of detection is an exciting area of protein structure analysis.

ACKNOWLEDGEMENTS

This work was supported in part from the following sources: the Elsa U. Pardee Foundation (K. E. D. & S. E. W.), Department of the Army Grant #DAMD17-94-J-4272 (K. E. D. & S. E. W.), Department of the Army Career Development Award #DAMD17-94-J-4161 (K. E. D.), Department of Veterans Affairs Medical Research Funds (S. E. W.) and Department of Energy contract #DE-AC04-91AL-65030 (W. E. M.) Content of the information herein does not necessarily reflect the position of the policy of the U. S. government, and no official endoresement should be inferred.

REFERENCES

1 Carlson, T. A., 1975 in Photoelectron and Auger spectroscopy, Plenum Press, NY.

2 Robinson, J. W., 1991 in Practical Handbook of Spectroscopy, CRC Press, Boca Raton,

FL.

3 Worley, C. M., Vannet, M. D., Ball, G. L. and Moddeman, W. E., 1987 Surface chemistry of a microcoated energetic material, pentaerythritoltetranitrate (PETN). Surface and Interface Analysis, 10:273.

4 Chiu, D., Tappel, A.L. and Millard, M.M., 1977 Improved procedure for x-ray photoelectron spectroscopy of selenium-glutathione peroxidase and application to the rat liver enzyme. Arch. Biochem. Biophys. 184:209.

5 Meisenheimer, R. G., Fisher, J. W. and Rehfeld, S. J., 1976 Thallium in human erythrocyte membranes: an x-ray photoelectron spectroscopy study. Biochem. Biophys. Res. Commun. 68, 994.

6 Pickart, L., Millard, M. M., Beiderman, B. and Thaler, M. M., 1978 Surface analysis and depth profiles of calcium in hepatoma cells during pyruvate-induced synthesis. Biochim. Biophys. Acta, 544:138.

7 Millard, M. M., Scherrer, R. and Thomas, R. S. 1976 Surface analysis and depth profile composition of bacterial cells by x-ray photoelectron spectroscopy and oxygen plasma etching. Biochem. Biophys. Res. Commun. 72:1209.

8 Peeling, J., Clark, D. T., Evans, M. and Boulter, D. 1976 Evaluation of the ESCA technique as a screening method for the estimation of protein content and quality in seed meals. J. Sci. Fd. Agric. 27:331.

9 Sigbahn, K., Mordling, C., Fahlman, A., Mordbert, R., Hedman, J., Johnsson, G., Bergmark, T., Karlsson, S. E., Lindgren, I. and Linberg, B., 1967 ESCA-Atomic, Molecular, and Solid State Structure Studied by Means of Electron spectroscopy, Nova Acta Regiae Soc. Sci. Upsaliensis Ser. IV Vol. 20.

10 Bumben, K. D. and Dev, S. B. 1988 Investigation of poly(L-amino acids) by x-ray photoelectron spectroscopy. Anal. Chem. 60:1393.

11 Clark, D. T., Peeling, J. and Colling, L., 1976 An experimental and theoretical investigation of the core level spectra of a series of amino acids, dipeptides and polypeptides. Biochim. Biophys. Acta 453:533.

12 Scofield, J. H., 1973 in Theoretical cross-sections from 1-1500 KeV, Lawrence Livermore Laboratory Report UCRL-51326.

13 Gendler, S. J., Spicer, A. P., Lalani, E. -N, Duhig, T., Peat, N., Burchell, J., Pemberton, L., Boshell, M. and Taylor-Papadimitriou, J., 1991 Structure and biology of a carcinoma-associated mucin, MUC1. Amer. Rev. Resp. Dis. 144:S42.

14 Hanisch, F. -G., Uhlenbruck, G., Peter-Katalinic, J., Egge, H., Dabrowski, J. and Dabrowski, U., 1989 Structures of neutral O-linked polylactosaminoglycans on human skim milk mucins. J. Biol. Chem. 264:872.

15 Gerken, T. A., Gupta, R and Jentoft, N., 1992 A novel approach for chemically deglycosylating O-linked glycoproteins. The deglycosylation of submaxillary and respiratory mucins. Biochemistry 31:639.

16 Gupta, R and Jentoft, N., 1989 Subunit structure of porcine submaxillary mucin. Biochemistry 28:6114.

@Figure = Fig. 1. Schematic representation of the XPS process.

@Figure = Fig. 2. Representative low resolution XPS spectrum of glycine showing the presence of carbon, nitrogen and oxygen characteristic of amino acids.

@Figure = Fig. 3. High resolution XPS C 1s spectra of (a) glycine, (b) polyglycine and (c) glucose showing unique patterns for the different carbon atoms in each compound. Jagged curves are the raw data and the smooth curves are the best fit approximations as described in the text.

@Figure = Figure 4. High resolution XPS N 1s spectra of (a) glycine, (b) polyglycine and (c) glucose showing nitrogen binding energy differences between zwitterion and amide structures. The data also shows the absence of nitrogen in the carbohydrate glucose. Jagged curves are the raw data and the smooth curves are the best fit approximations.

@Figure = Figure 5. High resolution XPS O 1s spectra of (a) glycine, (b) polyglycine and (c) glucose showing oxygen binding energy differences between carboxylate, amide and carbohydrate (alcohol). Jagged curves are the raw data and the smooth curves are the best fit approximations.

Table 1. Summary of Quantitative XPS Results on Mucin-Related Materials

Material	Atomic % Compositions		
	%C	%N	%O
Ala	52[1] (50)[2]	17 (17)	32(33)
Arg	53 (50)	32 (36)	16 (17)
Asp	46 (44)	12 (11)	40 (44)
Gly	43 (40)	21 (20)	36 (40)
His	52 (50)	17 (17)	32 (33)
Pro	63 (62)	17 (16)	30 (31)
Ser	45 (43)	14 (14)	41 (43)
Thr	53 (50)	13 (12)	37 (38)
Val	64 (62)	13 (12)	23 (31)
MUC1 peptide [3]	52 (53)	17 (16)	30 (31)

[1] Values given are the experimentally determined atomic % composition for each element in the corresponding amino acid. [2] Values in parentheses are the theoretically derived atomic % compositions for each element in the corresponding amino acid. [3] Amino acids present in the MUC1 peptide were combined in the molar ratios of $G_2S_2T_3A_4P_5HVDR$.

Table 2. Summary of Quantitative XPS Results on Mucins and Related Materials

Material	Atomic % Compositions[1]		
	%C	%N	%O
Carbohydrate, normal [2]	55 (50)	0.3 (0.4)	45 (49)
Carbohydrate, cancer [3]	55 (52)	3.4 (3.6)	42 (44)
Porcine mucin [4]	77	4.9	18
Porcine mucin, partially deglycosylated [5]	65	8.5	27
Bovine mucin [4]	72	3.2	25
Bovine mucin, partially deglycosylated [5]	67	9.7	28

[1] Values given are the experimentally determined atomic % composition for each element in the corresponding amino acid. Values in parentheses are the theoretically derived atomic % compositions for each element in the corresponding amino acid. [2] Carbohydrates common to normal mucins (13, 14) were combined in the molar ratios of $Gal_{12}GlcNAc_{11}GalNAc_1$ where Gal = galactose, GlcNAc = N-acetylglucosamine and GalNAc = N-acetylgalactosamine. [3] Carbohydrate common to cancer-associated mucins (13) were combined in the molar ratios of $NANA_1Gal_1GalNAc_1$, where NANA = N-acetylneuraminic acid. [4] Mucins (from porcine stomach and bovine submaxillary gland) were purchased from Sigma Chemical Co (St. Louis, MO) [5] Mucins were partially deglycosylated by periodate oxidation (15).

Table 3. Summary of Binding Energies for Glycine, Polyglycine and Glucose: High Resolution Data.

		E_b, eV		
		Glycine (12 runs)	Polyglycine (8 runs)	Glucose (4 runs)
C 1s				
	α-C	286.19 ± 0.07	286.42 ± 0.07	
	carboxylate	288.38 ± 0.07		
	amide		288.42 ± 0.07	
	alcohol			286.60 ± 0.03
	anomeric			287.94 ± 0.05
N 1s				
	zwitterion	401.45 ± 0.05		
	amide		400.19 ± 0.05	
O 1s				
	carboxylate	531.15 ± 0.06		
	amide		531.78 ± 0.06	
	alcohol			532.88 ± 0.04
	pyranose ring			533.62 ± 0.07

E_b given are the average energies of the indicated number of runs ± the standard deviation.

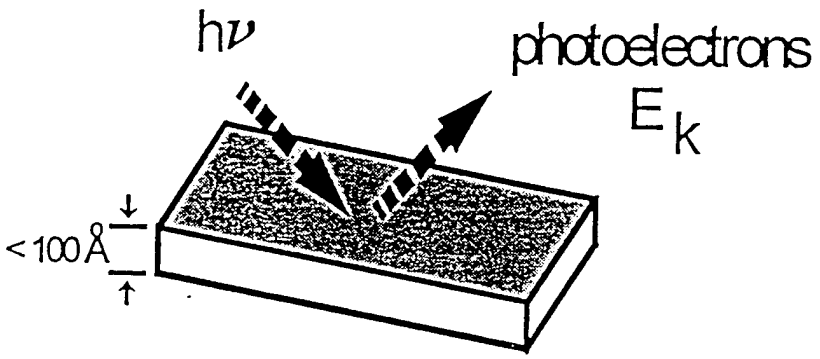

$$E_b = h\nu - E_k - w$$

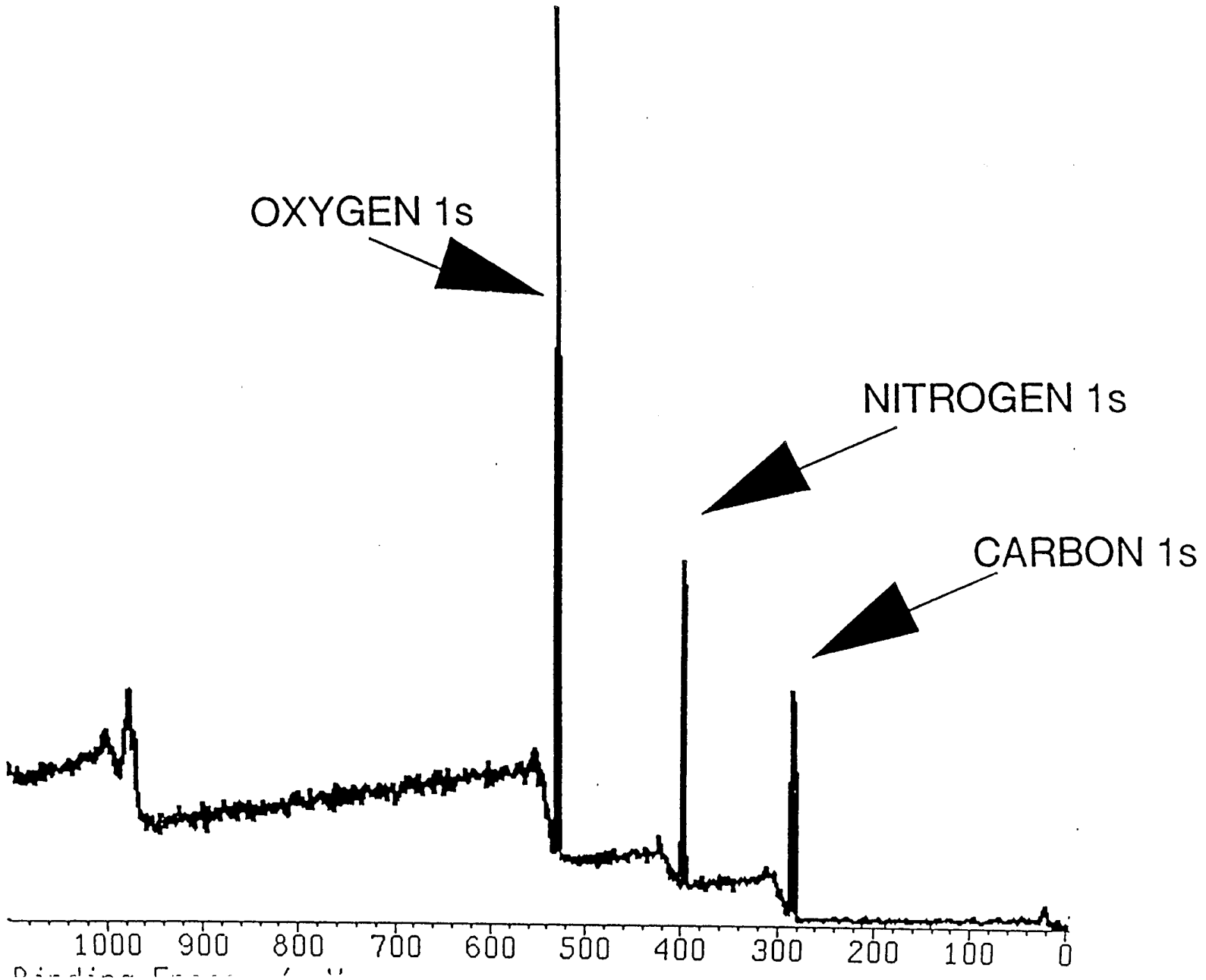
OXYGEN 1s
NITROGEN 1s
CARBON 1s
1000
900
800
700
600
500
400
300
200
100
0

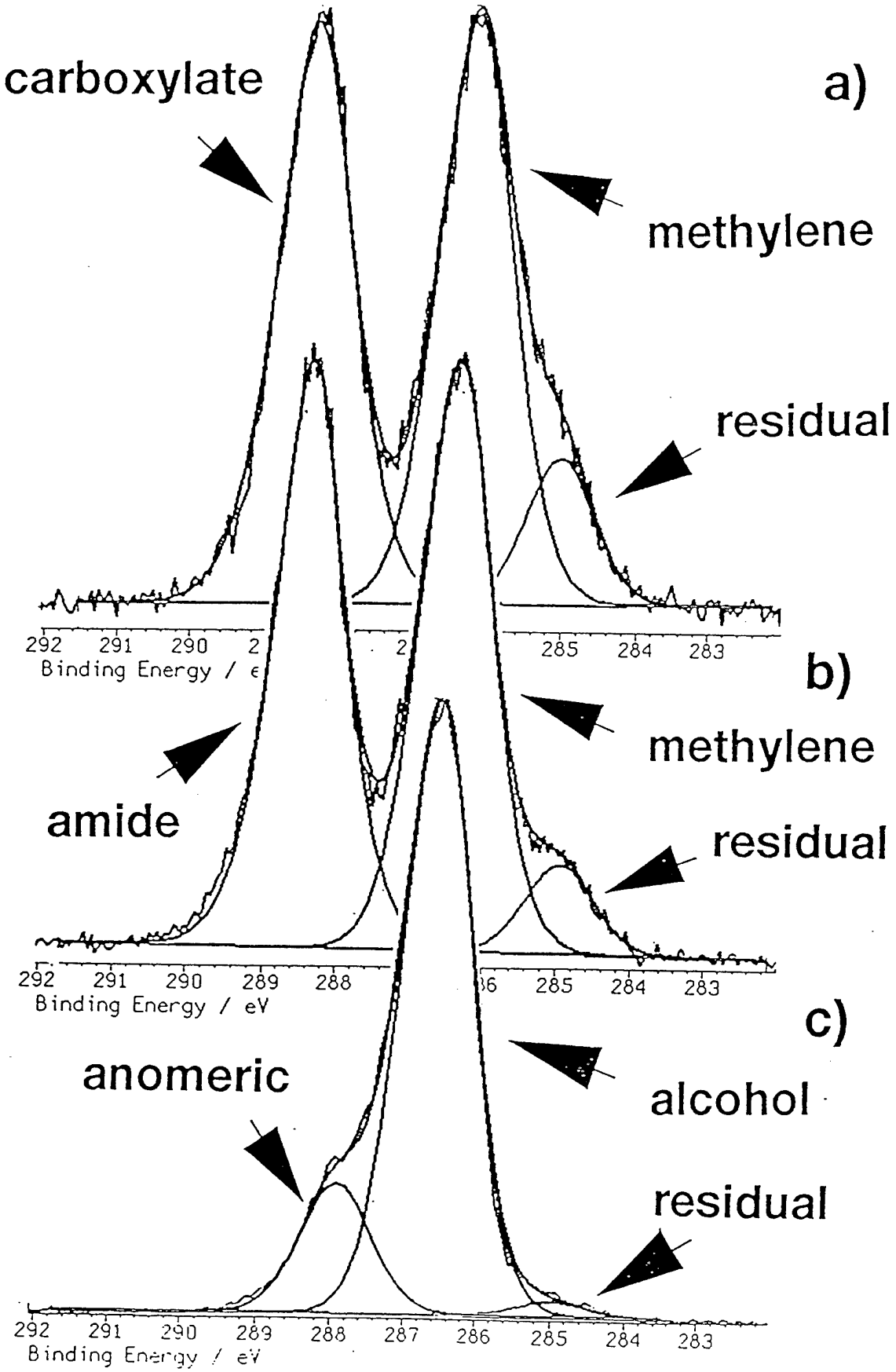
carboxylate
a)
methylene
residual
292 291 290
Binding Energy / e
285 284 283
b)
amide
methylene
residual
292 291 290 289 288
Binding Energy / eV
285 284 283
c)
anomeric
alcohol
residual
292 291 290 289 288 287 286 285 284 283
Binding Energy / eV

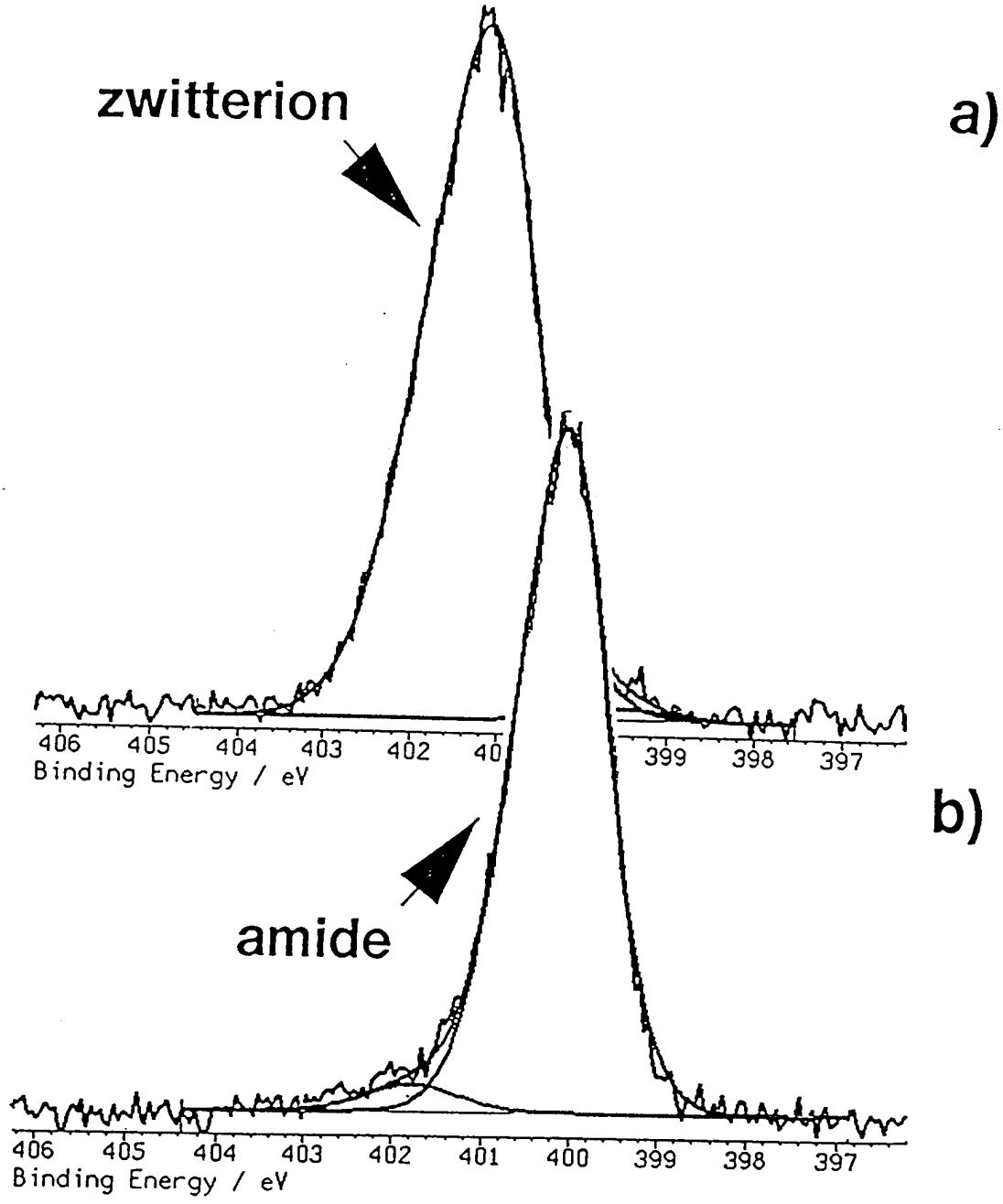
zwitterion
a)
406 405 404 403 402 40
399 398 397
Binding Energy / eV
b)
amide
406 405 404 403 402 401 400 399 398 397
Binding Energy / eV
c)
406 405 404 403 402 401 400 399 398 397
Binding Energy / eV

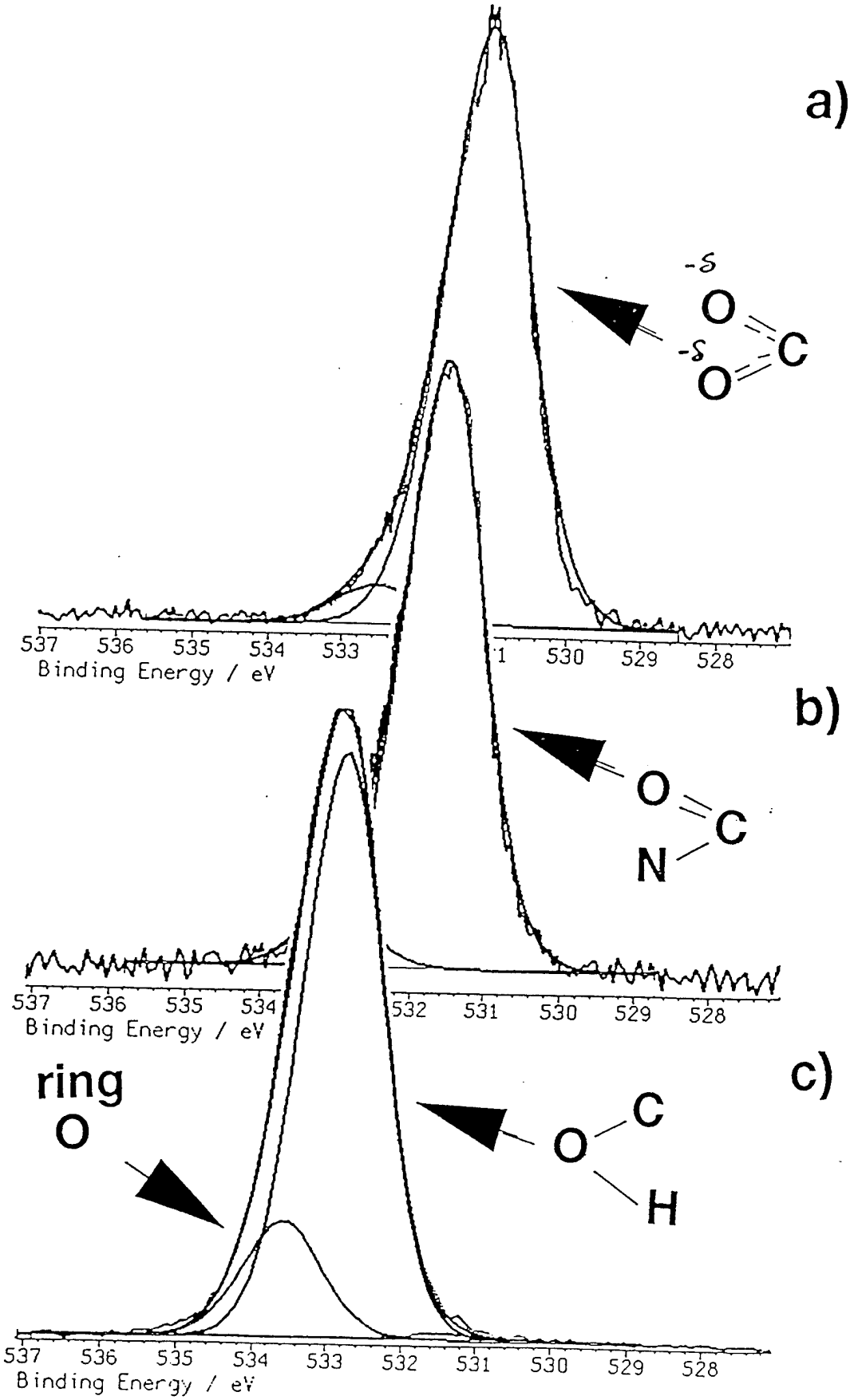
a)
-δ
O
C
-δ
O
537 536 535 534 533
1 530 529 528
Binding Energy / eV
b)
O
C
N
537 536 535 534
532 531 530 529 528
Binding Energy / eV
c)
ring
O
O
C
H
537 536 535 534 533 532 531 530 529 528
Binding Energy / eV

CELLULAR IMMUNOLOGY **160,** 199–204 (1995)

Irreversible Inhibition of Human Natural Killer Cell Natural Cytotoxicity by Modification of the Extracellular Membrane by the Adenine Nucleotide Analog 5′-*p*-(Fluorosulfonyl)benzoyl Adenosine[1,2]

KENNETH E. DOMBROWSKI,*,†,[3] J. CATHERINE CONE,*,[4] JAY M. BJORNDAHL,†,‡ AND CATHERINE A. PHILLIPS*,†

Department of Veterans Affairs Medical Center, Amarillo, Texas 79106; †Department of Internal Medicine, Texas Tech University Health Sciences Center, Amarillo, Texas 79106; and ‡Harrington Cancer Center, Amarillo, Texas 79106

Received March 15, 1994; accepted October 24, 1994

Extracellular adenine nucleotides are inhibitors of the human natural killer cell line NK3.3 natural cytotoxicity activity. Natural cytotoxicity was inhibited approximately 26% by 1 m*M* ATP and 21% by 1 m*M* ADP. 5′-Adenylyl imidodiphosphate, a nonhydrolyzable ATP analog, inhibited natural cytotoxicity by 41% at a concentration of 1 m*M* and >97% at a concentration of 10 m*M*. In contrast, AMP was not inhibitory. Adenosine was a weak inhibitor of natural cytotoxicity and may represent an alternate regulatory pathway. Removal of the nucleotides resulted in the restoration of control levels of natural cytotoxicity activity. The affinity label 5′-*p*-(fluorosulfonyl)benzoyladenosine (5′-FSBA) is a synthetic analog of ATP or ADP containing an electrophilic fluorosulfonyl group capable of covalently modifying proteins at adenine di- and triphosphate nucleotide-binding sites. Natural cytotoxicity was irreversibly inhibited by modification of the extracellular membrane of NK3.3 cells by 5′-FSBA. This inhibition was concentration dependent with an I_{50} ~100 μ*M* and complete inhibition at 1 m*M*. Modification of NK3.3 by 5′-FSBA did not affect the formation of effector–target cell conjugates; however, granule release was inhibited. This targets the site of inhibition by 5′-FSBA modification to a pathway preceding granule release. Irreversible, covalent modification of surface adenine nucleotide-binding proteins by 5′-FSBA provides a probe to study the role of specific adenine nucleotide-binding proteins in the extracellular regulation of natural killer cytolytic activity by adenine nucleotides.

INTRODUCTION

Natural killer (NK)[5] cells are LGL which spontaneously kill susceptible target cells in a non-major histocompatibility complex-restricted manner and without prior sensitization (3). Lysis of target cells is mediated by two mechanisms: natural cytotoxicity and antibody-dependent cellular cytotoxicity (3, 4). Cytolytic activity proceeds through three general steps: target cell recognition, programming for lysis, and granule release (4). The intracellular and extracellular regulation of these processes has not been fully elucidated.

Natural cytotoxicity of nonstimulated, peripheral blood LGL was shown to be inhibited by extracellular nucleotides in micromolar concentrations (5, 6). However, cell populations used in these investigations were not pure, thus leading to questions concerning whether the cytolytic activity observed was in fact due to NK cells. Recently, freshly isolated and characterized, nonstimulated, peripheral blood NK cells were shown to be

[1] This work was supported in part by funding from the Texas Tech University Health Sciences Center seed grant program (K.E.D., C.A.P.), the Amarillo Area Foundation (C.A.P.), the Department of Veterans Affairs (C.A.P., James M. Trevillyan, and Stephen E. Wright), the Elsa U. Pardee Foundation (K.E.D. and Stephen E. Wright), Department of the Army Career Development Award Grant DAMD17-94-J-4161 (K.E.D.), and Department of the Army Grant DAMD17-94-J-4272 (K.E.D. and Stephen E. Wright). Content of the information herein does not necessarily reflect the position or the policy of the U.S. government, and no official endorsement should be inferred.

[2] Parts of this work have been presented in preliminary form at the Eighth Natural Killer Cell Workshop and the First Meeting of The Society for Natural Immunity, St. Petersburg, FL, October 4–6, 1992 (1), the Tenth Texas Immunology Conference, Richardson, TX, November 13–15, 1992, and the annual meeting of the American Association of Immunologists, Denver, CO, May 21–25, 1993 (2).

[3] To whom correspondence should be addressed at the Department of Internal Medicine, Texas Tech University Health Sciences Center, 1400 Wallace Blvd., Amarillo, TX 79106. Fax: (806) 354-5549.

[4] Current address: Department of Medicine, Division of Hematology/Oncology (Slot 508), University of Arkansas for Medical Sciences, Little Rock, AR 72205.

[5] Abbreviations used: NK cell, natural killer cell; LGL, large granular lymphocyte; IL-2, interleukin 2; DMF, *N,N*-dimethylformamide; 5′-FSBA, [*p*-(fluorosulfonyl)benzoyl]-5′-adenosine; AMPPNP, 5′-adenylyl imidodiphosphate; FSB, fluorosulfonylbenzoyl; FSB-OMe, fluorosulfonlybenzoic acid methyl ester; PMSF, phenylmethylsulfonyl fluoride; DTNB, dinitrothiobisbenzoic acid; N-CBZ-Lys, *N*-carbobenzoxy-lysine; E:T, effector cell to target cell ratio.

0008-8749/95 $6.00

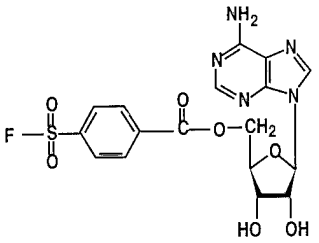

FIG. 1. Structure of 5′-FSBA.

susceptible to inhibition by adenine nucleotides, while IL-2-stimulated NK cells were not inhibited at the same nucleotide levels (7). Here, we present evidence that the cytolytic activity of the human IL-2-dependent NK cell line NK3.3 (8) is inhibited reversibly by low millimolar concentrations of extracellular adenine nucleotides. We also examine the irreversible inhibition of the effect of the cytolytic activity of this cell line by the adenine nucleotide affinity label 5′-FSBA (9) (Fig. 1). 5′-FSBA contains an electrophilic fluorosulfonyl group capable of reacting with nucleophilic amino acids in the ATP or ADP binding pockets of proteins. In an extended conformation, the fluorosulfonyl group may be located in a position equivalent to the β- or γ-phosphoryl groups of ATP or ADP (9). 5′-FSBA has been shown to covalently modify the human NK cell line NK3.3 (10). The use of covalent modifying reagents specific for adenine nucleotide-binding proteins on the surface of NK cells could prove to be a useful technique in elucidating the role of such proteins in the extracellular regulation of NK cell cytolytic activity by permitting the investigator to dissect their respective activity from other cellular responses.

MATERIALS AND METHODS

Materials. Nucleotides were purchased as the disodium salts from Sigma Chemical Company (St. Louis, MO). Sodium [^{51}Cr]chromate was purchased from NEN Research Products (DuPont; Boston, MA). RPMI 1640, penicillin/streptomycin, and L-glutamine were purchased from GIBCO BRL (Gaithersburg, MD). Lymphocult-T, a source of cellular growth factors, was purchased from Biotest Diagnostics (Denville, NJ). K562 and Raji cells were purchased from American Type Culture Collection (Rockville, MD). Calcein and dihydroethidium were purchased from Molecular Probes (Eugene, OR). Rehatuin fetal bovine serum was purchased from Intergen Co. (Purchase, NY). All other chemicals were of reagent grade purity.

Cell culture and maintenance. The NK3.3 cell line (8) was a generous gift from Dr. Jacki Kornbluth (University of Arkansas for Medical Sciences, Little Rock, AR). Cells were maintained in RPMI 1640 medium containing 15% fetal bovine serum and 15% Lymphocult-T as described previously (8, 10). NK3.3 cell cytolytic activity was assayed 16–24 hr after feeding.

Treatment of NK3.3 with extracellular adenosine and adenine nucleotides. To assess the effect of extracellular adenosine and adenine nucleotides on NK3.3 cytolytic activity, these compounds were added directly to the cytotoxicity assays to the final concentrations (either 1 or 10 m*M* as indicated in the figures) without preincubation. Nucleotides were prepared as 100× stock solutions in RPMI 1640, pH 7.2. Alternatively, NK3.3 cells were preincubated in the presence or absence of extracellular adenosine and adenine nucleotides for 1 hr at 37°C in RPMI 1640 without fetal bovine serum at the concentrations indicated above. After the preincubation period, the cells were pelleted, washed, and resuspended in fresh RPMI 1640 containing 10% fetal bovine serum and fresh adenosine or nucleotide at the final concentrations indicated. The cytolytic activity was assayed as described below.

Modification of NK3.3 with 5′-FSBA, FSB-OMe, and PMSF. 5′-FSBA was prepared by the method of Pal *et al.* (11). FSB-OMe was prepared by methanolysis of fluorosulfonyl benzoyl chloride overnight at room temperature. The highly reactive acid chloride is completely converted to the methyl ester by this procedure. The methanol is evaporated and the solid FSB-OMe is dissolved in DMF. NK3.3 cells were modified by 5′-FSBA (0.01–10 m*M*), FSB-OMe (1 m*M*), or PMSF (1 m*M*) solubilized in DMF as described by Dombrowski *et al.* (10). Briefly, NK3.3 cells ($>1 \times 10^6$ cells) were suspended in serum-free RPMI 1640. The potential covalent-modifying reagents were added to the cell suspension to achieve the final concentrations indicated and sufficient DMF was added to bring the final concentration of DMF to 2.5%. The final volume of the modification reaction was held at 200 μl. Following the modification reaction, cells were pelleted and washed once with RPMI 1640 to remove excess reagent. Cells were then resuspended in RPMI 1640 containing 10% fetal bovine serum and assayed for cytolytic activity. The viability of the NK3.3 cells after modification in all cases was >90% by trypan blue exclusion and spontaneous ^{51}Cr release was <10%.

Cytotoxicity assays. Natural cytotoxicity was assayed using sodium [^{51}Cr]chromate-loaded K562 target cells as described by Brunner *et al.* (12). The E:T ratios routinely used were sequential halving dilutions ranging from 20:1 to 0.3:1, unless otherwise specified. All assays were performed in triplicate. ^{51}Cr released into the supernatants was quantified using a Beckman 4000 gamma counter. Percentage specific release of ^{51}Cr was calculated as: %specific release = [(cpm test − cpm spontaneous)/(cpm maximum − cpm spontaneous)] × 100. Cytolytic activity (LU) was determined by exponential fit of specific ^{51}Cr release using the program provided by Pross *et al.* (13).

Conjugate formation assay. Formation of NK3.3 and K562 conjugates was monitored by flow cytometric analysis according to a modified procedure of Luce *et al.* (14). Briefly, NK3.3 cells modified by 5′-FSBA (2×10^6/ml) were loaded with 100 μM calcein. K562 cells were loaded with 40 μg/ml dihydroethidium. Control cells were treated identically to the 5′-FSBA-modified cells except that 5′-FSBA was omitted from the modification reaction. Following 3×10 ml washes with RPMI 1640, cells were resuspended at 5×10^6 cells/ml in RPMI 1640 containing 10% fetal bovine serum, 25 mM Hepes, pH 7.2, and placed on ice. Aliquots (25 μl) of NK3.3 and K562 were transferred together into a microfuge tube and centrifuged at maximum speed in a microfuge for 2 sec. Pelleted cells were incubated at 37°C for 6 min. Following incubation the pellet was gently resuspended in 3 ml PBS containing 0.2% albumin. Conjugate formation was analyzed on an Epics Elite flow cytometer (Coulter Cytometry, Hialeah, FL). Conjugates were defined by the cell population that was positive for both calcin and dihydroethidium. A total of 10,000 cells were analyzed.

Measurement of serine esterase activity. Granzyme (a serine esterase) activity secreted into the supernatant as a result of cytolytic activation (granule release) was measured as described by Bajpai and Brahmi (7). Briefly, 1×10^6 NK3.3 cells (FSBA-modified or nonmodified) were incubated with 1×10^6 K562 cells in a final volume of 1 ml of RPMI 1640 containing 10% fetal bovine serum for 4 hr at 37°C. The cells were pelleted and granzyme activity in the supernatant was determined by measuring the absorbance change at 405 nm in an assay mixture which contains 0.2 mM DTNB and 0.2 mM N-CBZ-Lys.

RESULTS

Effect of extracellular adenine compounds on natural cytotoxicity. Figure 2 shows that the specific ^{51}Cr release from K562 target cells increases with increasing E:T ratio. The assay was linear with time and between E:T ratios of 1.25:1 to 20:1.

Figure 3 shows that ATP and ADP inhibited natural cytotoxicity 26 and 21% of control activity at a concentration of 1 mM and at E:T ratios <5:1 and at LU_{10}. AMPPNP (a nonhydrolyzable ATP analog) inhibited natural cytotoxicity 41% of control activity at 1 mM and >97% at 10 mM. AMP did not effect natural cytotoxicity at 1 mM. Adenosine gave ~30% inhibition of natural cytotoxicity at 1 mM.

NK cells lyse Raji cells to a lesser, but significant, extent than K562 through natural cytotoxicity (<10%). Natural cytotoxicity against Raji target cells was also inhibited by adenine nucleotides to a similar extent as are K562 target cells (data not shown).

Preincubation of each nucleotide with NK3.3 cells for 1 hr at 37°C followed by assay for natural cytotoxicity

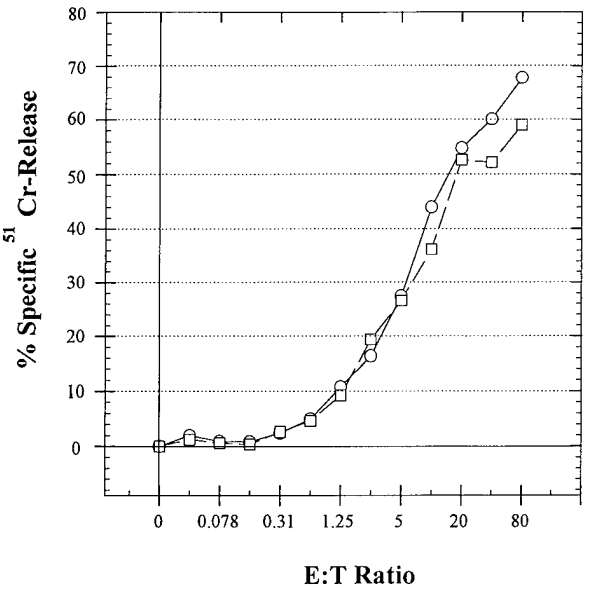

FIG. 2. Effect of DMF on natural cytotoxicity. Representative experiment of three separate experiments demonstrating the linearity of the natural cytotoxicity assay and effect of DMF on natural cytotoxicity. Cells were incubated for 1 hr at 37°C in RPMI 1640 in the absence (○) or presence (□) of 2.5% DMF. ^{51}Cr release experiments were performed as described under Materials and Methods.

activity did not increase the extent of inhibition (data not shown). Furthermore, removal of the nucleotides after preincubation and assay in fresh medium containing no exogenous nucleotides resulted in restoration of control levels of natural cytotoxicity activity (Fig. 3). These data demonstrate that the inhibition of natural cytotoxicity by adenine di- and triphosphate nucleotides and adenosine are reversible.

Effect of 5′-FSBA on natural cytotoxicity. Figure 2 shows that DMF (necessary for the solubilization of 5′-FSBA) at a concentration of 2.5% does not significantly affect natural cytotoxicity up to an E:T ratio of 80:1. 5′-FSBA does not affect the membrane integrity of NK3.3 cells (10) and is impermeant to the membrane (15). Modification of NK3.3 cells with 5′-FSBA shows a dose-dependent inhibition of natural cytotoxicity activity with increasing 5′-FSBA concentrations (Fig. 4). Complete inhibition of natural cytotoxicity activity was obtained with 1 mM of the affinity label. This inhibition was not a result of a noncovalent interaction since extensive washing of the cells following modification did not restore cytolytic activity.

To rule out the possibility that inhibition observed through modification by 5′-FSBA was not due to nonspecific modifications by the fluorosulfonyl group, FSB-OMe, containing only the fluorosulfonyl covalent modifying moiety, was assayed for its ability to inhibit natural cytotoxicity. Figure 4 shows that both FSB-OMe and PMSF (a structural analog of FSB-OMe and serine pro-

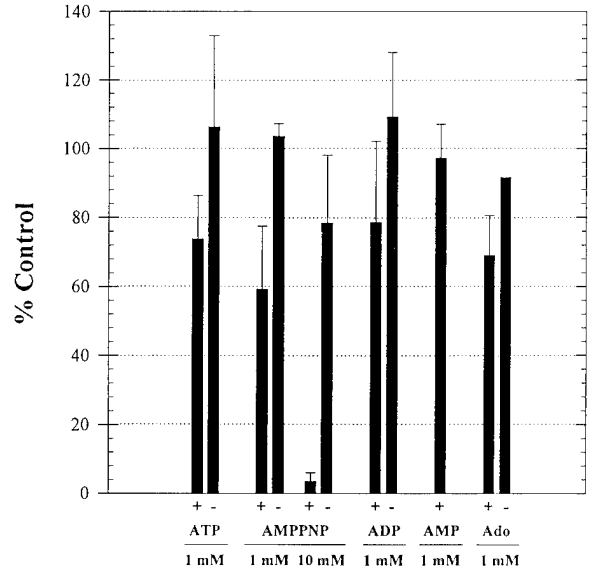

FIG. 3. Effect of extracellular adenosine and adenine nucleotides on NK cell natural cytotoxicity. Cells were assayed 16–24 hr after feeding. Cells were preincubated with the compounds indicated for 1 hr at 37°C as described under Materials and Methods and washed twice with RPMI 1640 containing 10% fetal bovine serum. NK3.3 cells were then combined with ^{51}Cr-loaded K562 target cells and natural cytotoxicity activity was determined as described under Materials and Methods in the presence (+) or absence (−) of exogenous adenine or nucleotides. (Note: AMP was not considered to be an inhibitor; therefore, the corresponding [−] sample was not necessary to be determined.) Percentage control was determined either at individual E:T ratios or from comparison of the LU_{10} as described under Materials and Methods. Results are reported as the means ± SD of at least three experiments.

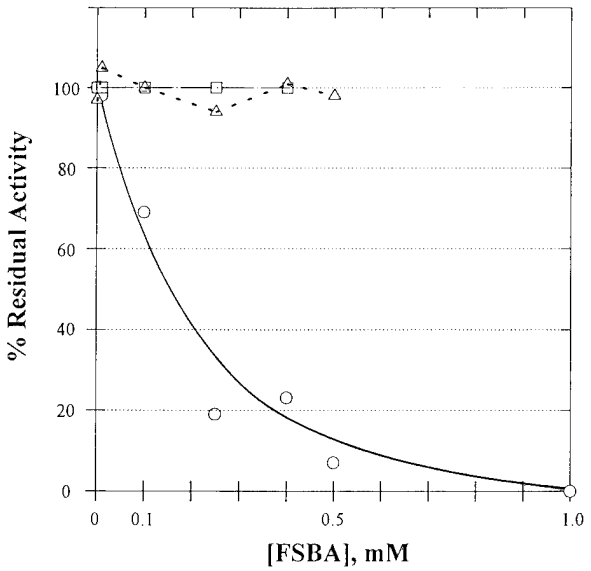

FIG. 4. Inhibition of natural cytotoxicity by modification of NK3.3 by 5′-FSBA. Representative experiment of three separate experiments demonstrating the dose–response inhibition of natural cytotoxicity by 5′-FSBA. NK3.3 cells were preincubated with the various concentrations of (○) 5′-FSBA, (□) FSB-OMe, and (△) PMSF for 1 hr prior to assay. The cells were pelleted, washed, and resuspended in fresh medium without the inhibitors and assayed for natural cytotoxicity activity as described under Materials and Methods.

tease inhibitor) are not inhibitors of natural cytotoxicity at concentrations of 5′-FSBA which give nearly complete inhibition of natural cytotoxicity. These results suggest that the entire 5′-FSBA molecule is necessary for the irreversible inhibition.

NK cells do not normally recognize other NK cells as target cells. Modification of NK3.3 by 5′-FSBA raises the question of whether surface modification of these cells causes them to become target cells. Thus, the inhibition observed would be due to a loss in effector cells resulting in a lower E:T and, hence, apparent inhibition. To verify this, ^{51}Cr-loaded NK3.3 cells and ^{51}Cr-loaded NK3.3 cells modified by 1 m*M* 5′-FSBA served as "target cells." These target cells were not lysed by non-5′-FSBA-modified NK3.3 effector cells in a 4-hr ^{51}Cr release assay with E:T ratios up to 20:1 (Fig. 5). These data indicate that the inhibition of natural cytotoxicity after modification by 5′-FSBA was a result of an inhibition of the cytolytic mechanism.

Effect of 5′-FSBA modification on E:T conjugate formation. To target the site of inhibition resulting from modification by 5′-FSBA, the E:T conjugate formation was examined. Figure 6 (left) shows that no E:T conju-

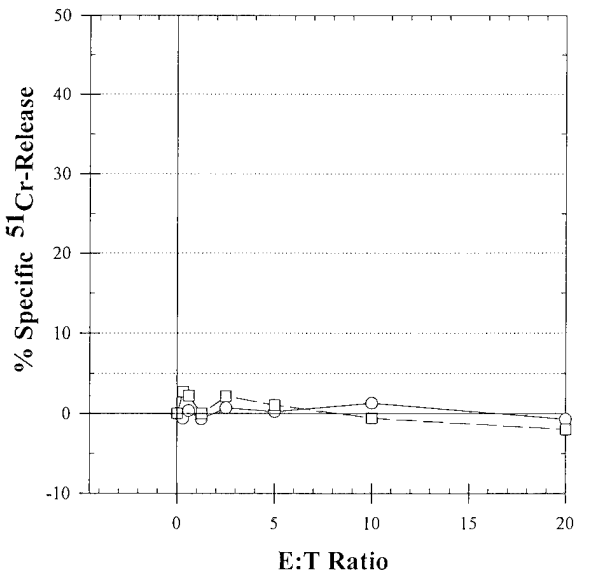

FIG. 5. The 5′-FSBA-modified NK3.3 as potential target cells. (○) NK3.3 cells were modified by 5′-FSBA as described under Materials and Methods. (□) Control NK3.3 cells were incubated in 2.5% DMF. Both cell populations were washed, pelleted, and loaded with ^{51}Cr as described under Materials and Methods. These ^{51}Cr-loaded NK3.3 cells were considered "target cells." Fresh NK3.3 (non-5′-FSBA-modified or DMF-treated) were the "effector cells." Effector and target cells were combined in the ratios indicated and incubated in RPMI 1640 containing 10% fetal bovine serum for 4 hr at 37°C. The percentage specific ^{51}Cr release was determined as described for a natural cytotoxicity assay.

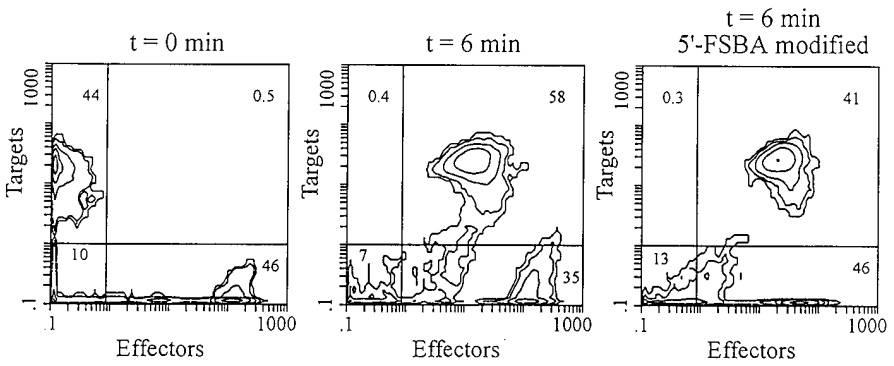

FIG. 6. Effect of 5′-FSBA modification of NK3.3 on effector cell–target cell conjugate formation. Control cells were incubated with 2.5% DMF in parallel with cells modified by 5′-FSBA. Conjugate formation was assayed for twice as described under Materials and Methods. Conjugate formation was not affected by incubation cells with 2.5% compared to control cells not incubated with this solvent (data not shown). Numbers listed in each quadrant represent the percentage of cells in that quandrant. Left, t = 0 min, unmodified NK3.3 cells were mixed with K562 cells, pelleted, and immediately analyzed for conjugate formation; center, t = 6 min, unmodified control cells were mixed with K562 cells, pelleted, and analyzed for conjugate formation after a 6 min incubation at 37°C; right, NK3.3 cells modified by 5′-FSBA were mixed with K562 cells, pelleted, and analyzed for conjugate formation after a 6-min incubation at 37°C.

gate formation is detected upon mixing and pelleting effector cells and target cells, followed by immediate flow cytometry analysis. Conjugate formation was observed when the cells were incubated for 6 min before analysis (Fig. 6, center). Figure 6 (right) shows that conjugate formation is not affected by the modification of NK3.3 cells with 5′-FSBA.

Effect of 5′-FSBA modification on granzyme activity. To further target the site of inhibition resulting from modification by 5′-FSBA, the release of lytic granules was examined by measuring the granzyme release following E:T conjugate formation. Figure 7 shows that the granzyme activity assay is linear for at least 30 min from control cells, but that granzyme activity released into the supernatant following incubation with target cells is inhibited >90% in samples modified by 5′-FSBA. This result is consistent with the loss of cytolytic activity.

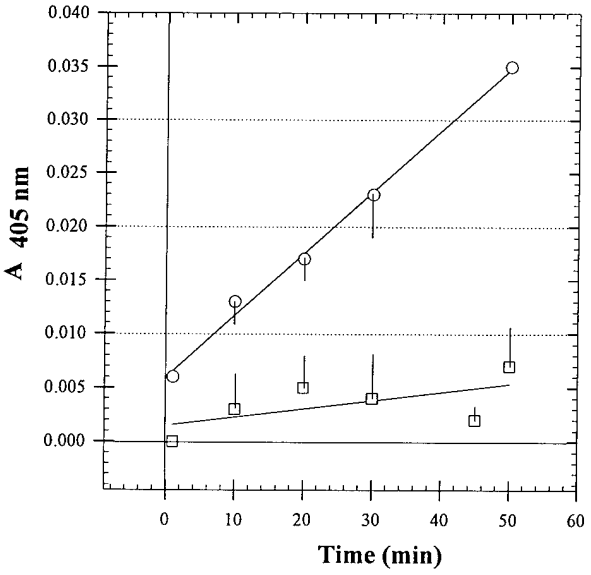

FIG. 7. Effect of 5′-FSBA modification of NK3.3 on granule release. NK3.3 cells were incubated in the absence (○) or presence (□) of 5′-FSBA. Granzyme release was measured by colorimetric assay at 405 nm as described under Materials and Methods. Data represent the means ± average deviation (n = 3).

DISCUSSION

Extracellular nucleotides have been described to have substantial stimulatory and inhibitory effects on the physiological processes and membrane integrity of a variety of lymphoid and nonlymphoid cells (16). In the NK cell system, extracellular adenine nucleotides inhibited the cytolytic activity of these nonstimulated, peripheral blood effector cells (5–7). However, IL-2-stimulated NK cells were suggested to be refractory to inhibition of cytolytic activity by extracellular adenine nucleotides (7). Here, we demonstrated that extracellular adenine nucleotides are inhibitory to NK cell cytolytic activities using the IL-2-dependent human natural killer cell line NK3.3 model system.

Natural cytotoxicity is inhibited by extracellular nucleotides with increasing negative charge: whereas ATP, AMPPNP, and ADP are inhibitory, AMP is not. The inhibition resulting from the di- and triphosphate nucleotides is reversible. In contrast, the inhibition observed by modification of NK3.3 cells by the adenine nucleotide affinity label 5′-FSBA is not reversible. 5′-FSBA covalently modifies NK3.3 cells by acting as an ATP or ADP analog (10).

It is interesting to note that the inhibition of NK3.3 natural cytotoxicity by 5′-FSBA and adenine nucleotides parallels the inhibition of the ectoATPase identified on this cell line (10). The fact that adenosine is inhibitory to natural cytotoxicity, but not to ectoATPase activity, may suggest an alternate, extracellular-initiated mechanism of cell-mediated events, possibly through a P_1 pu-

rinergic receptor as initially suggested for murine NK cells (5).

5′-FSBA and nucleotides are impermeable to the cell membrane (15) and do not affect the membrane integrity of this NK cell line (2, 10). As such the inhibition of natural cytotoxicity observed would appear to be mediated through a cell-surface nucleotide-binding protein resulting in an inhibition of a signal transduction pathway required for the cytolytic mechanism to proceed.

The specific protein(s) modified by 5′-FSBA and the mechanism of inhibition of cytolytic function is yet to be determined. The use of the characterized human NK cell line NK3.3 will facilitate the study of the interactions of extracellular nucleotides and the affinity label 5′-FSBA on the extracellular regulatory mechanisms of cell-mediated cytotoxicities.

ACKNOWLEDGMENTS

We thank Dr. Jacki Kornbluth for the NK3.3 cell line. We also thank Dr. James M. Trevillyan for his many discussions of this work and Dr. Naziha F. Nuwayhid for review of this manuscript.

REFERENCES

1. Dombrowski, K. E., Cone, J. C., and Phillips, C. A., *Nat. Immun.* **11,** 290, 1992.
2. Dombrowski, K. E., Trevillyan, J. M., Cone, J. C., Lu, Y., and Phillips, C. A., *J. Immunol.* **150,** 208A, 1993. [Abstract 1188]
3. Anderson, S. K. (1993) *In* "NK Cell Medicated Cytotoxicity: Receptors, Signaling and Mechanisms" (E. Lotzova and R. B. Herberman, Eds.), Chap. 1, pp. 1–14, CRC Press, Boca Raton, FL.
4. O'Shea, J., and Ortaldo, J. R., *In* "The Natural Killer Cell" (C. E. Lewis and J. O 'D. McGee, Eds.), pp. 1–40, IRL Press, Oxford, 1992.
5. Henriksson, T., *Immunol. Lett.* **7,** 171, 1983.
6. Schmidt, A., Ortaldo, J. R., and Herberman, R. B., *J. Immunol.* **132,** 146, 1984.
7. Bajpai, A., and Brahmi, Z., *Cell. Immunol.* **148,** 130, 1993.
8. Kornbluth, J., Flomenberg, N., and Dupont, B., *J. Immunol.* **129,** 2831, 1982.
9. Colman, R. F., *In* "Protein Function: A Practical Approach," pp. 77–99, IRL Press, Oxford, 1989.
10. Dombrowski, K. E., Trevillyan, J. M., Cone, J. C., Lu, Y., and Phillips, C. A., *Biochemistry* **32,** 6515, 1993.
11. Pal, P. K., Wechter, W. J., and Colman, R. F., *J. Biol. Chem.* **250,** 8140, 1975.
12. Brunner, K. T., Engers, H., and Cerrotini, J. C., *In "In Vitro*: Methods of Cell Mediated Immunity against Viruses" (B. Bloom and J. David, Eds.), Academic Press, New York, 1976.
13. Pross, H. F., Baines, M. G., Rubin, P., Shragge, P., and Patterson, M. S., *J. Clin. Immunol.* **1,** 51, 1981.
14. Luce, G. G., Sharrow, S. O., and Shaw, S., *BioTechniques* **3,** 270, 1985.
15. Bennett, J. S., Colman, R. F., and Colman, R. W., *J. Biol. Chem.* **253,** 7346, 1978.
16. Luthje, J., *Klin. Wochenschr.* **67,** 317, 1989.

Antigen Recognition by CTL Is Dependent upon EctoATPase Activity[1]

Kenneth E. Dombrowski,[2*†] Yong Ke,[‡] Linda F. Thompson,[§] and Judith A. Kapp[‡]

*Department of Veterans Affairs Medical Center, †Department of Internal Medicine, Texas Tech University Health Sciences Center, Amarillo, TX 79106; ‡Winship Cancer Center and Department of Pathology, Emory University School of Medicine, Atlanta, GA 30322; and §Immunobiology and Cancer Program, Oklahoma Medical Research Foundation, Oklahoma City, OK 73104

Alloantigen-specific and OVA-specific $CD8^+$ CTL were shown here to express an ectoATPase. These CTL also express an ectoADPase, but do not express detectable levels of an ectoAMPase. $CD8^+$ CTL transported adenosine into their cytoplasm at a rate of 2.3×10^{-11} mmol/min/10^5 cells. In contrast, adenosine uptake was 34-fold lower when ATP was used as the source of the nucleoside. This was consistent with the lack of ectoAMPase and suggests that the role of ectoATPase is not in the salvage of extracellular nucleotides. 5′-p-(fluorosulfonyl)benzoyl adenosine (5′-FSBA) is an ATP analogue affinity label that irreversibly inhibits CTL ectoATPase. Cells made ectoATPase activity deficient by modification with 5′-FSBA were not susceptible to potential lytic effects of extracellular ATP with less than 20% specific lysis at 20 mM of exogenous ATP. However, cells modified by 5′-FSBA were unable to kill their respective target cells. Complete inhibition of cell-mediated killing was observed with 1 mM 5′-FSBA. CTL modified by 5′-FSBA also failed to secrete TNF-α and IFN-γ after activation by the appropriate Ag. Killing was also inhibited by 5′-adenylylimidodiphosphate (a nonhydrolyzable ATP analogue), but not by ATP, ADP, α, β-methylene ADP (a nonhydrolyzable ADP analogue), AMP, or adenosine. Blockage of CTL activity by 5′-FSBA was not reversed by addition of ADP, suggesting that hydrolysis of ATP is an essential ectoATPase-mediated signal for CTL activation. These results suggest that ectoATPase is essential for Ag recognition and/or effector activities of CTL. *The Journal of Immunology,* 1995, 154: 6227–6237.

Extracellular adenine nucleotides display a variety of effects on a number of different cell types (for review, see Ref. 1). Effects of ATP include membrane permeabilization (1), induction of apoptosis (2–4), organic anion transport in hepatocytes (5), and stimulation of Ca^{2+} mobilization in thymocytes (6, 7), smooth muscle (8), and neuroblastoma cell lines (9–11). Extracellular ADP is involved in the control of platelet aggregation and regulation of vascular tone (1). The specific actions of extracellular AMP are less well defined. Extracellular adenosine has substantial effects in vasodilation (12) and the regulation of neurotransmitter release (13), possibly through the modulation of intracellular cAMP levels. The extracellular action of adenine nucleotides is mediated by purinergic receptors (14) and by extracellular, cell-associated nucleotidases, termed ectonucleotidases.

Ectonucleotidases are expressed by cells in, or lining, the lumen of blood vessels where high concentrations of extracellular nucleotides occur (1). Each enzyme is responsible for the removal of specific phosphate groups from extracellular adenine nucleotides. EctoATPase (1, 15–17) catalyzes the hydrolysis of the γ phosphate of ATP to ADP and P_i,[3] whereas ectoADPase is specific for the

Received for publication January 17, 1995. Accepted for publication March 28, 1995.

The costs of publication of this article were defrayed in part by the payment of page charges. This article must therefore be hereby marked *advertisement* in accordance with 18 U.S.C. Section 1734 solely to indicate this fact.

[1] This work was supported in part by a Texas Tech University Health Sciences Center seed grant (K.E.D.), the Elsa U. Pardee Foundation (K.E.D.), Department of Army Career Development Award Grant DAMD17-94-J-4161 (K.E.D.), and Department of Army Medical Research and Materiel Command Grant DAMD17-94-J-4272 (K.E.D.), the American Cancer Society Grant IM-617A (J.A.K.), and Research Grants AI-18220 (L.F.T.), GM-39699 (L.F.T.), and AI-13987 (J.A.K.) from the National Institutes of Health. Content of the information herein does not necessarily reflect the position or the policy of the U.S. government, and no official endorsement should be inferred.

[2] Address correspondence and reprint requests to Dr. Kenneth E. Dombrowski, Department of Internal Medicine, Texas Tech University Health Sciences Center, 1400 Wallace Blvd., Amarillo, TX 79106

[3] Abbreviations used in this paper: P_i, inorganic phosphate; 5′-FSBA, 5′-*p*-(fluorosulfonyl)benzoyl adenosine; OVA-CTL, OVA-specific CTL; AMPCP, α, β-methylene ADP; AMPPNP, 5′-adenylylimidodiphosphate; DMF, dimethylformamide; ectoATPDase, ectoATP diphosphohydrolase; PMS, phenazine methosulfate; XTT, sodium 3′-[1-(phenylaminocarbonyl)-3,4-tetrazolium]-bis(4-methoxy-6-nitro)benzene sulfonic acid hydrate; ecto-5′-NT, ecto-5′-nucleotidase.

0022-1767/95/$02.00

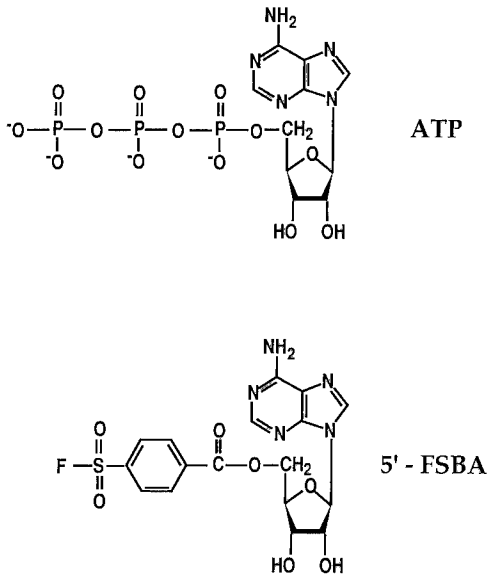

FIGURE 1. Structural comparison of ATP and 5′-FSBA.

hydrolysis of ADP to AMP and P_i (1, 18). EctoATP-diphosphohydrolase (ectoATPDase), like ectoATPase, acts on ATP as a substrate, but forms AMP by the sequential removal of the γ and β phosphate groups (19–23). EctoAMPase, also known as ecto-5′-nucleotidase or CD73 (24), catalyzes the hydrolysis of AMP to adenosine and P_i. Adenosine is transported across the cell membrane and either degraded to uric acid or integrated into purine salvage pathways (1, 25).

In the immune system only ectoATPases and ectoAMPases have been described and characterized. EctoATPases are expressed by polymorphonuclear leukocytes (15), lymphocytes (26–29), macrophages (30), NK cells (31–33), and CTL (33, 34). EctoAMPases are present on subpopulations of human T (35, 36) and B lymphocytes (37). In T lymphocyte subpopulations, CD73 (an ectoAMPase) provides a costimulatory signal for activation and proliferation (35, 38–40). In T and B lymphocytes, a deficiency of ecto-5′-nucleotidase activity is apparent in patients with common variable immunodeficiency, congenital X-linked agammaglobulinemia, severe combined immunodeficiency, and a variety of other immunodeficiency diseases (37 and references therein).

The physiologic role of ectoATPases expressed by bone marrow-derived cells is not known. The role of ectoATPase in lymphoid cell function is being examined by using competitive nucleotide analogue antagonists and the adenine nucleotide affinity label 5′-*p*-(fluorosulfonyl)benzoyl adenosine (5′-FSBA, Fig. 1) (31, 32), a structural analogue of ATP and ADP (41). 5′-FSBA is well suited for studies of extracellular regulation because it does not cross the cell membrane (42). This affinity label contains a reactive fluorosulfonyl group at a position that is equivalent to the β or γ phosphoryl group of ATP. When 5′-FSBA modifies a protein at or near an ATP- or ADP-binding site, covalent attachment of this affinity reagent is achieved by electrophilic substitution of the fluoro group by basic or other nucleophilic amino acid side chain residues frequently found in nucleotide binding pockets (41).

In a murine system, ectoATPase was postulated to protect CTL effector cells from the potential lytic effects of extracellular ATP released during granule exocytosis (34). However, we have shown that a human NK cell line made deficient in ectoATPase activity through inhibition by 5′-FSBA was not susceptible to the potential lytic effects of extracellular ATP (31, 32). Thus, the primary role of ectoATPase in NK cells is not for the protection of that effector cell population from extracellular ATP. Moreover, ectoATPase is required for the cytolytic activity of NK cells because 5′-FSBA modification blocks natural cytotoxicity (43) and Ab-dependent cellular cytotoxicity (32) (K. E. Dombrowski, J. M. Bjorndahl, J. C. Cone, and C. A. Phillips, manuscript in preparation).

In this paper we have asked whether the functions of murine $CD8^+$ CTL that express an ectoATPase are dependent upon this enzyme. We demonstrate that Ag-specific responses are inhibited by modification with 5′-FSBA under conditions that inhibit the ectoATPase activity. Thus, ectoATPase activity is required for Ag recognition and/or the activation of effector function in $CD8^+$, MHC class I-restricted, cytotoxic T cells.

Materials and Methods

ATP was purchased as the disodium salt from Sigma Chemical Co. (St. Louis, MO). [γ-^{32}P]ATP, [2-^{3}H]adenosine and [2-^{3}H]ATP were purchased from Amersham (Arlington Heights, IL). Sodium [^{51}Cr]chromate was purchased from NEN Research Products (DuPont, Boston, MA). DMF was purchased from Aldrich (Milwaukee, WI). 5′-FSBA was prepared by condensation of adenosine with fluorosulfonylbenzoyl chloride according to the method of Pal et al. (44). All chemicals were of reagent grade purity.

Ag

Purified chicken OVA (grade VI) was purchased from Sigma and dissolved in PBS, pH 7.4. CFA containing *Mycobacterium tuberculosis* strain H37Ra was purchased from Difco Laboratories (Detroit, MI). To prepare the OVA-CFA emulsion, 1.0 ml of soluble OVA in PBS was added to 1.0 ml oil phase of CFA and mixed vigorously, using two glass syringes connected through a three-way valve.

Animals and immunization procedures

Female C57BL/10 (H-2^b) and BALB/c (H-2^d) mice, 8 to 12 wk old, were purchased from The Jackson Laboratory (Bar Harbor, ME). C57BL/10 mice were injected s.c. in the hind footpads with 100 μg of OVA in CFA or copolymer adjuvants (45, 46). Spleen cells were dispersed into single cell suspensions and restimulated in vitro as described by Moore et al. (47).

Cell culture and maintenance

The tumor cells used as CTL targets were MHC class II-negative EL-4 (H-2^b thymoma derived from C57BL/6 mice), E.G7-OVA (EL-4 transfected with the chicken OVA cDNA gene (47) provided by Dr. M. J. Bevan, University of Washington, Seattle, WA) and P815 (H-2^d mastocytoma derived from DBA/2 mice) (American Type Culture Collection,

Rockville, MD). WEHI164.13 is a fibrosarcoma clone that is highly sensitive to TNF-α (48). All cell lines were cultured in the complete medium consisting of RPMI 1640 (Mediatech, Washington, DC) supplemented with 10% (v/v) FCS (HyClone, Logan, UT), 1 mM L-glutamine and 1 mM sodium pyruvate (Life Technologies, Inc., Grand Island, NY), 50 μM 2-ME (Sigma), 100 IU/ml penicillin and 100 μg/ml streptomycin (Mediatech), and 50 μg/ml gentamicin sulfate (Sigma), at 37°C in 6% CO_2 in air.

Long-term CTL lines

Long-term CTL lines derived from splenic mononuclear cells were used as the source of CTL for all experiments. OVA-specific CTL (OVA-CTL) were generated by incubating 35×10^6 splenic mononuclear cells from C57BL/10 mice that had been primed 10 days earlier with 100 μg OVA in CFA or copolymer adjuvants with 3×10^6 of γ-irradiated (20,000 rad; 1 rad = 0.01 Gy) E.G7-OVA cells in 10 ml of complete medium (49). Spleen cells containing primed CTL precursors were harvested after 7 days. Long-term lines were established by weekly stimulation of 2.5×10^6 CTL with 25×10^6 irradiated (2000 rad) syngeneic spleen cells as filler cells and 1×10^6 irradiated E.G7-OVA in 10 ml of complete medium plus 5% (v/v) rat Con A supernatant (40-h supernatant of Con A-stimulated rat spleen cells) as a source of T cell growth factors. The resulting CTL lines recognize E.G7-OVA but not the parental EL-4 cells. These cells are specific for the $OVA_{257-264}$ epitope in association with H-2K^b as previously described (50, 51).

Alloantigen-specific CTL were generated by incubating 50×10^6 splenic mononuclear cells from C57BL/10 (H-2^b) mice with 50×10^6 of γ-irradiated (2000 rad) spleen cells from BALB/c (H-2^d) mice in 10 ml of complete medium. After 7 days, 5×10^6 of cytotoxic effector cells were harvested and restimulated with 25×10^6 irradiated (3000 rad) BALB/c spleen cells plus 5% Con A supernatant. Long-term bulk lines have been generated by weekly stimulation following the same protocol. This CTL line recognizes P815 (H-2^d) targets but not syngeneic (EL-4) targets.

The Ag-specific OVA-CTL and the alloantigen-specific B10α-BALB/c CTL lines were determined to be 100% CD8$^+$ by FACS analysis. CTL were purified by density gradient separation using Histopaque-1077 (Sigma).

EctoATPase activity assays

EctoATPase activity was measured using [γ-^{32}P]ATP as substrate and counting the amount of $^{32}P_i$ released into the supernatants after precipitation of nucleotides with activated charcoal as described previously (31). Each assay mixture contained 1×10^4 cells in a final volume of 200 μl with 0.3 mM ATP and 0.3 μCi/assay. The specific radioactivity of the ATP substrate was generally 1×10^{13} cpm/mol.

To assay potential inhibitors of ectoATPase activity, known inhibitors of other classes of ATPases were added directly to the assay mixture: ouabain and vanadate are inhibitors of the plasma membrane (P-type) class of ATPases (52, 53), nitrate is an inhibitor of the vacuolar (V-type) class of ATPases (54), vanadate and azide are inhibitors of the mitochondrial (F-type) class of ATPases (54), and fluoride is an inhibitor of phosphatases (52). AMPPNP (Li salt) (Sigma) is a nonhydrolyzable analogue of ATP and is a known inhibitor of ectoATPase (31). AMPCP (sodium salt) (Sigma) is a nonhydrolyzable analogue of ADP and inhibitor of ectoADPases.

The kinetic parameters of K_m and V_{max} were determined by Lineweaver-Burk plots using ATP substrate concentrations ranging from 25 to 300 μM. The type of inhibition and inhibitor constants for AMPPNP and AMPCP were determined by Dixon plot analysis at three substrate concentrations (0.3 mM, 0.15 mM, and 0.075 mM) using inhibitor concentrations ranging from 25 to 200 μM.

EctoAMPase activity assays

EctoAMPase enzyme activity was assayed on intact cells by measuring the conversion of [^{14}C]inosine 5′-monophosphate to [^{14}C]inosine as previously described (55). Enzyme activity was expressed as nanomoles of product formed/hour/10^6 cells.

Uptake of extracellular adenosine

Uptake of adenosine and ATP was performed as described previously (56). Briefly, 100 μl of CTL (1×10^6 cells/ml) in RPMI 1640 containing 10% FCS were incubated with 100 μl of a 45-mM solution of [2-^{3}H]adenosine (22 Ci/mmol) or a 40-mM solution of [2-^{3}H]ATP (19 Ci/mmol) for the times indicated. The cells were quickly pelleted and washed three times with RPMI 1640 plus 10% FCS to remove exogenous adenosine or ATP. The radioactivity incorporated into the cells was determined by scintillation counting using a Beckman LS 5801 liquid scintillation counter.

Cytotoxicity assays

Target cells (1×10^6) were loaded with 100 to 200 μCi sodium [^{51}Cr]chromate (DuPont, Boston, MA) in Tris-phosphate buffer, pH 7.4, by incubation at 37°C for 1 h. After washing, a standard 4-h cytotoxicity assay (57) was conducted in triplicate by incubating 1×10^4 ^{51}Cr-loaded targets with 1×10^5 effector cells (E:T ratio = 10:1) in 200 μl of complete medium. Aliquots of the supernatant (100 μl) were harvested and the radioactivity was detected in a gamma counter (Wallac, Turku, Finland). Experimental data were converted to percentage of specific lysis as calculated: percent specific lysis = (release by CTL − spontaneous release)/(maximal release − spontaneous release). Maximal release was determined by the addition of 1% Triton X-100 (EM Science, Gibbstown, NJ). Spontaneous release in the absence of effector cells was generally less than 15% of the maximal release in all experiments. Results are reported as the mean of triplicates ± SD of representative experiments.

Modification of CTL by 5′-FSBA

OVA-specific and alloantigen-specific CTL were modified by 5′-FSBA solubilized in DMF or with DMF alone as described previously (31, 43). The final concentration of DMF was held constant at 2.5%. After the modification reaction, cells were pelleted and washed once with RPMI 1640 to remove excess 5′-FSBA, resuspended in complete medium, and assayed for cytolytic activity. The viability of the CTL cells after modification was >90% by trypan blue exclusion.

Effect of extracellular adenine nucleotides on cytolytic activity

In some experiments, viable CTL were preincubated with up to 10 mM of exogenous ATP, AMPPNP (a nonhydrolyzable ATP analogue antagonist of ATPase activity; 31, 43), ADP, AMPCP (a nonhydrolyzable ADP analogue antagonist of ADPase activity), AMP, or adenosine in serum-free RPMI 1640 at 37°C for 1 h. Target cells were then added and cytolytic activity was measured as described above.

Challenge of CTL with extracellular ATP

To determine whether ectoATPase protects CTL from lysis by extracellular ATP, CTL were loaded with 100 to 200 μCi sodium [^{51}Cr]chromate for 1 h at 37°C. They were subsequently treated with 2.5% DMF alone, or 1 mM 5′-FSBA in 2.5% DMF at 37°C for 1 h. After washing, CTL cells were incubated with titrated concentrations of ATP at 37°C for 4 h. Supernatants were counted for radioactivity and percentage of specific lysis was determined as: percent specific lysis = (release in the presence of ATP − spontaneous release)/(maximal release − spontaneous release).

Cytokine production assays

CTL were incubated with unlabeled targets at an E:T ratio of 10:1. After 4 h at 37°C, supernatants were harvested and assayed for IFN-γ or TNF-α. IFN-γ was determined by ELISA as described by the manufacturer (PharMingen). Briefly, an ELISA plate was coated with rat anti-mouse IFN-γ capture mAb (4 μg/ml) and incubated overnight at 4°C. The plate was then blocked with 10% FCS in PBS. Titrated rIFN-γ standards and test samples were added and incubated overnight at 4°C. Biotinylated rat anti-mouse IFN-γ detecting mAb (4 μg/ml) was then added and incubated at 22°C for 45 min. Avidin-peroxidase (2.5 μg/ml) was then added and incubated again at 22°C for 30 min. Finally, 2,2′-azino-di[3-ethylbenzthiazoline sulfonate] substrate containing H_2O_2 was

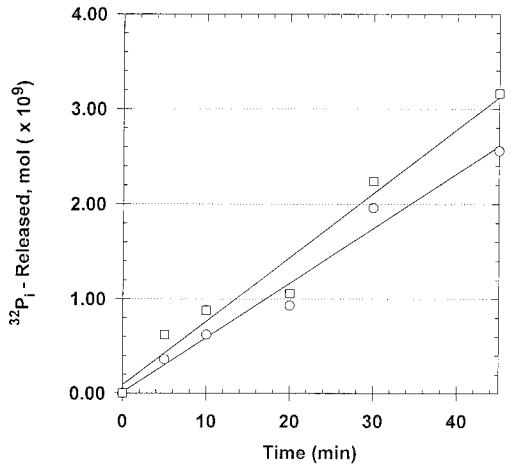

FIGURE 2. Expression of ectoATPase by CTL. EctoATPase activity expressed by OVA-CTL (□) and B1OαBALB/c CTL (○) was measured using 2.5 × 10^4 CTL and [γ-^{32}P]ATP as substrate as described in *Materials and Methods*. The $^{32}P_i$ released into the supernatant was determined by scintillation counting after charcoal precipitation of the nucleotides. The specific radioactivity of the ATP substrate in this representative experiment was 1.1 × 10^{13} cpm/mol.

added. The colorimetric reaction was developed at 22°C and absorbance at 405 nm was read using an automatic microplate reader (Molecular Devices Corp., Menlo Park, CA). After each step, the plate was washed extensively with 1% Tween in PBS. The concentrations (nanograms per milliliter) of murine IFN-γ in samples were calculated from a standard curve. Results are reported as the mean of triplicates ± SD for a representative experiment performed at least three times.

TNF-α was detected using WEHI164.13 (48) a cell line that is lysed by TNF-α. Briefly, WEHI164.13 target cells were seeded into 96-well, flat-bottom plates at 1.5 to 2.0 × 10^4 cells/well. Test supernatants were then added at a final volume of 200 μl/well and incubated at 37°C for 24 h. In control wells, only complete medium was added to target cells. Lysis of WEHI64.13 cells was determined by colorimetric reaction using tetrazolium salt XTT (Diagnostic Chemicals, Oxford, CT), and PMS (Aldrich) as described by Roehm et al. (58). Absorbance was read at 450 nm. Percentage of dead cells was calculated as following: percentage of dead cells = 100 − (absorbance in wells with test supernatant/absorbance in control wells) × 100. Results are reported as the mean of triplicates ± SD for representative experiments.

Results

Identification of T cell-associated ectoATPases

Two murine class I MHC-restricted $CD8^+$ CTL lines, an OVA-CTL, and an alloantigen-specific B10α-BALB/c CTL (H-2^b anti-H-2^d), were assayed for expression of ectoATPase activity. Incubation of these cells with [γ-^{32}P]ATP demonstrated that both released $^{32}P_i$ that was linear with time (Fig. 2).

To determine whether the observed ATPase activity was membrane associated or an intracellular enzyme that was secreted or released, CTL were incubated for 20 min under standard assay conditions without ATP and pelleted. If the ATPase activity was secreted or released, it would appear in the supernatant; conversely, activity associated with the pellet would indicate a cell-associated enzyme. Assay of both fractions demonstrated that 90 to 95% of the ATPase activity was cell associated (Table IA). This suggests that the ATPase is an ectoenzyme.

Table I. *Characterization of CTL ectoATPase*

A. Cellular Location and Kinetic Parameters

Cell line	Cellular location[b]	K_m[c] (μM)	V_{max}[c] (nmol/min)
OVA-CTL	95% cell associated	67	20
B10α-BALB/c-CTL	90% cell associated	163	220

B. Inhibitors of CTL EctoATPase

Inhibitor	OVA-CTL (% control)[d]	B10α-BALB/c-CTL (% control)[d]
Ouabain, 1 mM	95	93
No_3^-, 100 mM	97	85
VO_4^-, 500 μM	87	87
N_3^-, 1 mM	101	85
F^-, 10 mM	95	86
AMPPNP, 1 mM	25	ND
AMPCP, 1 mM	59	ND
5′-FSBA, 1 mM	12	10

[a] All assays were performed at 37°C for 20 min in triplicate as described in *Materials and Methods*.

[b] CTL (1 × 10^4 cells) were incubated for 20 min at 37°C in RPMI 1640 without FCS, pelleted, and resuspended in fresh RPMI 1640; supernatant was saved. ATP was added to a concentration of 0.3 mM containing 0.3 μCi of [^{32}P]ATP to each supernatant and resuspended cell pellet. Percentage of cell-associated activity was determined by (activity of resuspended cell pellet)/(total ectoATPase activity of 1 × 10^4 CTL).

[c] K_m and V_{max} for each CTL cell line were determined by Lineweaver-Burk plots using 25 to 300 μM ATP.

[d] CTL (1 × 10^4 cells) were assayed for ATPase activity in the presence of compounds indicated. Values indicated are the percentage of control samples not containing any exogenous inhibitors.

Examination of the enzymatic reaction products by TLC on silica gel F254 (EM Science, Gibbstown, NJ) and a solvent system of isobutyric acid/NH_4OH/H_2O (66/33/1; v/v/v) demonstrated ADP and AMP were both produced by hydrolysis of ATP. When ADP was used as substrate, AMP was the only product detected. No adenosine could be detected using ATP or ADP as substrate. These results suggest that the CTL do not express ectoAMPase. When specifically assayed for ectoAMPase, the activity was below the level of detection (<0.4 nmol/h/10^6 cells) (Fig. 3). These results suggest that $CD8^+$ CTL express either an ectoATPase and an ectoADPase, or an ectoATPDase.

EctoATPase activity of both CTL cell lines followed Michaelis-Menton kinetics. $CD8^+$ CTL hydrolyzed ATP at rates of 2.7 × 10^{-15} mol/min/cell and 2.3 × 10^{-15} mol/min/cell for the OVA-CTL and B10α-BALB/c CTL, respectively (Fig. 2). The K_m^{ATP} and V_{max} were 67 μM and 20 nmol $^{32}P_i$ released/min, respectively, for the OVA-CTL and 163 μM and 220 nmol $^{32}P_i$ released/min, respectively, for the B10α-BALB/c CTL (Table IA).

To characterize further the ectoATPase, CTL expressing this enzyme activity were assayed in the presence of compounds that are known inhibitors specific for other classes of ATPases (P-, V-, and F-type and ectoATPDase)

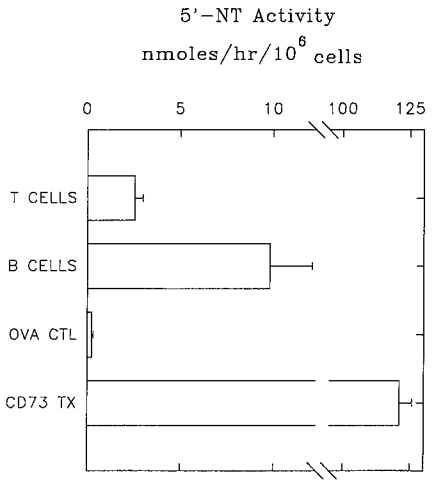

FIGURE 3. Ecto-5′-nucleotidase activity of OVA-CTL. Ecto-5′-NT enzymatic activity was assayed by measuring the conversion of [^{14}C]IMP to [^{14}C]inosine as previously described (55) and is expressed as nanomoles/hour/10^6 cells. Nonspecific nucleotide phosphatase activity, resistant to inhibition by the ecto-5′-NT inhibitor AMPCP, was subtracted. The results shown are the mean ± SD of triplicate determinations. The ecto-5′-NT activity of OVA-CTL was beneath the limits of detection (0.4 nmol/h/10^6 cells) and is shown in comparison to that of murine spleen T and B lymphocytes as well as to Jurkat cells transfected with CD73 cDNA (59). The splenic T cell preparation consisted of total spleen cells depleted of B cells by panning on plates coated with sheep anti-mouse IgG (Cappell, Durham, NC). The specific B cell preparation consisted of total spleen cells depleted of T cells by panning on plates coated with anti-CD3 mAb 145–2C11 (a gift of Dr. J. Bluestone, University of Chicago, Chicago, IL).

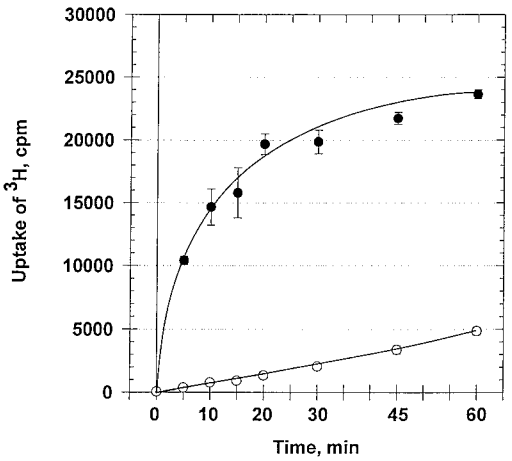

FIGURE 4. Uptake of adenosine by OVA-CTL. OVA-CTL (1×10^5 cells in 100 μl of serum-free RPMI 1640) were incubated with a 45-mM solution of [2-^{3}H]adenosine (●) or a 40 mM solution of [2-^{3}H]ATP (○) for the indicated times and as described in *Materials and Methods*. At each time point, the cells were pelleted and washed. Incorporation was determined by scintillation counting of the cell fraction. The specific radioactivity of [2-^{3}H]adenosine and [2-^{3}H]ATP was 22 Ci/mmol and 19 Ci/mmol, respectively. The data are the means ± SD of triplicate determinations.

and phosphatases, but not inhibitors of ectoATPase. The concentrations of ouabain, NO_3^- (P-type ATPase inhibitor), VO_4^- (P- and F-type ATPase inhibitor), N_3^- (F-type ATPase and ectoATPDase inhibitor) and F^- (phosphatase inhibitor) used are at least 100-fold higher than the K_i for the respective compound. Table IB shows that both the OVA-CTL and B10α-BALB/c CTL are not significantly inhibited by any of these ATPase inhibitors. The fact that both ADP and AMP (products of ectoATPDase) are produced by CTL incubated with ATP suggests that the enzymatic activity observed might be an ectoATPDase. However, N_3^- did not inhibit the hydrolysis of ATP by CTL. Therefore, the observed nucleotide-hydrolyzing activities expressed by CTL are most likely caused by two distinct enzymes: an ectoATPase and an ectoADPase.

AMPPNP is a competitive inhibitor of the NK cell ectoATPase (31) and also an inhibitor of the CTL ectoATPase (Table IB). Dixon plot analysis (data not shown) demonstrated that the inhibition was competitive with respect to ATP with a K_i of 146 μM. AMPCP was also an inhibitor of phosphate release, but weaker than that produced by AMPPNP (Table IB). Dixon plot analysis (data not shown) demonstrated that the inhibition was also competitive with respect to ATP with a K_i of 245 μM.

Uptake of adenosine by CTL

Adenosine is readily transported across the cell membrane of $CD8^+$ CTL at an initial rate of 2.3×10^{-11} mmol/min/10^5 cells (Fig. 4). ATP and other nucleotides are not transported: they must first be degraded to the nucleoside (56). In fact, CTL incubated with [2-^{3}H]ATP transported only 6.8×10^{-13} mmol of adenosine/min, 34-fold less efficient than adenosine transport. The slow uptake of [2-^{3}H]ATP is consistent with the lack of ectoAMPase expression by these CTL.

Does ectoATPase protect CTL from lytic activity of ATP?

We have used two CTL lines as a model system to examine the postulated role of ectoATPase in protecting T cells from the potential lytic effects of extracellular ATP released from the lytic granules of CTL (34). Modification of OVA-CTL and B10α-BALB/c CTL with the adenine nucleotide affinity label 5′-FSBA-inhibited ectoATPase activity a maximum of ~90% at a concentration of 1 mM (Table IB; Fig. 5). Inhibition of ectoATPase activity by 5′-FSBA was dose dependent with an ID_{50} of ~0.1 mM (Fig. 5). No further inhibition of activity could be achieved even after a second round of modification with 5′-FSBA.

^{51}Cr-loaded CTL were treated with or without 1 mM 5′-FSBA in the presence of DMF at 37°C for 60 min. The

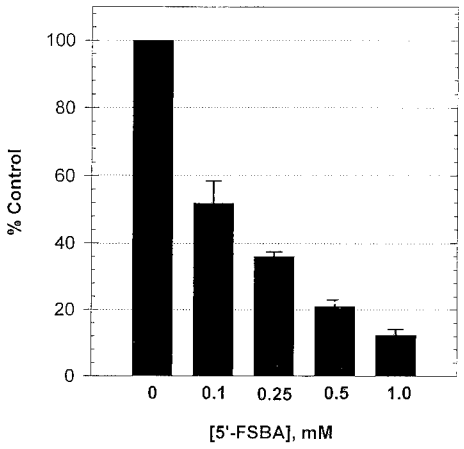

FIGURE 5. Inhibition of ectoATPase by 5′-FSBA. OVA-CTL (1×10^6 cells) were incubated in 200 μl of serum-free RPMI 1640 and 2.5% final concentration of DMF or with the indicated concentrations of 5′-FSBA in DMF for 1 h at 37°C as described in *Materials and Methods.* The CTL were pelleted and resuspended in fresh serum-free RPMI 1640 at a concentration of 1×10^6 cells/ml and assayed for ectoATPase activity as described in *Materials and Methods.* Data are represented as the mean ± SD of triplicate determinations.

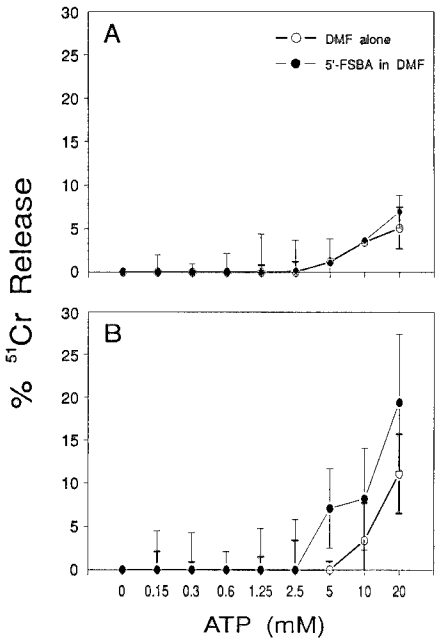

FIGURE 6. Lysis of CTL by extracellular ATP. Alloantigen-specific CTL (B10α-BALB/c CTL) (*A*) or OVA-CTL (*B*) were loaded with 100 to 200 μCi ^{51}Cr at 37°C for 60 min. ^{51}Cr-loaded CTL were then treated with either 1 mM 5′-FSBA dissolved in DMF (●) or with DMF only (○) at 37°C for 60 min. In both instances, the final concentration of DMF was 2.5%. After washing, 1×10^4 of ^{51}Cr-loaded cells were plated into a 96-well, U-bottom plate and incubated with the indicated concentration of ATP in a volume of 200 μl/well. Supernatants were harvested after a 4-h incubation at 37°C and the radioactivity was measured by gamma counting. Specific lysis of ^{51}Cr-loaded target cells is reported as percentage of ^{51}Cr release.

CTL were incubated at 37°C for 4 h with or without various concentrations of exogenous ATP (Fig. 6). The specific ^{51}Cr-release was less than 10% in B10α-BALB/c CTL (Fig. 6*A*) and less than 20% in OVA-CTL (Fig. 6*B*) at 20 mM ATP. There were no statistical differences of ^{51}Cr release between modified and control cells. CTL were no more sensitive to ATP lysis when the ectoATPase activity was inhibited. Thus, we conclude that ectoATPase is not present to protect T cells from the lytic effects of extracellular ATP.

Inhibition of CTL activities

To assess whether modification of ectoATPase affected the cytolytic activity of CTL, B10α-BALB/c CTL and OVA-CTL were pretreated with various concentrations of 5′-FSBA (up to 1 mM) in the presence of DMF, which is necessary for the solubilization of 5′-FSBA. As shown in Figure 7, 2.5% DMF alone did not affect cytolytic activity of either CTL line. However, cytolytic activity of both lines was profoundly inhibited by 5′-FSBA. Inhibition was dose dependent with complete inhibition of cytolytic activity occurring at ~1 mM of 5′-FSBA. Moreover, there was a linear relationship between percentage of specific lysis of targets with increasing E:T ratios at a given concentration of 5′-FSBA (data not shown).

Because 5′-FSBA inhibited the cytolytic activity of $CD8^+$ CTL lines, we next determined whether modification of CTL by 5′-FSBA affected the Ag-induced secretion of lymphokines. CTL do not produce lymphokines if unstimulated or if incubated with an irrelevant Ag, such as EL-4 (Fig. 8). Stimulation with the appropriate Ag triggers release of IFN-γ in both lines. Secretion of IFN-γ was inhibited in both B10α-BALB/c CTL (Fig. 8*A*) and OVA-CTL (Fig. 8*B*) in a dose-dependent manner by 5′-FSBA. B10α-BALB/c CTL were more sensitive to inhibition than OVA-CTL with near complete inhibition occurring at 0.5 mM 5′-FSBA.

Production or secretion of TNF-α by CTL also requires incubation with the appropriate Ag (Fig. 9). The same supernatants that were tested for IFN-γ were screened for TNF-α. TNF-α secretion was also inhibited in a dose-dependent fashion by reaction with 5′-FSBA in both alloantigen-specific CTL (Fig. 9*A*) and OVA-CTL (Fig. 9*B*).

Effect of extracellular adenine nucleotides on CTL activity

Because 5′-FSBA inhibits the cytolytic activity of CTL, the effects of the nucleotides themselves on the cytolytic activity were also examined. ATP, at a concentration of 10 mM, did not cause a significant release of ^{51}Cr from the target cells (Fig. 10). Also, ATP, ADP, and AMP at concentrations of 10 mM did not inhibit the cytolytic activity

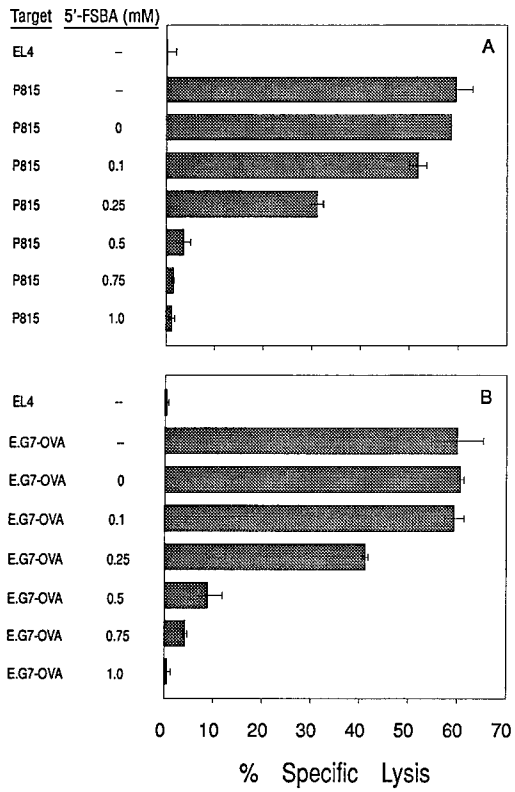

FIGURE 7. Inhibition of CTL activity by 5′-FSBA. B10α-BALB/c CTL (*A*) or OVA-CTL (*B*) were pretreated with various concentrations of 5′-FSBA dissolved in DMF as indicated or with DMF alone (lane = "0") at 37°C for 60 min, or untreated (lane = "–"). In samples containing DMF, the final concentration of this solvent was 2.5%. EL-4, P815, and E.G7-OVA tumor target cells were loaded with 100 to 200 μCi of ^{51}Cr at 37°C for 60 min. After washing, 1×10^5 CTL effector cells were incubated with 1×10^4 ^{51}Cr-labeled target cells (E:T ratio = 10:1) at 37°C for 4 h. Radioactivity of supernatants was measured by gamma counting. Percentage of specific lysis of ^{51}Cr-loaded target cells was calculated as described in *Materials and Methods*.

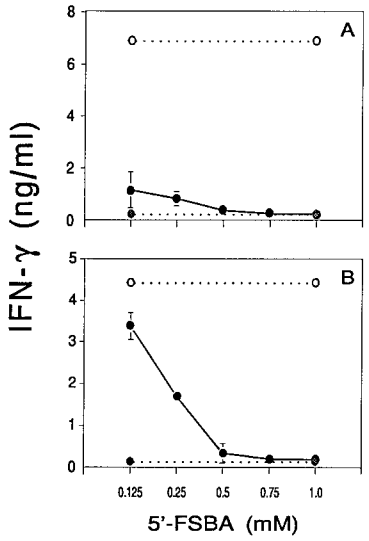

FIGURE 8. Inhibition of IFN-γ production of CTL by 5′-FSBA. B10α-BALB/c CTL (*A*) or OVA-CTL (*B*) were pretreated with various concentrations of 5′-FSBA as indicated, or untreated. CTL effector cells were then incubated with P815 (*A*) or E.G7-OVA (*B*) targets at an E:T ratio of 10:1. After 4 h at 37°C, supernatants were collected and measured for IFN-γ production by ELISA as described in *Materials and Methods*. Untreated B10α-BALB/c CTL incubated with P815 and EL-4 were used as positive and negative controls, displayed as upper and lower dotted lines, respectively (*A*). Untreated OVA-CTL incubated with E.G7-OVA and EL-4 were used as positive and negative controls, displayed as upper and lower dotted lines, respectively (*B*).

of either OVA-CTL (Fig. 10) or the B1OαBALB/c CTL (not shown). The reversible ectoATPase inhibitor, AMP-PNP, inhibited the cytolytic activity of both CTL but required higher concentrations than 5′-FSBA. By contrast, AMPCP was not inhibitory (Fig. 10). Similar results were obtained using the alloantigen-specific CTL (not shown). These results are consistent with the inhibition of cytolytic activity by 5′-FSBA and suggest that the hydrolysis of extracellular ATP is required for the effector cell functions described above.

EctoATPase catalyzes the hydrolysis of ATP to ADP and P_i: an ADPase further degrades the ADP to AMP. This raises the possibility that inhibition of CTL activity by inhibiting ectoATPase activity might be an indirect result of the lack of ADP or AMP. However, exogenous ADP or AMP did not circumvent the 5′-FSBA-induced inhibition of CTL activity (Fig. 11). Thus, hydrolysis of ATP is, most likely, the essential ectoATPase-dependent signal for CTL activation.

Discussion

The alloantigen-specific and OVA-specific $CD8^+$ CTL tested in these experiments express an ectoATPase, confirming earlier studies (33, 34) that demonstrated ATPase activity by a subset of T cells. In addition, we found that these CTL degraded ADP to AMP, suggesting that they also express an ectoADPase. The hydrolysis of both ATP and ADP might be accounted for by the presence of an ectoATPDase (19–23). However, the ATPase and ADPase activities of these CTL are most probably mediated by distinct enzymes because azide, a potent inhibitor of ectoATPDase (19–23), did not inhibit the hydrolysis of ATP observed here.

The nucleotide affinity label 5′-FSBA and nucleotide analogues have allowed us to begin to dissect the role of adenine nucleotides and ectoATPase in the extracellular regulation of CTL. It is clear from the studies presented here, and similar studies on NK cells (31, 32), that ectoATPase is not present to protect effector cells from the postulated lytic effects of extracellular ATP (1, 34). Furthermore, although $CD8^+$ CTL transported adenosine

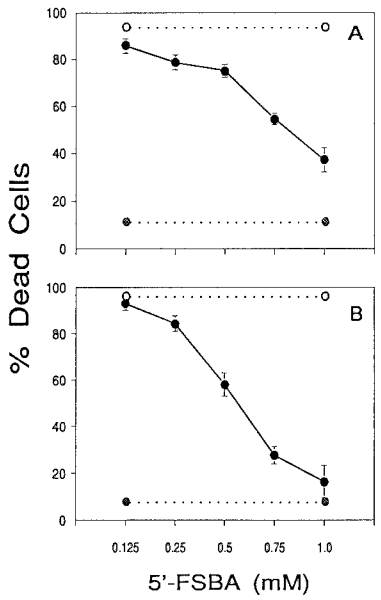

FIGURE 9. Inhibition of TNF-α production of CTL by 5′-FSBA. B10α-BALB/c CTL (*A*) or OVA-CTL (*B*) were pretreated with various concentrations of 5′-FSBA as indicated, or untreated. CTL effector cells were then incubated with P815 (*A*) or E.G7-OVA (*B*) targets at an E:T ratio of 10:1. After 4 h at 37°C, supernatants were harvested, frozen and thawed, and then added to the TNF-α-sensitive WEHI164.13 cells at 200 μl/well in a 96-well, flat-bottomed plate. After incubation at 37°C for 24 h, lysis of WEHL164.13 cells by TNF-α was determined by colorimetric reaction using XTT and PMS. Absorbance was read at 450 nm. The percentage of dead cells was calculated as described in *Materials and Methods*. Untreated B10α-BALB/c CTL incubated with P815 and EL-4 were used as positive and negative controls, displayed as upper and lower dotted lines, respectively (*A*). Untreated OVA-CTL incubated with E.G7-OVA and EL-4 were used as positive and negative controls, displayed as upper and lower dotted lines, respectively (*B*).

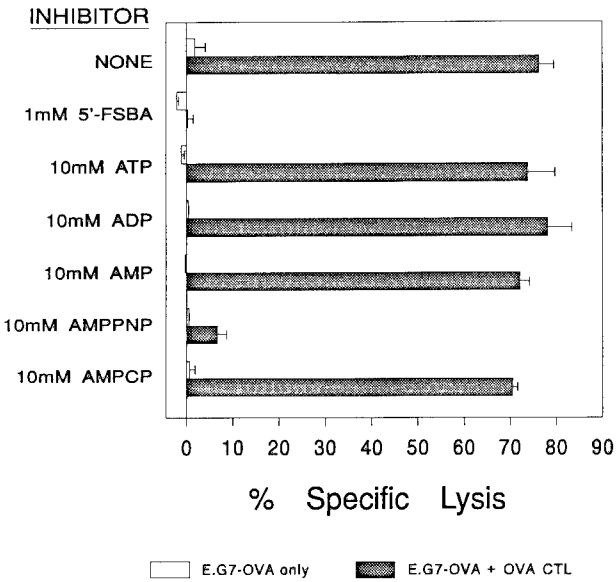

FIGURE 10. Effect of extracellular adenine nucleotides on cytolytic activity. OVA-CTL (1×10^5 cells) were pretreated with the indicated concentrations of 5′-FSBA, ATP, ADP AMP, AMPPNP, or AMPCP at 37°C for 60 min, or untreated. E.G7-OVA tumor target cells were labeled with 100 to 200 μCi of ^{51}Cr at 37°C for 60 min and 1×10^4 ^{51}Cr-loaded target cells were added to 1×10^5 CTL effector cells (E:T ratio = 10:1) and incubated at 37°C for 4 h. The final concentrations of the soluble, reversible inhibitors ATP, ADP, AMP, AMPPNP, and AMPCP were maintained at 10 mM. Radioactivity of supernatants was measured by gamma counting. Lysis of EL-4 targets by OVA-CTL was negligibly low and is not shown.

across the plasma membrane, adenosine was not generated from ATP by CTL, suggesting that the CTL lack ectoAMPase, an enzyme previously identified as CD73 that is expressed by some human T and B cells (24). Lack of ectoAMPase by the CTL was verified directly by measuring the conversion of IMP to inosine. Thus, CTL ectonucleotidases differ from rat liver canalicular membrane ectonucleotidases that are involved in the degradation of ATP to the nucleoside for transport (56). More importantly, $CD8^+$ CTL cells covalently modified by 5′-FSBA lost ectoATPase activity and lost their ability to kill target cells. Inhibition of ectoATPase by AMPPNP also resulted in the inhibition of cytolytic activity. The inhibition of cytolytic activity by AMPPNP was weaker than that produced by 5′-FSBA, probably because AMPPNP is a reversible inhibitor, whereas 5′-FSBA covalently binds to ectoATPase providing irreversible inhibition. Inhibition of CTL activation was not reversed by ADP or AMP, suggesting that hydrolysis of ATP is responsible for signaling rather than indirect mechanisms mediated by the lack of ADP or AMP.

In addition to the inhibition of the cytolytic activity of $CD8^+$ CTL, cytokine secretion from both $CD8^+$ CTL lines was also inhibited in cells modified by 5′-FSBA. The production of INF-γ was more sensitive to inhibition by 5′-FSBA than production of TNF-α in both cell lines. The explanation for these differences in sensitivity is currently unknown.

The inhibition of cytolytic activity in $CD8^+$ CTL is similar to the inhibition of the cytolytic activity by NK cells. In the NK cell system, ectoATPase activity was also inhibited by 5′-FSBA and AMPPNP. Moreover, inhibition of the ectoATPase by 5′-FSBA inhibited natural cytotoxicity (43) and Ab-dependent cellular cytotoxicity by NK cells (33) (K. E. Dombrowski, J. M. Bjorndahl, J. C. Cone, and C. A. Phillips, manuscript in preparation). Like CTL, ADCC by NK cells was not inhibited by ADP. However, NK cell natural cytotoxicity was inhibited by ADP. The explanation for these differences is not clear, but may reflect different activation mechanisms between natural cytotoxicity and ADCC. Differences in the nucleotide inhibition patterns between CTL and NK cells could be

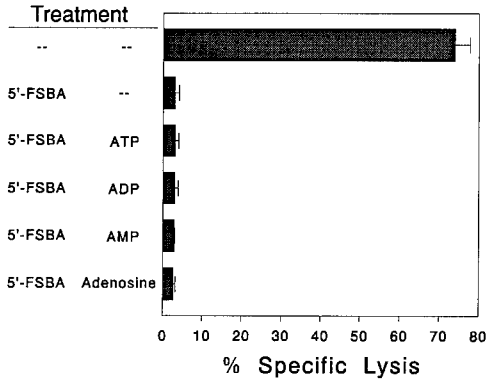

FIGURE 11. Do extracellular adenine nucleotides reverse 5′-FSBA-mediated inhibition of CTL activity? OVA-CTL were pretreated with 1 mM 5′-FSBA at 37°C for 60 min, or untreated. After washing, treated or untreated effector cells were incubated with ^{51}Cr-labeled E.G7-OVA targets at an E:T ratio of 10:1, together with either 1 mM ATP, 1 mM ADP, 1 mM AMP, 1 mM adenosine or medium as indicated. After a 4-h incubation at 37°C, radioactivity in the supernatants was measured by gamma counting. Lysis of EL-4 targets by OVA-CTL was negligibly low and is not shown.

explained by end-product inhibition of ectoATPase by ADP (31). Because NK cells do not express an ecto-ADPase (31), accumulation of ADP might cause feedback inhibition of natural cytotoxicity. By contrast, CTL express an ectoADPase that converts ADP to AMP, thus reducing the potential for feedback inhibition by ADP.

The observations reported above suggest that hydrolysis of ATP by ectoATPase is required for Ag recognition by CTL. It does not seem likely that the inhibition of killing and lymphokine secretion are mediated through a P_2 receptor because 5′-FSBA does not inhibit P_2 purinoceptor-mediated responses (60). Also, both ATP and AMPPNP are agonists of the P_2 class of purinergic receptors (14), but only AMPPNP is an inhibitor (antagonist) of the CTL-mediated killing. Furthermore, if a P_2 receptor was involved in down-regulating cytolytic activity and cytokine secretion, it would be expected that ADP and AMPCP also inhibit these activities because both are also agonists of P_2 receptors. However, neither of these adenine nucleoside diphosphates had any effect on cell-mediated killing. These results suggested that hydrolysis of ADP is not necessary for Ag recognition and that ectoADPase activity serves some other cellular function.

The role of ectoATPase activity in Ag recognition by CTL is not known. In an NK system, inhibition of ectoATPase by 5′-FSBA does not inhibit E:T conjugate formation (43), but does inhibit Ca^{2+} mobilization triggered by cross-linking the FcγRIII receptor (CD16) expressed by these cells (K. E. Dombrowski, J. M. Bjorndahl, J. C. Cone, and C. A. Phillips, manuscript in preparation). In some T cells, exogenous ATP stimulates intracellular Ca^{2+} flux (6, 7), whereas AMPPNP does not (6). In addition, TCR interaction with peptide-MHC complexes or insolubilized anti-receptor Ab induces the mobilization of Ca^{2+} (reviewed in Refs. 61 and 62). Thus, the hydrolysis of extracellular ATP may be an essential step in Ca^{2+} mobilization mediated by TCR and FcR triggering.

EctoATPase activity is not detectable on naive splenic T cells (K. E. Dombrowski, Y. Ke, and J. A. Kapp, unpublished observations) suggesting that expression of the enzyme is a consequence of T cell activation. This is also similar to the NK system in which the ectoATPase is induced by IL-2 and other cytokines (32, 33). The observation that these CTL lines express the enzyme continuously probably reflects the fact that long-term T cell lines do not resume a resting state in vitro. Nevertheless, the ectoATPase is required for activation of these CTL lines by Ag. Whether the enzyme is required for the initial recognition of Ag via the TCR or for a down-stream event cannot be determined from these studies because the assays were performed several hours after interactions between T cells and their targets. Studies are currently underway to examine earlier events after interaction of CTL and target cells.

Acknowledgments

We thank Linda Kapp, Kenneth Brewer, and Aletha Laurent for their excellent technical assistance, Dr. Don Dennis for his valuable discussions, Donna L. Scott for typing this manuscript, and Diantha Steinhilper for her graphic assistance.

References

1. Luthje, J. 1989. Origin, metabolism and function of extracellular adenine nucleotides in the blood. *Klin. Wochenschr. 67:317.*
2. Pizzo, P., M. Murgia, A. Zambon, P. Zanovello, V. Bronte, D. Pietrobon, and F. DiVirgilio. 1992. Role of P_{2Z} purinergic receptors in ATP-mediated killing of Tumor Necrosis Factor (TNF)-sensitive and TNF-resistant L929 fibroblasts. *J. Immunol. 149:3372.*
3. Zheng, L. M., A. Zychlinsky, C.-C. Liu, D. M. Ojcius, and J. D.-E. Young. 1991. Extracellular ATP as a trigger for apoptosis or programmed cell death. *J. Cell Biol. 112:279.*
4. Zanovello, P., V. Bronte, A. Rosato, P. Pizzo, and F. DiVirgilio. 1990. Responses of mouse lymphocytes to extracellular ATP. II. Extracellular ATP causes cell type-dependent lysis and DNA fragmentation. *J. Immunol. 145:1545.*
5. Campbell, C. G., D. C. Spray, and A. W. Wolkoff. 1993. Extracellular ATP^{4-} modulates organic anion transport by rat hepatocytes. *J. Biol. Chem. 268:15399.*
6. Lin, J., R. Krishnaraj, and R. G. Kemp. 1985. Exogenous ATP enhances calcium influx in intact thymocytes. *J. Immunol. 135:3403.*
7. Gouy, H., D. Cefani, S. B. Christensen, P. Debre, and G. Bismuth. 1990. Ca^{2+} influx in human T lymphocytes is induced independently of inositol phosphate production by mobilization of intracellular Ca^{2+} stores: a study with the Ca^{2+} endoplasmic reticulum-ATPase inhibitor thapsigargin. *Eur. J. Immunol. 20:2269.*
8. Gerwins, P., and B. B. Fredholm. 1992. ATP and its metabolite adenosine act synergistically to mobilize intracellular calcium via the formation of inositol 1,4,5-trisphosphate in a smooth muscle cell line. *J. Biol. Chem. 267:16081.*
9. Chueh, S.-H., and L.-S. Kao. 1993. Extracellular ATP stimulates calcium influx in neuroblastoma × glioma hybrid NG108–15 cells. *J. Neurochem. 61:1782.*
10. Chueh, S.-H., L.-S. Hu, and S.-L. Song. 1994. Two distinct ATP signaling mechanisms in differentiated neuroblastoma × glioma hybrid NG108–15 cells. *Mol. Pharmacol. 45:532.*

11. Chueh, S.-H., and L.-S. Kao. 1994. Calcium signaling induced by bradykinin is synergistically enhanced by high K^+ in NG108–15 cells. *Am. J. Physiol. 266 (Cell Physiol. 35):C1006.*
12. Pelleg, A., C. M. Hurt, and E. L. Michelson. 1990. Cardiac effects of adenosine and ATP. *Ann. NY Acad. Sci. 603:19.*
13. Williams, M. 1990. Purine nucleosides and nucleotides as central nervous system modulators. *Ann. NY Acad. Sci. 603:93.*
14. Burnstock, G. 1990. Overview: purinergic mechanisms. *Ann. NY Acad. Sci. 603:1.*
15. DePierre, J. W., and M. L. Karnovsky. 1974. Ecto-enzymes of the guinea pig polymorphonuclear leukocyte. II. Properties and suitability as markers for the plasma membrane. *J. Biol. Chem. 249:7121.*
16. Karnovsky, M. L. 1986. In *Cellular Biology of Ectoenzymes.* G. W. Kreutzberg, M. Reddington, and H. Zimmerman, eds. Springer-Verlag, Berlin, pp. 1–13.
17. Lin, S.-H. 1990. Liver plasma membrane ecto-ATPase: purification, localization, cloning and functions. *Ann. NY Acad. Sci. 603:394.*
18. Moodie, F. D. L., H. Baum, P. J. Butterworth, and T. J. Peters. 1991. Purification and characterisation of bovine spleen ADPase. *Eur. J. Biochem. 202:1209.*
19. Picher, M., R. Beliveau, M. Potier, D. Savaria, E. Rousseau, and A. R. Beaudoin. 1994. Demonstration of an ectoATP-diphosphohydrolase (E. C.3.6.1.5.) in non-vascular smooth muscles of the bovine trachea. *Biochim. Biophys. Acta. 1200:167.*
20. Picher, M., Y. P. Cote, R. Beliveau, M. Potier, and A. R. Beaudoin. 1993. Demonstration of a novel type of ATP-diphosphohydrolase (EC 3.6.1.5) in the bovine lung. *J. Biol. Chem. 268:4699.*
21. Cote, Y. P., M. Picher, P. St-Jean, R. Beliveau, M. Potier, and A. R. Beaudoin. 1991. Identification and localization of ATP-diphosphohydrolase (apyrase) in bovine aorta: relevance to vascular tone and platelet aggregation. *Biochim. Biophys. Acta 1078:187.*
22. Cote, Y. P., J. G. Filep, B. Battistini, J. Gauvreau, P. Sirois, and A. R. Beaudoin. 1992. Characterization of ATP-diphosphohydrolase activities in the intima and media of the bovine aorta: evidence for a regulatory role in platelet activation in vitro. *Biochim. Biophys. Acta 1139:133.*
23. Cote, Y. P., S. Ouellet, and A. R. Beaudoin. 1992. Kinetic properties of type-II ATP diphosphohydrolase from the tunica media of the bovine aorta. *Biochem. Biophys. Acta 1160:246.*
24. Dorken, B., P. Moller, A. Pezzotto, R. Schwartz-Albiez, and G. B. Moldenhauer. 1989. Cell antigens: CD73. In *Leucocyte Typing IV: White Cell Differentiation Antigens,* W. Knapp, B. Dörken, E. P. Rieber, H. Stein, W. R. Gilks, R. E. Schmidt, A. E. G. Kr. von dem Borne, eds. Wiley, New York and Oxford, UK, pp. 102–104.
25. Schrader, J., R. M. Berne, and R. Rubio. 1972. Uptake and metabolism of adenosine by human erythrocyte ghosts. *Am. J. Physiol. 223:159.*
26. Kragballe, K., and J. Ellegaard. 1978. ATPase activity of purified human normal T- and B-lymphocytes. *Scand. J. Haematol. 20:271.*
27. Barankiewicz, J., M. Hui, A. Cohen, and H.-M. Dosch. 1989. Differential expression of ecto-nucleotide metabolic enzymes during immunoglobulin gene rearrangements in human pre-B-cells. *Adv. Exp. Med. Biol. 253B:455.*
28. Barankiewicz, J., H.-M. Dosch, R. Cheung, and A. Cohen. 1979. Relationship between extracellular and intracellular nucleotide metabolism in human lymphocytes. *Adv. Exp. Med. Biol. 253B:475.*
29. Barankiewicz, J., and A. Cohen. 1990. Extracellular ATP metabolism in B and T lymphocytes. *Ann. NY Acad. Sci. 603:380.*
30. Steinberg, T. H., H. P. Buisman, S. Greenberg, F. DiVirgilio, and S. C. Silverstein. 1990. Effects of extracellular ATP on mononuclear phagocytes. *Ann. NY Acad. Sci. 603:120.*
31. Dombrowski, K. E., J. M. Trevillyan, J. C. Cone, Y. Lu, and C. A. Phillips. 1993. Identification of an ectoATPase expressed by the human natural killer cell line NK3.3. *J. Immunol. 150:208A (Abstr. 1188).*
32. Dombrowski, K. E., J. C. Cone, and C. A. Phillips. 1993. Identification and functional role of an ectoATPase activity associated with NK33 cells. *Natural Immunity 11:290.*
33. Bajpai, A., and Z. Brahmi. 1993. Regulation of resting and IL-2-activated human cytotoxic lymphocytes by exogenous nucleotides: role of IL-2 and ectoATPases. *Cell. Immunol. 148:130.*
34. Filippini, A., R. E. Taffs, T. Agui, and M. V. Sitkovsky. 1990. EctoATPase activity in cytolytic T-lymphocytes: protection from the cytolytic effects of extracellular ATP. *J. Biol. Chem. 265:334.*
35. Dianzani, U., V. Redoglia, M. Bragardo, C. Attisano, A. Bianchi, D. DiFranco, U. Ramenghi, H. Wolff, L. F. Thompson, A. Pileri, and M. Massaia. 1993. Co-stimulatory signal delivered by CD73 molecule to human $CD45RA^{hi}CD45RO^{lo}$ (naive) $CD8^+$ T lymphocytes. *J. Immunol. 151:3961.*
36. Edwards, N. L., E. W. Gelfand, L. Burk, H.-M. Dosch, and I. H. Fox. 1979. Distribution of 5′-nucleotidase in human lymphoid tissues. *Proc. Natl. Acad. Sci. USA 76:3474.*
37. Thompson, L. F., J. M. Ruedi, R. D. O'Connor, and J. F. Bastian. 1986. Ecto-5′-nucleotidase expression during human B cell development: an explanation for the heterogeneity in B lymphocyte ecto-5′-nucleotidase activity in patients with hypogammaglobulinemia. *J. Immunol. 137:2496.*
38. Massaia, M., L. Perrin, A. Bianchi, J. Ruedi, C. Attisano, D. Altieri, G. T. Rijkers, and L. F. Thompson. 1990. Human T cell activation: synergy between CD73 (ecto-5′-nucleotidase) and signals delivered through CD3 and CD2 molecules. *J. Immunol. 145:1664.*
39. Massaia, M., A. Pileri, M. Boccadoro, A. Bianchi, A. Palumbo, and U. Dianzani. 1988. The generation of alloreactive cytotoxic T lymphocytes requires the expression of ecto-5′-nucleotidase activity. *J. Immunol. 141:3768.*
40. Thompson, L. F., J. M. Ruedi, A. Glass, M. G. Low, and A. H. Lucas. 1989. Antibodies to 5′-nucleotidase (CD73), a glycosyl-phosphatidylinositol-anchored protein, cause human peripheral blood T cells to proliferate. *J. Immunol. 143:1815.*
41. Colman, R. F. 1989. Affinity labeling. In *Protein Function: A Practical Approach.* IRL Press, Oxford, UK, p. 77.
42. Bennett, J. S., R. F. Colman, and R. W. Colman. 1978. Identification of adenine nucleotide binding proteins in human platelet membranes by affinity labeling with 5′-p-fluorosulfonyl benzoyl adenosine. *J. Biol. Chem. 253:7346.*
43. Dombrowski, K. E., J. C. Cone, J. M. Bjorndahl, and C. A. Phillips. 1995. Irreversible inhibition of human natural killer cell natural cytotoxicity by modification of the extracellular membrane by the adenine nucleotide analogue 5′-*p*-(fluorosulfonyl)benzoyl adenosine. *Cell. Immunol. 160:199.*
44. Pal, P. K., W. J. Wechter, and R. F. Colman. 1975. Affinity labeling of the DPNH site of bovine liver glutamate dehydrogenase by 5-fluorosulfonyl benzoyl adenosine. *J. Biol. Chem. 250:8140.*
45. Ke, Y., R. L. Hunter, and J. A. Kapp. 1995. Induction of humoral and cytolytic responses by ovalbumin in TiterMax or a new synthetic co-polymer. *Vaccine Res. 4:1.*
46. Ke, Y., Y. Li, and J. A. Kapp. 1995. Ovalbumin injected with complete Freund's adjuvant stimulates cytolytic responses. *Eur. J. Immunol. 25:549.*
47. Moore, M. W., R. R. Carbone, and M. J. Bevan. 1988. Introduction of soluble protein into the class I pathway of antigen processing and presentation. *Cell 54:777.*
48. Espevik, T., and J. Nissen-Meyer. 1986. A highly sensitive cell line, WEHI 164 clone 13, for measuring cytotoxic factor/tumor necrosis factor from human monocytes. *J. Immunol. Methods 95:99.*
49. Li, Y., Y. Ke, P. D. Gottlieb, and J. A. Kapp. 1994. Delivery of exogenous antigen into the major histocompatibility complex class I and class II pathways by electroporation. *J. Leukocyte Biol. 56:616.*
50. Carbone, F. R., S. J. Sterry, M. Butler, S. Rodda, and M. W. Moore. 1992. T cell receptor alpha-chain determines the specificity of residue 262 within the Kb-restricted, ovalbumin 257–264 determinant. *Int. Immunol. 4:861.*
51. Rotzschke, O., K. Falk, S. Stevanovic, G. Jung, P. Walden, and H.-G. Rammensee. 1991. Exact prediction of a natural T cell epitope. *Eur. J. Immunol. 21:2891.*
52. Lin, S.-H. 1985. The rat liver plasma membrane high affinity (Ca^{2+}-Mg^{2+})-ATPase is not a calcium pump: comparison with ATP-dependent calcium transporter. *J. Biol. Chem. 260:10976.*

53. Carofoli, E. 1994. Biogenesis: plasmic membrane calcium ATPase: 15 years of work on the purified enzyme. *FASEB J. 8:993.*
54. Harvey, W. R. 1992. Physiology of V-ATPases. *J. Exp. Biol. 171:1.*
55. Thompson, L. F., G. R. Boss, H. L. Spiegelberg, I. V. Jansen, R. D. O'Connor, T. A. Waldman, R. N. Hamburger, and J. E. Seegmiller. 1979. Ecto-5′-nucleotidase activity in T and B lymphocytes from normal subjects and patients with congenital X-linked aggammaglobulinemia. *J. Immunol. 123:2475.*
56. Che, M., T. Nishida, Z. Gatmaitan, and I. M. Arias. 1992. A nucleoside transporter is functionally linked to ectonucleotidases in rat liver canalicular membrane. *J. Biol. Chem. 267:9684.*
57. Brunner, K. T., H. Engers, and J. C. Cerrotini. 1976. The ^{51}Cr release assay as used for quantitative measurement of cell-mediated cytolysis in vitro. In *In Vitro Methods in Cell Mediated and Tumor Immunity.* B. R. Bloom and J. R. David, eds. Academic Press, N.Y., pp. 423–428.
58. Roehm, N. W., G. H. Rodgers, S. M. Hatfield, and A. L. Glasbrook. 1991. An improved colorimetric assay for cell proliferation and viability utilizing the tetrazolium salt XTT. *J. Immunol. Methods 142: 257.*
59. Resta, R., S. W. Hooker, A. B. Laurent, J. K. Shuck, Y. Misumi, Y. Ikehara, G. A. Koretzky, and L. F. Thompson. 1994. Glycosyl phosphatidylinositol membrane anchor is not required for T cell activation through CD73. *J. Immunol. 153:1046.*
60. Fedan, J. S., and S. J. Lamport. 1990. P2-purinoceptor antagonists. *Ann. NY Acad. Sci. 603:182.*
61. Fitch, F. W., M. D. McKisic, D. W. Lancki, and T. F. Gajewski. 1993. Differential regulation of murine T lymphocyte subsets. *Annu. Rev. Immunol. 11:29.*
62. Abbas, A. K., M. E. Williams, H. J. Burstein, T.-L. Chang, P. Bossu, and A. H. Lichtman. 1991. Activation and functions of $CD4^+$ T-cell subsets. *Immunol. Rev. 123:5.*

ANTIGEN-SPECIFIC CYTOTOXIC T-LYMPHOCYTE (CTL) RESPONSE INDUCED BY TUMOR-SPECIFIC MUC1 MUCIN PEPTIDE FROM HUMANS WITH ADENOCARCINOMAS.

Stephen E. Wright,[1,2] Karen E. Lowe, Sohel Talib, Lydia Kilinski, Kenneth E. Dombrowski,[1] Jane S. Lebkowski, and Ramila Philip. [1]Veterans Administration Medical Center and Depts. of [1]Internal Medicine, and [2]Cell Biology and Biochemistry, Texas Tech University Health Sciences Center, Amarillo, TX 79106 and Depts. of Molecular Biology and Cancer Biology, Applied Immune Sciences, Inc. Santa Clara, CA 95054.

One of the challenging goals in breast cancer immunotherapy is to increase tumor-specific cell-mediated immune response. Mucins are glycoproteins expressed by ductal epithelial cells of a variety of tissues, including breast, ovary and pancreas. Breast, ovarian and pancreatic carcinomas produce an abundance of highly immunogenic, aberrantly glycosylated mucins with shorter carbohydrate side chains than those of mucins expressed by nonmalignant cells. Tumor-specific epitopes are exposed in the hypoglycosylated mucin, and it has been shown that deglycosylated normal mucin can induce tumor-specific monoclonal antibodies. Our approach is to use IL-2 and immunogenic mucin peptide ligands to activate and expand CTL from humans with adenocarcinomas that will recognize the tumor-specific epitope. It has been observed that the T-cell receptor (TCR) Vβ repertoire may be restricted in humans with cancer. Since the TCR is involved in antigen recognition, T-cell activation, and the triggering of effector functions, it is of considerable significance to determine the TCR Vβ repertoire expressed by cells which have been treated with IL-2 and MUC1 mucin peptides. We have expanded peripheral blood lymphocytes from humans with adenocarcinomas using a native MUC1 mucin tandem repeat peptide (MUC1-mtr_1), a ($T^3 \rightarrow N^3$)MUC1-mtr_1 or immobilized anti-CD3, in the presence of IL-2 for a period of 14 days. The data indicate that the peptide-stimulated and expanded T-cells show antigen specific changes which were not induced by polyclonal activation and expansion.

Introduction

Mucins are polymorphic, O-linked glycosylated proteins expressed on the surface of ductal epithelial cells. The extracellular domain of mucins consists of 25 to 100 or more tandem repeats of a 20 amino acid sequence (1,2). The mucin glycosylation level is lower in cancer cells than in normal cells of ductal epithelial tissues (e.g., breast, ovary or pancreas) (3). This hypoglycosylation may result in the exposure of tumor-specific epitopes which are hidden in the fully glycosylated mucin. Some monoclonal antibodies raised against deglycosylated mucin have been shown to be tumor-specific (4-6). Previous studies showed that anti-mucin cytotoxicity is major histocompatibility complex (MHC) unrestricted. It is hypothesized that the mucin epitope can bind and activate the TCR in the absence of antigen processing and MHC presentation because of its highly repetitive , multivalent structure (7,8). Tumor-associated mucins may be effective target antigens for CTL in cancer immunotherapy.

Our aim is to stimulate and expand CTL that will specifically recognize and lyse adenocarcinoma cells. The strategy is to use tumor-specific mucin peptides to prime and activate T-cells from humans with adenocarcinomas, and to select CTL with the appropriate functional activity. We are using two mucin tandem repeat (mtr) peptides:

Native mucin (MUC1-mtr_1) **PDTRPADGSTAPPAHGVTSA**

Mutant mucin ([$T^3 \rightarrow N^3$]MUC1-mtr_1) **PDNRPADGSTAPPAHGVTSA**

The monoclonal antibody (mAb) tumor-specific epitope is PDTRP. T^3 is mutated to N^3 in ($T^3 \rightarrow N^3$)MUC1-mtr_1. Both peptides are recognized by the tumor-specific anti-mucin monoclonal antibody SM3, indicating that the T to N substitution does not alter antibody cross-reactivity. We determined the phenotype, proliferation, and cytotoxicity of T-cells from humans with adenocarcinomas which were cultured with mucin peptides. In order to see whether a dominant TCR repertoire develops in these cells in response to the tumor-specific mucin stimulation, we analyzed the patterns of TCR Vβ expression.

Materials and Methods

Cell culture conditions. Mononuclear cells (MC) from humans with adenocarcinomas were isolated by Ficoll-Hypaque density gradient centrifugation. Cells were cultured in AIM-V® serum free lymphocyte medium (GIBCO-BRL) in a 37°C humidified 5% CO_2 incubator as detailed below.

(a) MC were cultured with 100 IU/ml IL-2 and either 1 ug/ml MUC1-mtr_1 or 1 ug/ml ($T^3 \rightarrow N^3$)MUC1-mtr_1 for 14 days. The cells were harvested on day 17 (controls) or washed on day 14 and restimulated with either 1 ug/ml MUC1-mtr_1 or ($T^3 \rightarrow N^3$)MUC1-mtr_1 for 3 days and harvested on day 17.

(b) CD3 T cells were isolated from MC on day 0 on AIS CD3 microCELLector™ T-25 flasks containing immobilized anti-CD3 mAb. The adherent CD3 cells were cultured with 600 IU/ml IL-2. The cells were harvested on day 17 (controls) or washed on day 14 , cultured with either 1 ug/ml MUC1-mtr_1 or ($T^3 \rightarrow N^3$)MUC1-mtr_1, and harvested on day 17.

(c) CD3 T cells were isolated as in (b), and cultured with 600 IU/ml IL-2. On day 10, CD8 T cells were isolated from the CD3 cells using AIS CD8 microCELLector™ T-25 flasks. The adherent CD8 cells were harvested on day 17 (controls), or were washed on day 14, cultured with either 1 ug/ml MUC1-mtr_1 or ($T^3 \rightarrow N^3$)MUC1-mtr_1, and harvested on day 17.

(d) CD3 T cells were isolated as in (b), treated with 1 ug/ml soluble anti-CD28 mAb on day 0 and 600 IU/ml IL-2 on day 1. CD8 cells were isolated on day 10 and cultured as in (c).

Phenotyping. Cells (5 x 10^5 per aliquot) were obtained from day 13 ex vivo cultures, stained with fluorochrome-conjugated mAbs against CD4, CD8, CD56, and CD28, and analyzed by flow cytometry using the Becton Dickinson FACScan/Lysis II™ system.

Proliferation assays. Cells were adjusted to 1 x 10^6 cells/ml and dispensed at 100 ul per well of microtiter plates. Cells were incubated for 2 days, pulsed with [^{3}H]thymidine (1.0 uCi per well) and harvested after 24 hr. Radioactivity was measured by liquid scintillation counting.

Cytotoxicity assays. MCF7 breast cancer cell line which expresses underglycosylated mucin was used as the target cell line in a standard

chromium release assay. The MCF7 cells were labeled with ^{51}Cr (200 uCi per 1 x 10^7 cells) and 5 x 10^3 target cells/well were added to triplicate wells of microtiter plates. The effector cells were tested at indicated effector/target ratios. AIM-V medium was added in place of effector cells to the spontaneous ^{51}Cr release control wells. 10% Triton X-100 was added instead of effector cells to the maximum target lysis control wells. Cells were incubated for 4 hr. The supernatants were harvested and the radioactivity measured by liquid scintillation counting. The specific cytotoxicity was calculated by:

$$\% \text{ lysis} = \frac{(\text{mean experimental cpm} - \text{mean spontaneous cpm}) \times 100}{(\text{mean maximum cpm} - \text{mean spontaneous cpm})}$$

TCR Vβ analysis. For RT-PCR, mRNA was isolated from cells (≥ 10^6 per sample) using the Invitrogen Micro-FastTrack™ mRNA kit according to manufacturer's instructions. First strand cDNA was prepared from the poly(A)$^+$ mRNA using oligo dT primer and MMLV reverse transcriptase according to the GIBCO-BRL SuperScript™ protocol. The cDNA was amplified by Taq DNA polymerase in a 50 ul PCR for each of the 24 known TCR Vβ gene families. The PCR primers were from the Vβ T-Cell Receptor Typing Amplimer kit (Clontech), and were designed to have similar T_m's. The PCR profile was: denaturation at 94°C for 30 s, annealing at 55°C for 30 s, and extension at 72°C for 60 s for 30 cycles, followed by final extension at 72°C for 7 min on a Perkin Elmer Cetus 480 DNA thermal cycler. The amplified products were analyzed by 2% agarose gel electrophoresis and scanning laser densitometry (Molecular Dynamics 300A/ImageQuant system).

Conclusions

1.Tumor-specific mucin peptides provide a promising approach to stimulate the proliferation and tumor-specific cytotoxicity of CTL from MC of humans with adenocarcinomas.

2.The cultured MC exhibited greater proliferative and cytotoxic responses after mucin treatment than did $CD3^+$ or $CD8^+$ cells. The other (non-T) cells among the MC may serve as antigen presenting cells which, although unnecessary for T cell stimulation by mucin, may further enhance the mucin effects.

3.The native and mutant mucin peptides induced different TCR Vβ repertoires in the MC and $CD3^+$ cells. These results indicate that the single T to N amino acid substitution in the mAb tumor-specific mucin epitope can influence the mucin-TCR interaction.

4.Further studies are needed to establish the optimal culture conditions for expanding tumor-specific CTL subpopulations from MC, and to determine mucin peptide sequences that will produce the most effective CTL for cancer immunotherapy.

References

1.Gendler, S.J., Taylor-Papadimitriou, J., Duhig, T., Rothbard, J., and Burchell, J. (1988) J. Biol. Chem., 263, 12820-12823.

2.Lan, M.S., Batra, S.K., Qi, W.-N., Metzgar, R.S., Hollingsworth, M. A. (1990) J. Biol. Chem., 265, 15294-15299.

3.Hanisch, F.G., Uhlenbruck, G., Peter-Katalinic, J., Egge, H., Dabrowski, J., and Dabrowski, U. (1989) J. Biol. Chem., 264, 872-883.

4.Burchell, J., Gendler, S.J., Taylor-Papadimitriou, J., Girling, A., Lewis, A., Millis, R., and Lamport, D. (1987) Cancer Res., 47, 5476-5482.

5.Linsley, P.S., Brown, J.P., Magnani, J.L., and Horn, D. (1988) Cancer Res., 48, 2138-2148.

6.Perey, L., Hayes, D.F., Maimonis, P., Abe, M., O'Hara, C., and Kufe, D.W. (1992) Cancer Res., 52, 2563-2568.

7.Jerome, K.R., Barnd, D.L., Bendt, K.M., Boyer, C.M., Taylor-Papadimitriou, J., McKenzie, I.F.C., Bast, Jr., R.C., and Finn, O.J. (1991) Cancer Res., 51, 2908-2916.

8.Barnd, D.L., Lan, M., Metzgar, R.S., and Finn, O.J. (1989) Proc. Natl. Acad. Sci. USA, 86, 7159-7163.

Figure Legends:

Figure 1. Mucin Peptide Induced Expansion of CTL. PBMC from a breast cancer patient was cultured in the presence of anti-CD3, MUC1-mtr_1 + 100IU/ml rhIL2 or ($T^3 \rightarrow N^3$)MUC1-mtr_1 + 100 IU/ml IL2 for 14 days. The cells were counted on day 14 and fold expansion was calculated. Anti-CD3 activated cultures showed the highest level of expansion compared to the peptide stimulated cultures. Both MUC1-mtr_1 and ($T^3 \rightarrow N^3$)MUC1-mtr_1 showed comparable expansion.

Figure 2. Phenotype Analysis After Mucin Peptide Stimulation. a. mAbs used are for helper T cells (CD4), cytotoxic T cells (CD8), natural killer cells (CD56) and activated T cells (CD28). The PBMC cultured with MUC1-mtr_1 and the PBMC cultured with ($T^3 \rightarrow N^3$)MUC1-mtr_1 had similar profiles with respect to $CD4^+$(40%), $CD8^+$(30%), $CD56^+$(35-38%), and $CD28^+$(54-59%) subpopulations. The $CD3^+$T cell population had the expected $CD4^+$(49%), $CD8^+$(50%) composition and a slightly higher level of $CD28^+$(79%) cells. The $CD3^+$T cells treated with soluble anti-CD28 mAb displayed the highest level of $CD28^+$ cells (94%). b. In addition to CD4, CD8 and CD56, mAbs for memory T cells (CD45RO) and naive T cells (CD45RA) were used.

Figure 3. Proliferative Response After Peptide Restimulation. Proliferative response after mucin peptide treatment was highest for PBMC cultured initially with the mutant ($T^3 \rightarrow N^3$)MUC1-mtr_1. The PBMC cultured initially with the MUC1-mtr_1 proliferated slightly better than the $CD8^+$ cells cultured with or without the anti-CD28 mAb. The $CD8^+$ cells had been treated with mucin only during the last 3 days of culture. There was little difference in PBMC response to the MUC1-mtr_1 and ($T^3 \rightarrow N^3$)MUC1-mtr_1 peptides administered during the 3 day restimulation.

Figure 4. Cytotoxic Response After Peptide Restimulation (MCF7). Cytotoxic response against the MCF7 breast cancer cell line (effector/target ratios of (a)40:1 or (b) lower) was higher for the PBMC treated with either peptide than for the $CD3^+$ cells which had been exposed to either of the mucin peptides only during the last 3 or 5 days of culture.

Figure 5. TCR Analysis of Mucin Peptide Stimulated PBMC Cultures. a.-d. The predominant TCR Vß families expressed were Vß2, Vß4, Vß13, and Vß14. MUC1-mtr_1 and ($T^3 \rightarrow N^3$)MUC1-mtr_1 peptides had strikingly different effects. In general, the PBMC treated with MUC1-mtr_1 from day 0 expressed higher levels of Vß2, Vß4 and Vß14 than did the corresponding PBMC treated with ($T^3 \rightarrow N^3$)MUC1-mtr_1 from day 0. ($T^3 \rightarrow N^3$)MUC1-mtr_1 given to PBMC during the 3 day restimulation period drastically inhibited Vß expression, regardless of the initial mucin peptide treatment. The $CD3^+$ cells that had been given MUC1-mtr_1 during the last 3 days of culture showed enhanced Vß2 and Vß14, and decreased Vß13 compared to the mucin-free control. The ($T^3 \rightarrow N^3$)MUC1-mtr_1 repressed Vß2, Vß13 and Vß14 expression by the $CD3^+$ cells, but boosted the Vß4 expression by $CD3^+$ cells over two-fold compared to the mucin-free control or the MUC1-mtr_1 treatment. e. PBMCs were stimulated for 14 days and then restimulated for 3 days with indicated stimulants. Vβ gene expression was then determined by PCR of RNA of the cells.

Figure 6. Phenotype Analysis after Mucin Peptide Activation. Day 29 *ex vivo* phenotype analysis of an ovarian TIL using mAbs for helper T cells (CD4), cytotoxic T cells (CD8),

natural killer cells (CD56), memory T cells (CD45RO) and naive T cells (CD45RA). TIL cultured with IL2 alone, MUC1-mtr_1+IL2 or the ($T^3 \rightarrow N^3$)MUC1-mtr_1+IL2 had similar profiles with respect to the phenotype. All the three conditions had predominant $CD4^+$ and $CD45RO^+$ T cells. Both IL2 and ($T^3 \rightarrow N^3$)MUC1-mtr_1 cultured TIL showed a slight increase in $CD8^+$ T cells as compared to the MUC1-mtr_1 cultured T cells.

Figure 7. Cytotoxic Response After Mucin Peptide Stimulation (MCF7). Cytotoxic response against MCF7 target as measured by ^{51}Cr release assay was performed using ovarian TIL cultured with IL2 and peptides as effectors. TIL cultured in IL2 alone did not show any lysis against MCF7 at either 20:1 or 10:1 effector target ratios, whereas, both peptide stimulated cultures showed a significant level of lysis. Furthermore, ($T^3 \rightarrow N^3$)MUC1-mtr_1 stimulated T cells showed the highest level of lysis against the MCF7 target.

Figure 8. TCR Analysis of Mucin Peptide Stimulated Ovarian TIL. TCR analysis of ovarian TIL cultured in IL2 or peptides was performed. On day 29 the cells were harvested and TCR analysis was performed using an RNase protection assay. TIL cultured with IL2 alone showed Vβ 13.2 and 22.1 predominant populations of T cells. However, MUC1-mtr_1 stimulated cultures showed Vß 18.1 as the predominant population. Similarly, ($T^3 \rightarrow N^3$)MUC1-mtr_1 cultured TIL showed predominant Vß 2.1 and 5.2 positive population.

Fig.1

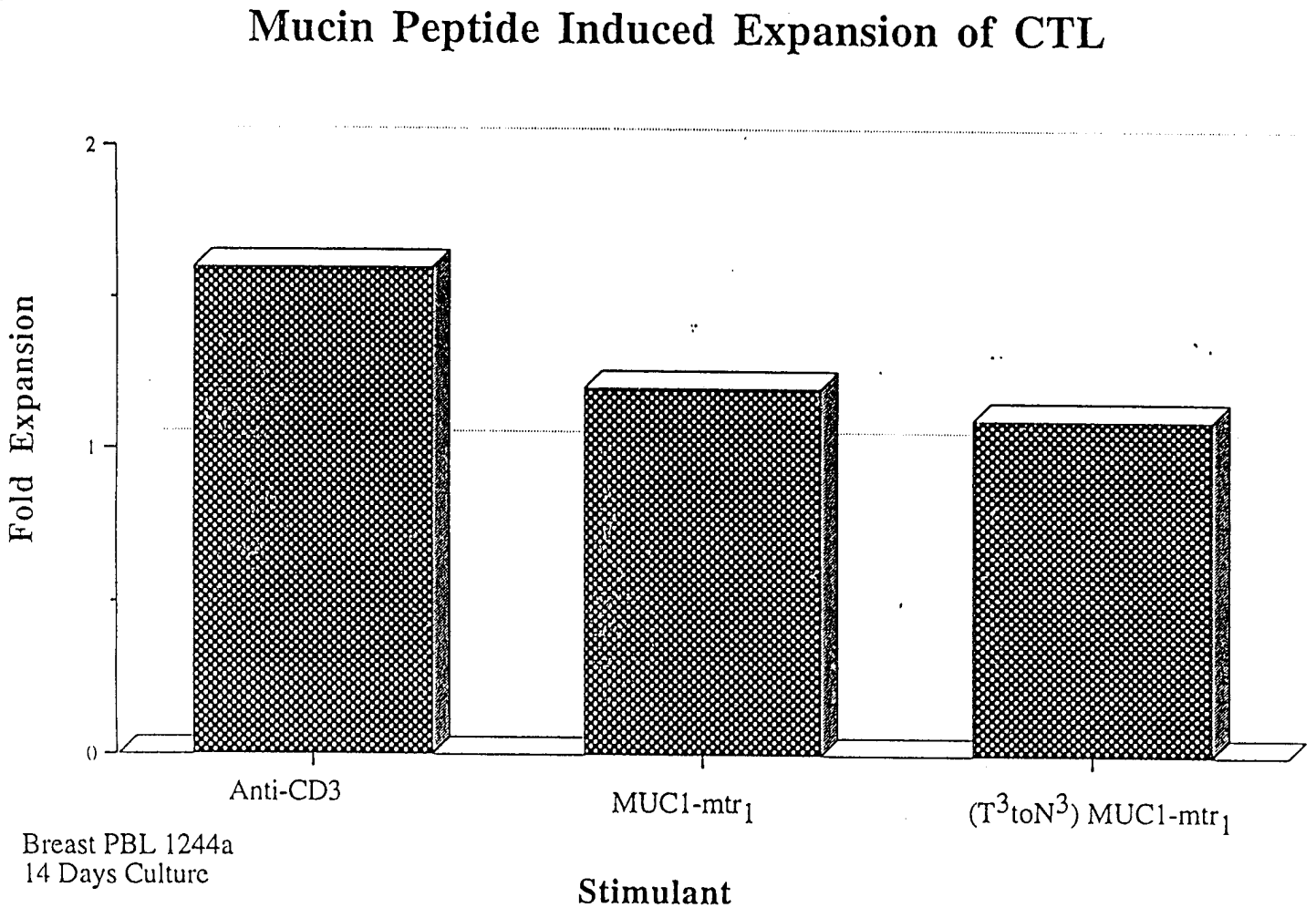
Mucin Peptide Induced Expansion of CTL
Fold Expansion
2
1
0
Anti-CD3
MUC1-mtr1
(T3toN3) MUC1-mtr1
Breast PBL 1244a
14 Days Culture
Stimulant

Fig.2a

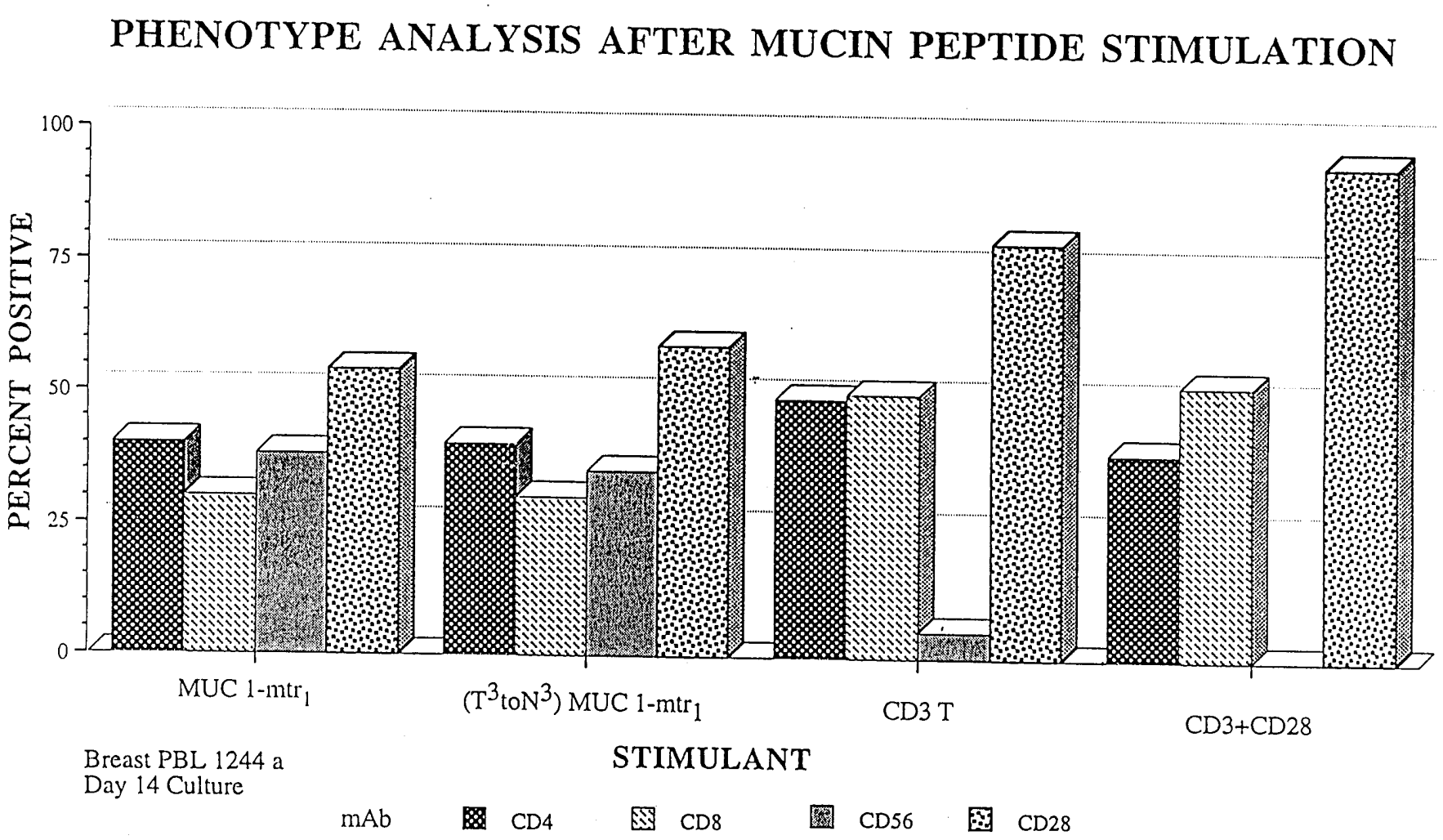
PHENOTYPE ANALYSIS AFTER MUCIN PEPTIDE STIMULATION
PERCENT POSITIVE
100
75
50
25
0
MUC 1-mtr1
(T3toN3) MUC 1-mtr1
CD3 T
CD3+CD28
STIMULANT
Breast PBL 1244 a
Day 14 Culture
mAb
CD4
CD8
CD56
CD28

Fig.2b

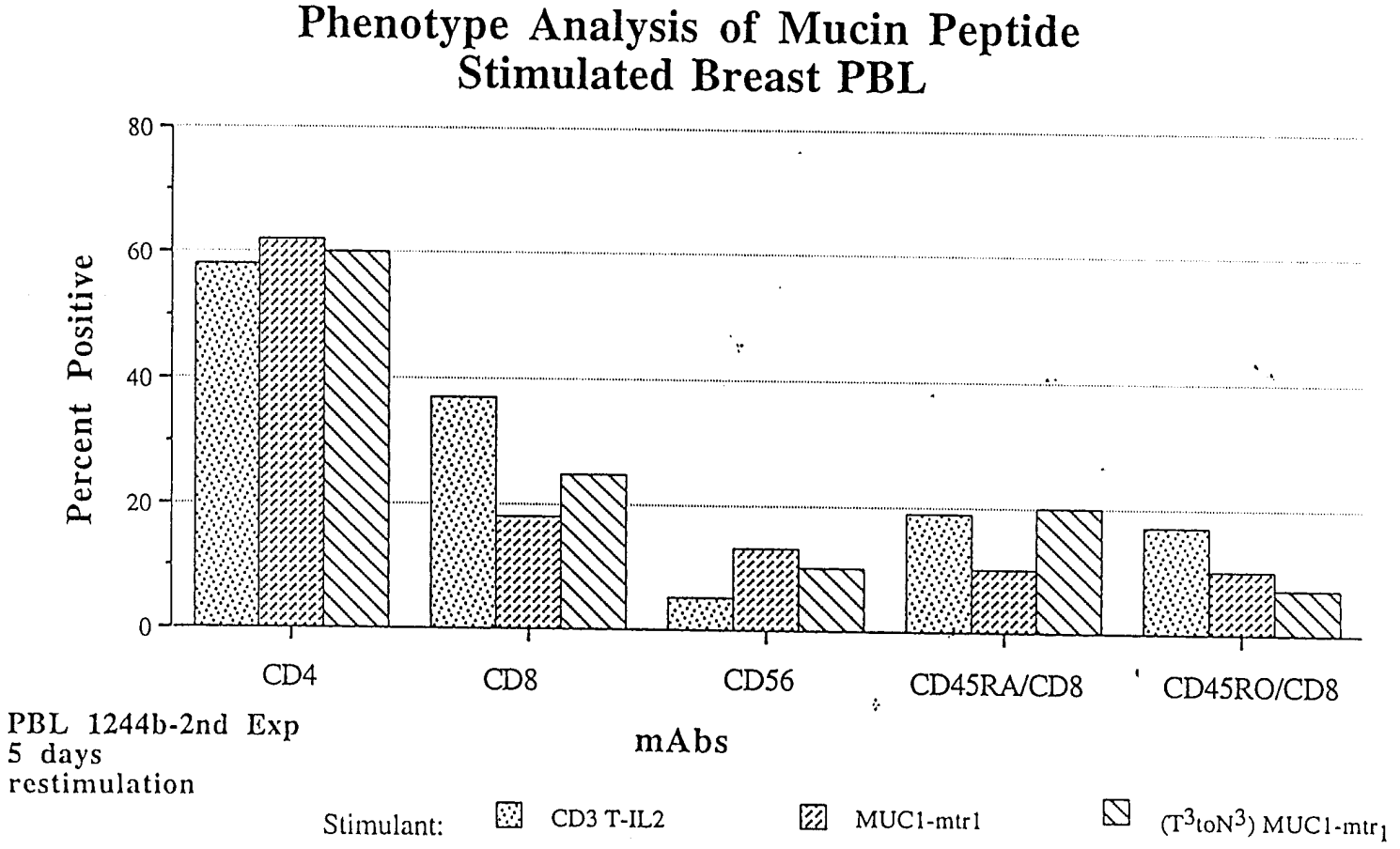
Phenotype Analysis of Mucin Peptide Stimulated Breast PBL
Percent Positive
80
60
40
20
0
CD4
CD8
CD56
CD45RA/CD8
CD45RO/CD8
mAbs
PBL 1244b-2nd Exp
5 days
restimulation
Stimulant:
CD3 T-IL2
MUC1-mtr1
(T3toN3) MUC1-mtr1

Fig.3

PROLIFERATIVE RESPONSE AFTER PEPTIDE RESTIMULATION

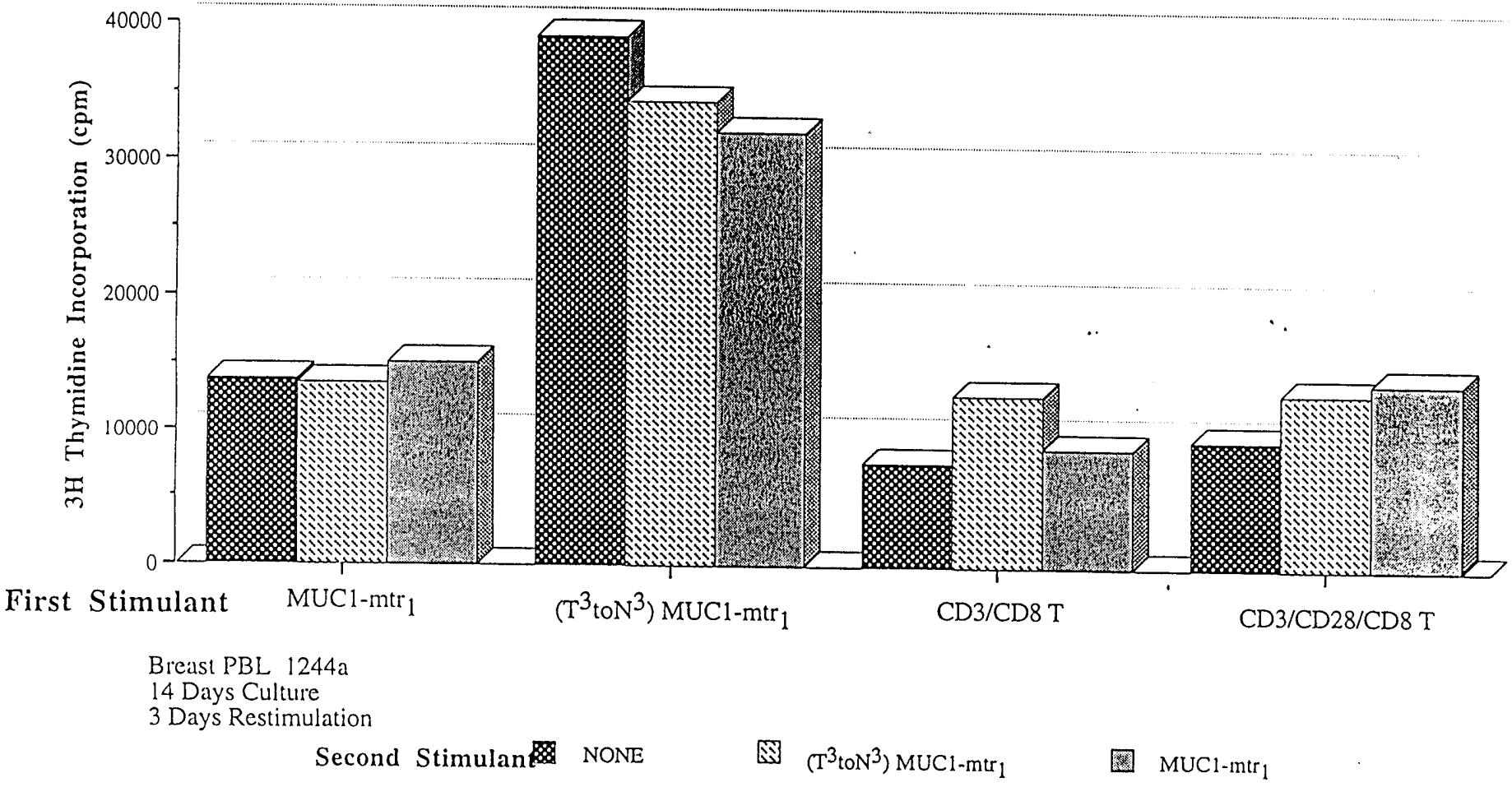

Fig. 4a

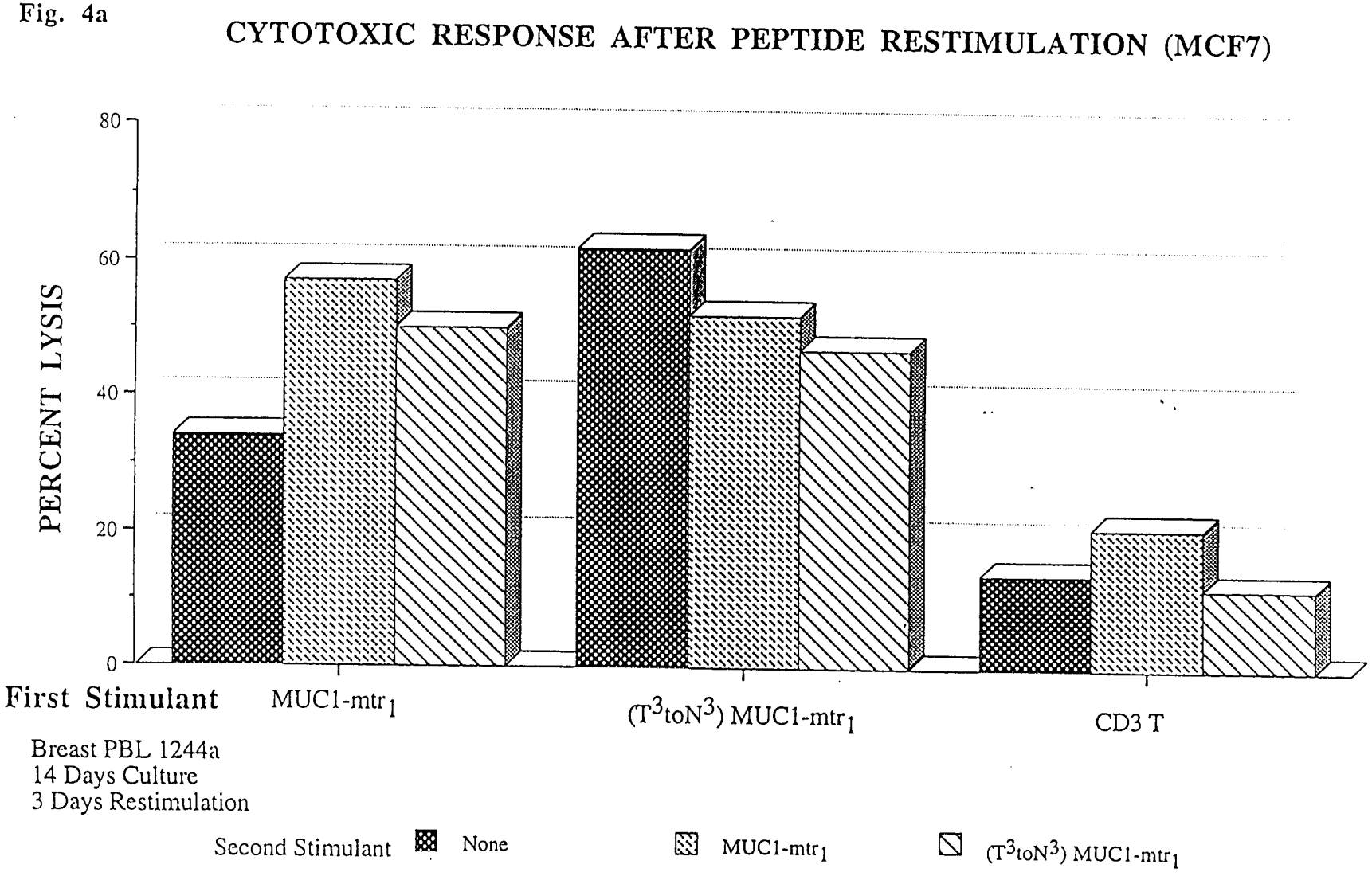
CYTOTOXIC RESPONSE AFTER PEPTIDE RESTIMULATION (MCF7)
PERCENT LYSIS
80
60
40
20
0
First Stimulant
MUC1-mtr1
(T3toN3) MUC1-mtr1
CD3 T
Breast PBL 1244a
14 Days Culture
3 Days Restimulation
Second Stimulant
None
MUC1-mtr1
(T3toN3) MUC1-mtr1

Fig.4b

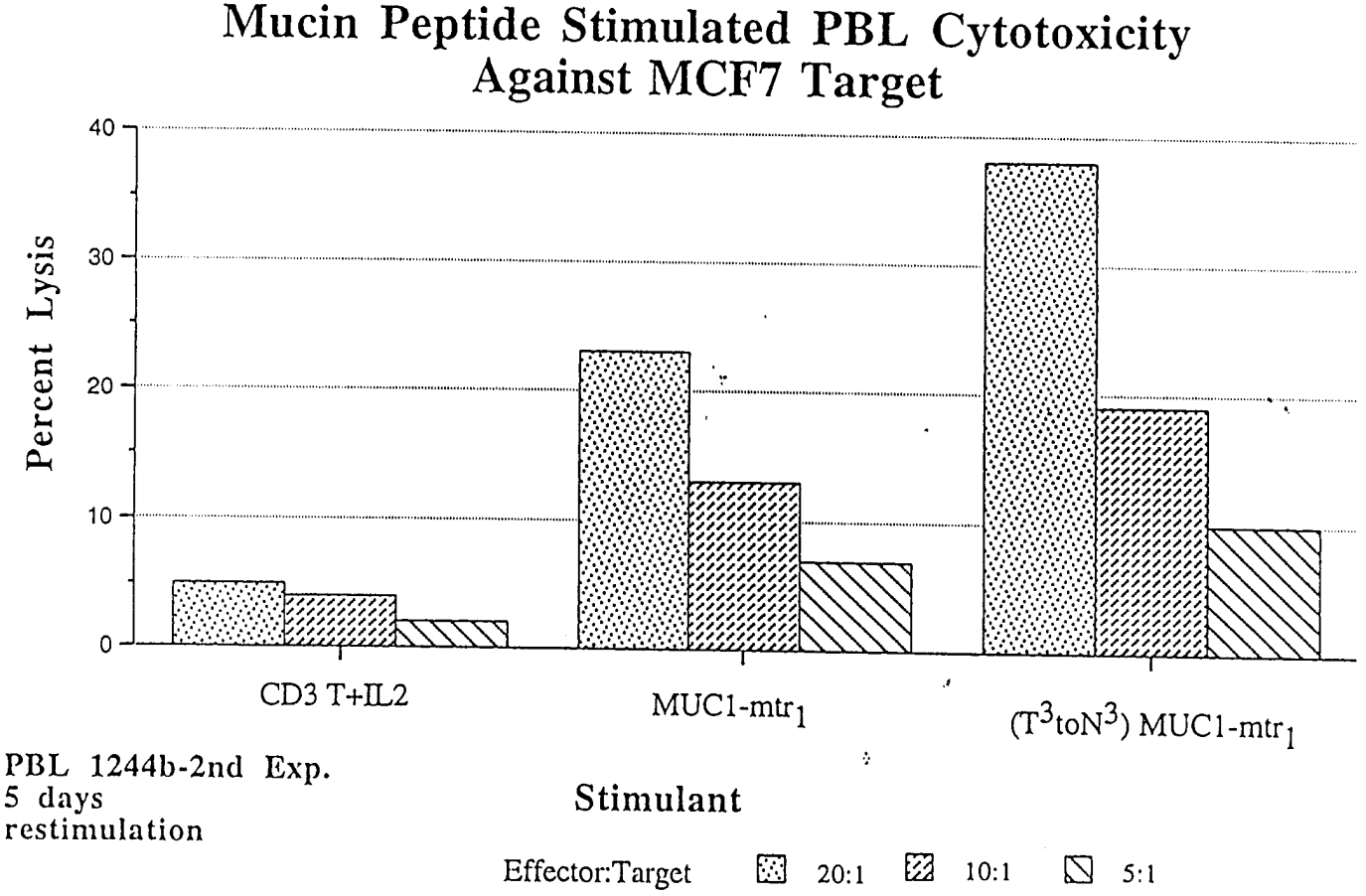

PBL 1244b-2nd Exp.
5 days
restimulation

fig. 5a

5a. TCR vB2 Expression in Response to Mucin Peptides

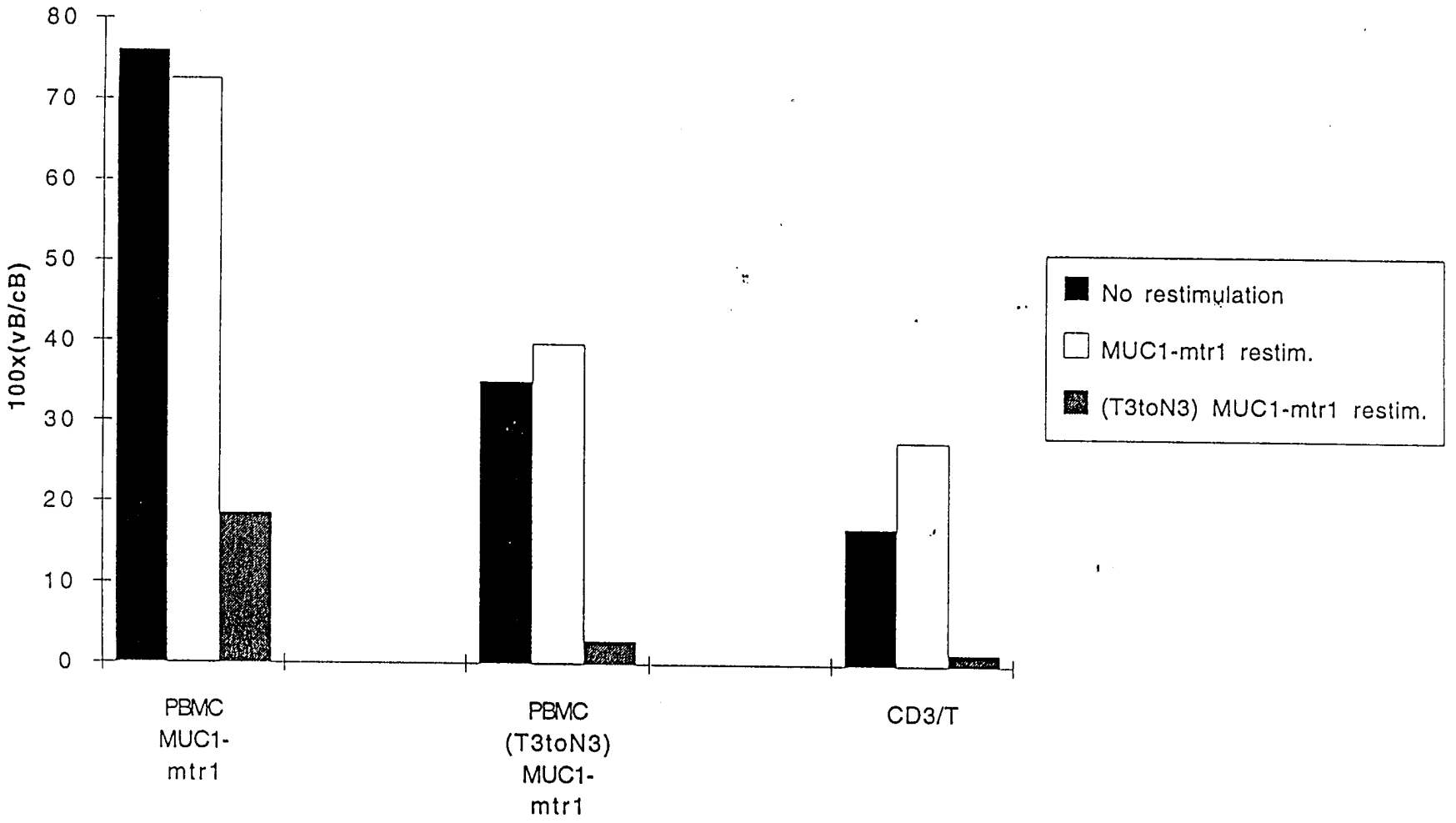

fig. 5b

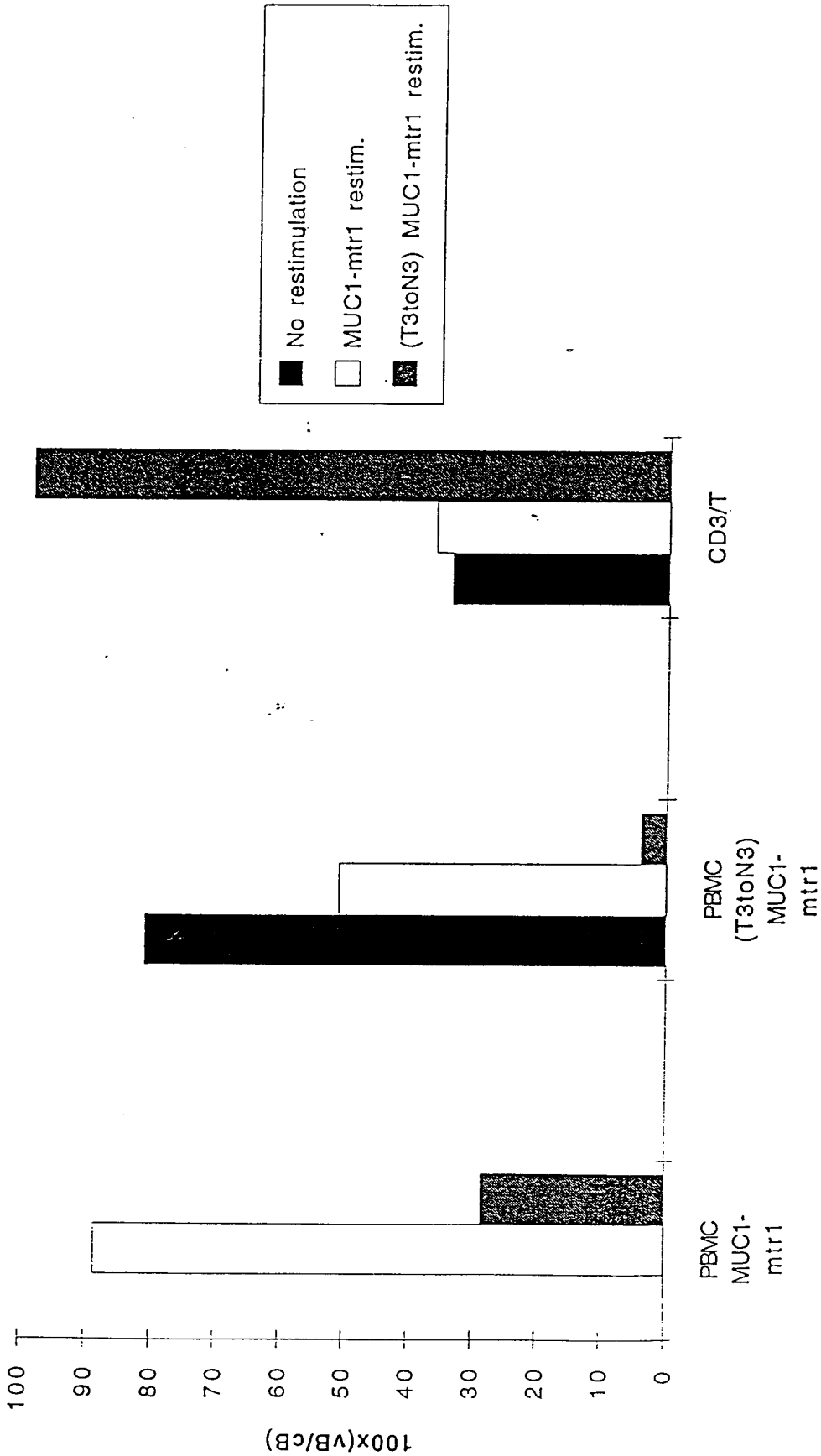
5b. TCR vB4 Expression in Response to Mucin Peptides
100x(vB/cB)
100
90
80
70
60
50
40
30
20
10
0
No restimulation
MUC1-mtr1 restim.
(T3toN3) MUC1-mtr1 restim.
PBMC MUC1-mtr1
PBMC (T3toN3) MUC1-mtr1
CD3/T

fig.5c

5c. TCR vB13 Expression in Response to Mucin Peptides

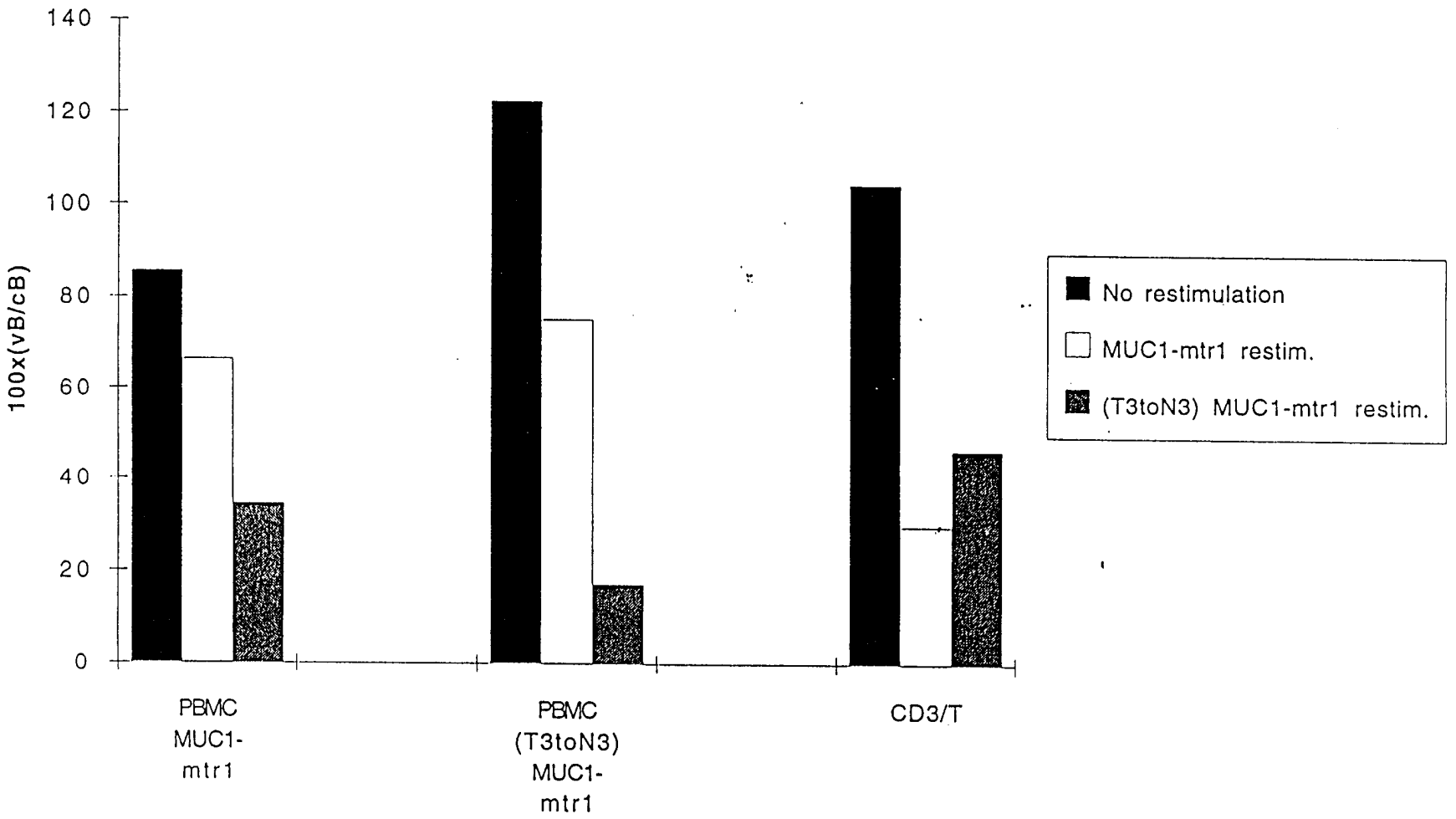

fig. 5d

5d. TCR vB14 Expression in Response to Mucin Peptides

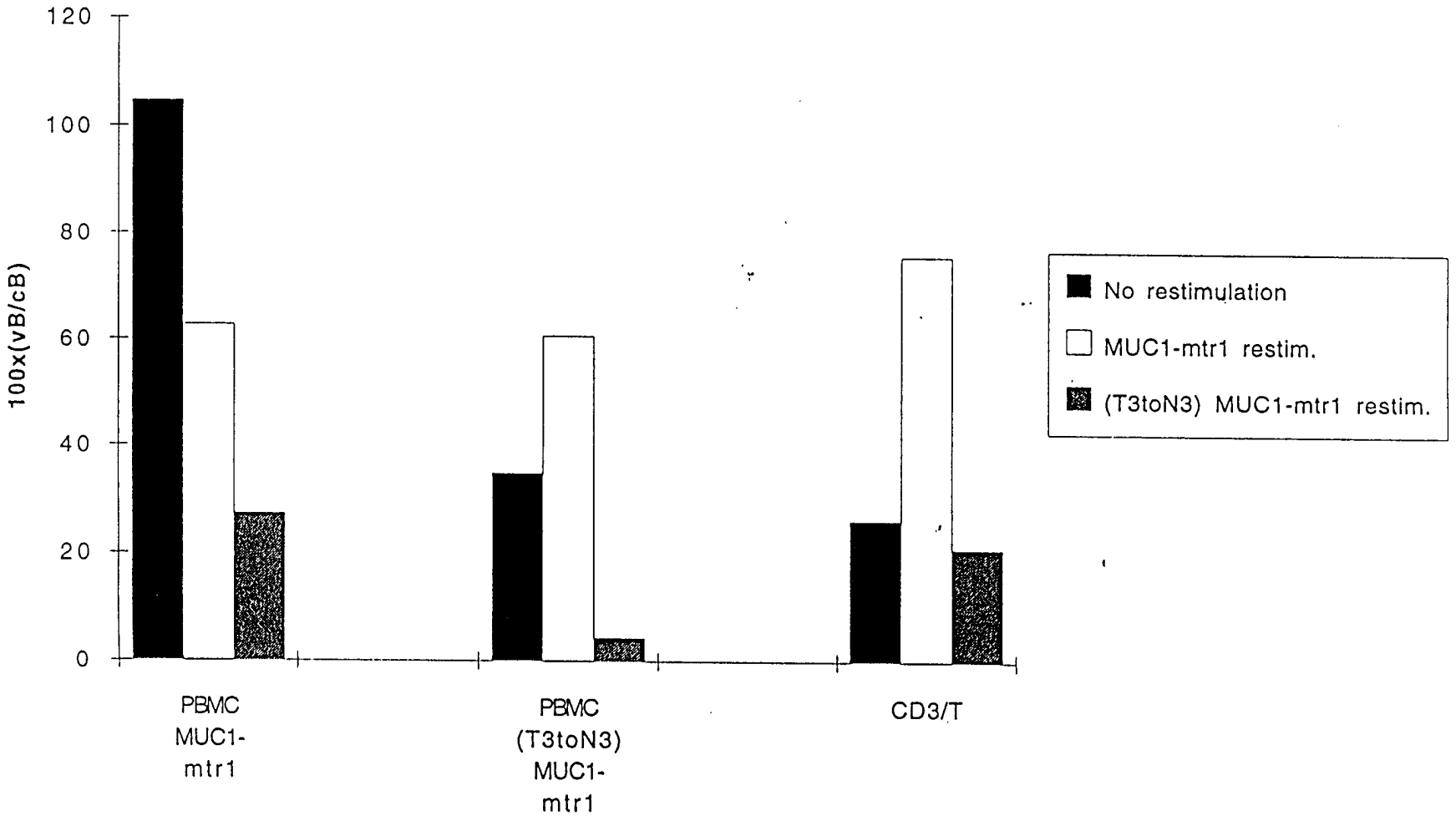

Fig.5e

TCR Analysis of Mucin Peptide Stimulated PBMC Cultures

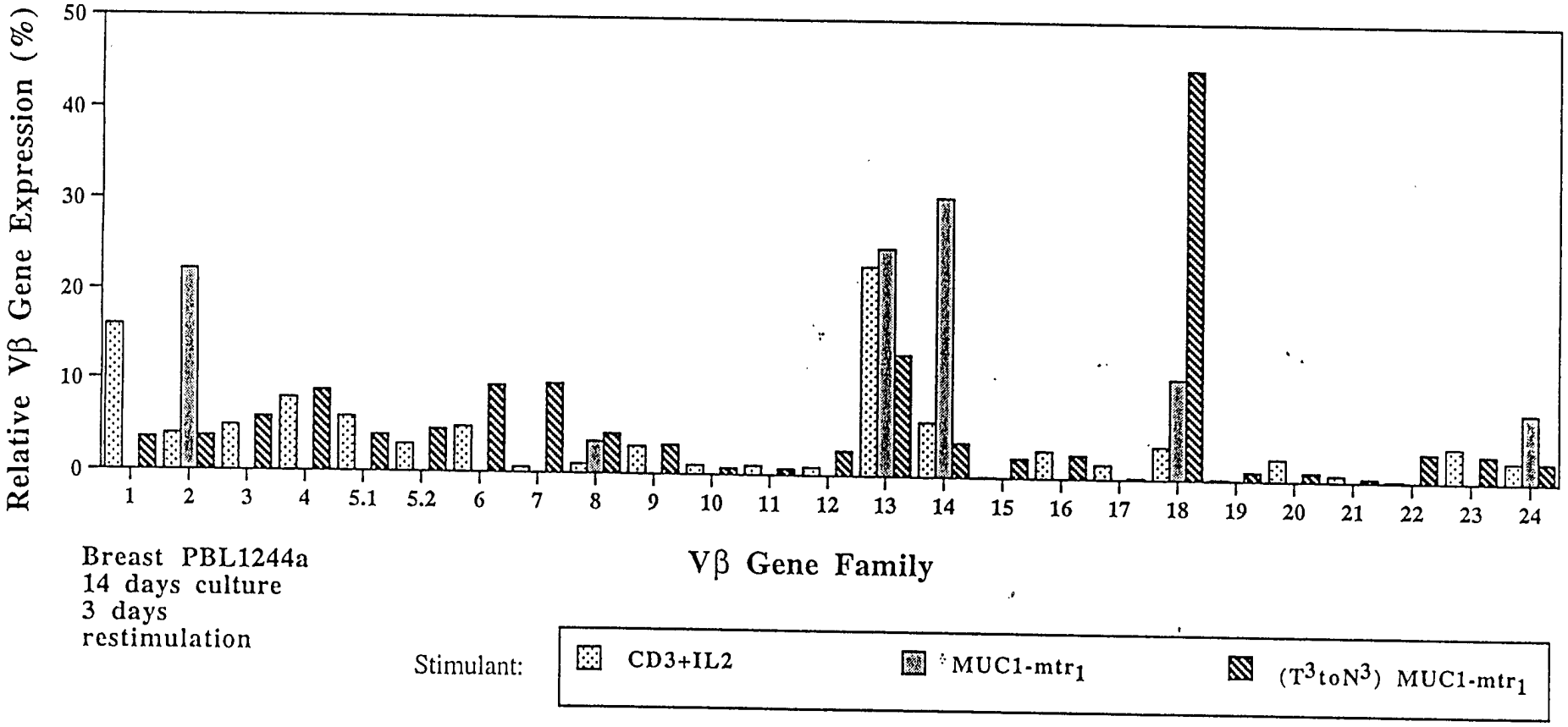

Fig. 6

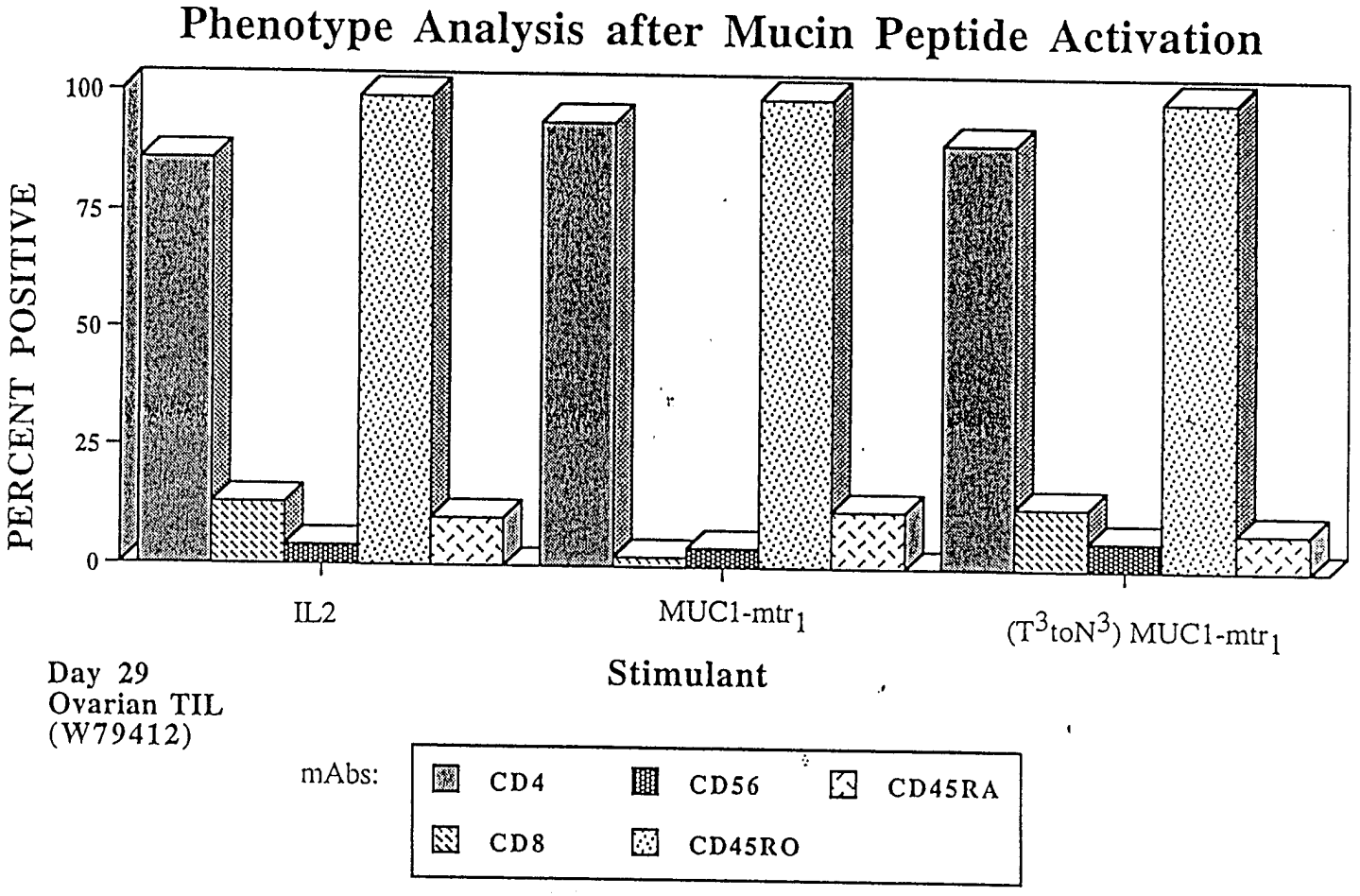
Phenotype Analysis after Mucin Peptide Activation
PERCENT POSITIVE
100
75
50
25
0
IL2
MUC1-mtr1
(T3toN3) MUC1-mtr1
Stimulant
Day 29
Ovarian TIL
(W79412)
mAbs:
CD4
CD56
CD45RA
CD8
CD45RO

Fig.7

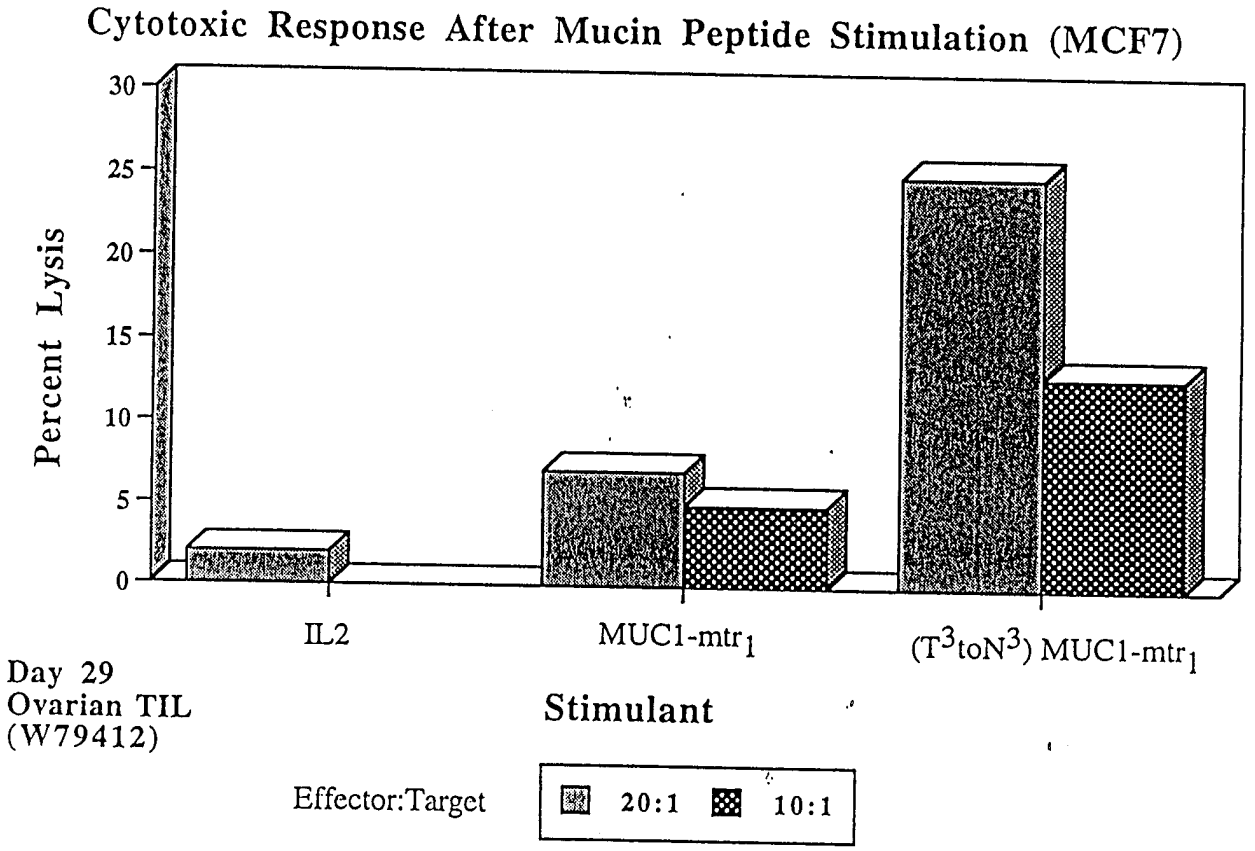
Cytotoxic Response After Mucin Peptide Stimulation (MCF7)
Percent Lysis
30
25
20
15
10
5
0
IL2
MUC1-mtr1
(T3toN3) MUC1-mtr1
Stimulant
Day 29
Ovarian TIL
(W79412)
Effector:Target
20:1
10:1

Fig.8

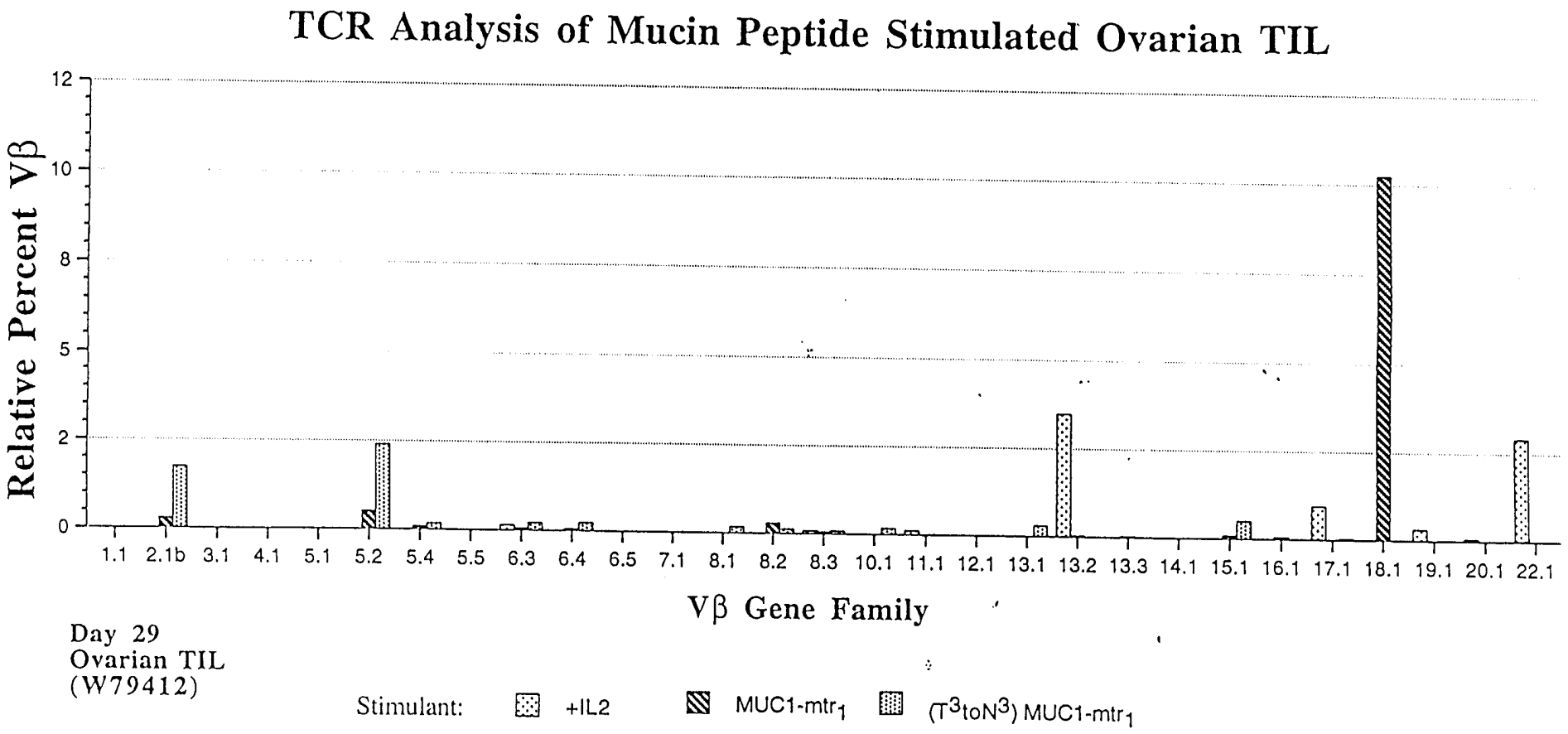
TCR Analysis of Mucin Peptide Stimulated Ovarian TIL
Relative Percent Vβ
12
10
8
5
2
0
1.1 2.1b 3.1 4.1 5.1 5.2 5.4 5.5 6.3 6.4 6.5 7.1 8.1 8.2 8.3 10.1 11.1 12.1 13.1 13.2 13.3 14.1 15.1 16.1 17.1 18.1 19.1 20.1 22.1
Vβ Gene Family
Day 29
Ovarian TIL
(W79412)
Stimulant:
+IL2
MUC1-mtr1
(T3toN3) MUC1-mtr1

SURFACE ANALYSIS OF PROTEINS AND RELATED MOLECULES BY X-RAY PHOTOELECTRON SPECTROSCOPY (XPS). Kenneth E. Dombrowski and Stephen E. Wright VA Medical Center and Dept. of Internal Medicine, Texas Tech University Health Sciences Center, Amarillo, TX 79106. Janine C. Birkbeck and William E. Moddeman. Mason and Hanger/Pantex Plant, Amarillo, Tx 79177

XPS is a surface-sensitive analytical technique which measures the binding energy of non-valence electrons of atoms in the first 100Å of a material. The binding energy can be related to the molecular bonding or oxidation state of an element. We have obtained XPS spectra on amino acids and polyamino acids which comprise the human MUC1 peptide PDTRPAPGSTAPPAHGVTSA. Characteristic binding energies (E_B) for carbon atoms ranged from 280 to 290 eV, 397 to 405 eV for nitrogen atoms and 529 to 536 eV for oxygen atoms. The precision is ± 0.1 eV. Within each range of E_B for each atomic species, different oxidation states were readily identifiable. Thus, a COO-zwitterion is distinguishable from an amide, alcohol and aliphatic carbons. XPS also yields information about the atomic composition molecules. Differences between the theoretical % composition and measured values generally differed by < 1%. A mutated T^3→N^3 MUC1 peptide has been analyzed by XPS. This mutation represents a 20% decrease in the number of hydroxyl groups present. XPS readily detected this decrease. Furthermore, we have begun to study the differences between components of protein and simple carbohydrates. Whereas amino acids exhibit a nitrogen composition of 10-20%, carbohydrates found on human mucins are generally composed of < 3% nitrogen. Work is directed to further refining the XPS differences among amino acids, peptides, proteins, and simple and complex carbohydrates in order to study the biochemistry of these human glycoproteins.

This work was supported in part by funds from the Elsa U. Pardee Foundation, Dept. of Veteran Affairs, Dept. of the Army, and Dept. of Energy.